

**The anti-inflammatory regulation of ATP-induced  
interleukin-1 $\beta$  release by short-chain fatty acids acetate,  
butyrate, propionate**

**Inaugural Dissertation**

for the degree of Doctor of Medicine

of the Faculty of Medicine

at the Justus-Liebig-University Giessen

submitted by

Herbolsheimer, Anna Isabel, born Chaveiro

from Mosbach (Baden)

Giessen (2023)

**From the Faculty of Medicine at the Justus-Liebig-University Giessen**

Department of General, Thoracic, Transplant and Pediatric Surgery

Laboratory of Experimental Surgery

First reviewer: Prof. Dr. Veronika Grau

Second reviewer: Prof. Dr. Soni Savei Pullamsetti

Date of Doctoral Defense: 24<sup>th</sup> June 2024

## Table of contents

1. Introduction .....	1
1.1 Monocytes and Macrophages .....	1
1.2 Toll-like receptor 4 signal transduction .....	4
1.3 P2X7 and P2X4 receptors.....	6
1.4 NLRP3-inflammasome .....	9
1.5 Interleukin-1 $\beta$ and Interleukin-18.....	11
1.6 Cholinergic system .....	13
1.7 Short-chain fatty acids (SCFAs).....	17
1.8 FFA2/FFA3 .....	22
1.9 Hypothesis .....	25
2. Materials and Methods .....	27
2.1 Materials and Chemicals .....	27
2.1.1 Reagents .....	27
2.1.2 Antibodies .....	31
2.1.3 Kits.....	32
2.1.4 Consumables .....	32
2.1.5 Equipment.....	35
2.1.6 Software .....	37
2.2 Methods .....	38
2.2.1 Human blood experiments .....	38
2.2.2 Mouse experiments .....	40
2.2.3 Statistical analysis.....	48
3. Results .....	50
3.1 Synthetic FFA2/FFA3 agonists inhibit the ATP-induced IL-1 $\beta$ release in hPBMCs and require the activity of nAChRs .....	50
3.1.1 The BzATP- or ATP-induced release of IL-1 $\beta$ .....	50
3.1.2 Involvement of P2X7 and P2X4 receptors in the BzATP- and ATP-induced secretion of IL-1 $\beta$ .....	51
3.1.3 Inhibition of IL-1 $\beta$ release via FFA2 agonist 4-CMTB .....	53
3.1.4 Inhibition of IL-1 $\beta$ release via FFA3 agonist AR420626.....	55
3.1.5 The signaling of the FFA2 involves nAChRs containing subunits $\alpha$ 7 and $\alpha$ 9/ $\alpha$ 10 .....	56

3.1.6 The signaling of the FFA3 involves nAChRs containing subunits $\alpha 7$ and $\alpha 9/\alpha 10$ .....	58
3.2 SCFAs and synthetic receptor agonists and the effect on the IL-1 $\beta$ release in mPBMCs from wild-type and FFA2 gene-deficient mice.....	60
3.2.1 The BzATP- or ATP-induced IL-1 $\beta$ release by wild-type mPBMCs.....	60
3.2.2 Inhibition of IL-1 $\beta$ release by wild-type mice via SCFAs.....	61
3.2.3 Inhibition of IL-1 $\beta$ release via SCFAs by wild-type and gene-deficient mPBMCs.....	63
3.2.4 Inhibition of IL-1 $\beta$ release via FFA2 and FFA3 agonists.....	65
3.2.5 Inhibition of IL-1 $\beta$ release via FFA2 and FFA3 agonists in wild-type and gene-deficient mice .....	66
3.3 SCFA and synthetic FFA agonists induce a cholinergic mechanism to inhibit the ATP-induced release of IL-1 $\beta$ by mouse BMDMs .....	69
3.3.1 Cell characterization via F4/80 staining .....	69
3.3.2 Double-staining of macrophages and the FFA2 within the murine colon .....	70
3.3.3 The BzATP or ATP induced release of IL-1 $\beta$ in mouse BMDMs .....	71
3.3.4 The inhibition of ATP-induced IL-1 $\beta$ release in mouse BMDMs via P2X7 receptor antagonist .....	73
3.3.5 The ATP-induced IL-1 $\beta$ release is blunted in the presence of P2X7 and P2X4 receptor antagonists .....	74
3.3.6 The influence of SCFAs and FFA2 and FFA3 agonists on the ATP-induced IL-1 $\beta$ release .....	77
3.3.7 The signaling of FFA2 and FFA3 involve nAChR containing $\alpha 7$ and $\alpha 9/\alpha 10$ .....	79
4. Discussion .....	83
4.1 Summary of the results .....	83
4.2 FFA-mediated regulation of ATP-dependent IL-1 $\beta$ secretion by hPBMCs.....	84
4.2.1 ATP receptor-dependent secretion of IL-1 $\beta$ .....	84
4.2.2 Involvement of the ATP receptors P2X4 and P2X7 .....	86
4.2.3 Control of IL-1 $\beta$ secretion by synthetic FFA2 and FFA3 agonists .....	88
4.2.4 Signaling of FFA2 and FFA3 via nAChRs.....	90
4.3 FFA-mediated regulation of ATP-dependent IL-1 $\beta$ secretion by mPBMCs.....	93
4.3.1 ATP receptor-dependent secretion of IL-1 $\beta$ .....	93
4.3.2 Control of IL-1 $\beta$ secretion by endogenous and synthetic FFA agonists.....	95
4.3.3 Role of FFA2 in the control of IL-1 $\beta$ secretion .....	96
4.4 FFA-mediated regulation of ATP-dependent IL-1 $\beta$ secretion by murine macrophages .....	98
4.4.1 Localization of FFA2-expressing macrophages in the murine colon .....	98

4.4.2 ATP receptor-dependent secretion of IL-1 $\beta$ .....	99
4.4.3 Involvement of the ATP receptors P2X4 and P2X7 .....	101
4.4.4 Control of IL-1 $\beta$ secretion by synthetic FFA agonists.....	102
4.4.5 Signaling of FFAs via nAChRs .....	103
<b>5. Conclusion.....</b>	<b>106</b>
<b>6. Summary .....</b>	<b>107</b>
6.1 German .....	107
6.2 English.....	108
<b>7. List of abbreviations.....</b>	<b>109</b>
<b>8. List of figures .....</b>	<b>113</b>
<b>9. List of tables.....</b>	<b>114</b>
<b>10. List of references .....</b>	<b>115</b>
<b>11. Supplementary Material.....</b>	<b>134</b>
<b>12. Note of thanks .....</b>	<b>148</b>

# 1. Introduction

## 1.1 Monocytes and Macrophages

The innate immune response is based on chemical, physical, humoral and cellular response mechanisms against invading pathogens (Janeway et al. 2001). Part of the cellular components are mononuclear phagocytes such as monocytes, macrophages, dendritic cells and further cells like granulocytes, mast cells and the natural killer cells (Janeway et al. 2001). For this thesis, the cellular response, specifically the monocyte and also the macrophage are of importance and will therefore be looked at more closely.

In the first part of this chapter, the monocyte with its characteristics will be reviewed. Then the macrophage, since monocytes differentiate into macrophages after tissue infiltration. At the end the cells used for most of the experiments for this thesis will briefly be explained.

The monocyte, being a type of leukocyte, is derived from the bone marrow and arises from precursor cells called promonocytes (van Furth and Cohn 1968). These migrate into the blood circulatory system upon specific stimuli (van Furth and Cohn 1968). Here, in the human blood, they make up less than 10% of the circulating nucleated cells (Prinyakupt and Pluempitiwiriyaewej 2015). Monocytes are known for their size, being the largest white blood cell measuring up to 20  $\mu\text{m}$  (Prinyakupt and Pluempitiwiriyaewej 2015). Their nucleus can be very heterogenous (Ziegler-Heitbrock 2000). Typically however, kidney-shaped bilobed nuclei are seen (Skinner and Johnson 2017).

Many functions of monocytes are known, primarily however their role in an immune response to infection (Yáñez et al. 2017). Important relevance, especially for this thesis, is revealed by the fact that activated monocytes show pro-inflammatory features, meaning they have the ability to produce and secrete interleukin-1 $\beta$  (IL-1 $\beta$ ) as well as other pro-inflammatory mediators and also being one of the leading cells to do so (Oppenheim et al. 1986; Rubartelli et al. 1990; Dinarello 2009; Canè et al. 2019). In an infectious setting, or under stress, in an autoimmune disease or due to trauma a higher relative or absolute number of circulating monocytes is common (Yáñez et al. 2017). On the other hand, a lower percentage of monocytes is found in the myelodysplastic syndrome (Saeed et al. 2017; Carrick and Begg 2008). Furthermore, monocytes, but also macrophages, are able to recognize a pathogen via pattern recognition receptors (PRRs) (Kawai and Akira 2010). A PRR, as the name says, is a protein that is found on for example the membrane

of cells and recognizes specific molecular structures mostly found on the surface of pathogens. The PRRs include the membrane toll-like receptors (TLRs) (Martinon et al. 2009; Iwasaki and Medzhitov 2015; Armant and Fenton 2002). These receptors, their pathogen recognition mechanism and the signal transduction will be explained in more detail in the next chapter. A relevant function of this TLR is to enable monocytes to act as antigen-presenting cells and activate further immune cells (Jakubzick et al. 2017). Additionally, monocytes are phagocytes and therefore remove microorganisms, dead or damaged cells (Canè et al. 2019; Guilliams et al. 2018).

Within 12-32 h, the monocytes infiltrate tissues upon tissue damage or infection guided by chemokines and differentiate into tissue specific macrophages and monocyte-derived dendritic cells, giving them an important role in immune response (Yáñez et al. 2017; Issekutz and Issekutz 1993; van Furth and Cohn 1968). The infiltration process is divided into different steps, the first being the so-called “tethering” of the monocyte to the endothelium (Maslin et al. 2005). Secondly, “loose rolling” along the surface following the “adhesion” to the endothelium (Maslin et al. 2005). In the final step, “diapedesis” between the endothelial cells takes place (Maslin et al. 2005).

Depending on the tissue, different names are given to the macrophages, such as microglia, histiocytes, Kupffer cells or alveolar macrophages, however all are part of the mononuclear phagocyte system (Ovchinnikov 2008). One of their main functions is to “catch” and engulf pathogens using their “arms” called filopodia (Kress et al. 2007). Having found a pathogen, foreign substances or cancer cells, these are engulfed and digested as a foreign substance by macrophages, which is called phagocytosis (Mahla et al. 2021). After that, the macrophage acts as an antigen presenting cell and presents peptides of own or foreign cells to T-cells, therefore activating the acquired immune system (Guerriero 2019). This presenting function is also seen in monocytes as mentioned in the paragraph above. Through releasing specific cytokines, the macrophages also have an anti-inflammatory role and therefore decrease immune reactions (Mills 2012). It has been thought that M1 macrophages encourage inflammation and M2 macrophages decrease inflammation (Mills 2012). This strict system has been criticized, since a higher complexity has been detected (Ransohoff 2016). Most macrophages found at sites of infection typically derive from monocytes, however some macrophages are already in the tissue independent of infection (Pittet et al. 2014). These then attract monocytes using cytokines (Pittet et al. 2014; Perdiguero and Geissmann 2016).

The macrophage has a lot of surface antigens in common with other immune cells such as the natural killer cells, B-lymphocytes and neutrophils (Ross 2000). To specifically identify the macrophage in mice, a monoclonal antibody called F4/80, like the antigen and was developed in 1981 (Austyn and Gordon 1981). This antibody did not react with other cells of hematopoietic origin, it showed to be directed to a surface antigen F4/80 specific to macrophages (Austyn and Gordon 1981). In the later years, however, other cells such as eosinophils and Langerhans cells were seen to express F4/80, reducing the specificity of the antibody developed (Hume et al. 1983; McGarry and Stewart 1991). This F4/80 antibody was used in this thesis, for an immunohistochemical staining to identify murine macrophages.

After having reviewed the similar functions and also the role monocytes and macrophages have in the defense against pathogens, it is comprehensible that a disbalance in any function can lead to various different pathological processes and can have an influence in the pathogenesis of some autoimmune diseases. Included are for example chronic bowel diseases, multiple sclerosis, rheumatoid arthritis, systemic sclerosis and diabetes type 1 (Ma et al. 2019).

Monocytes belong to the group of peripheral blood mononuclear cells (PBMCs) just like lymphocytes and other cells with a single non-fragmented nucleus (Delves et al. 2006). PBMCs are therefore classified as mononuclear cells and are well-studied components of the immune system (Delves et al. 2006). Since PBMCs circulate in the blood stream, they are easily isolated from peripheral blood by density gradient centrifugation, these cells are often used *in vitro* for research as a cellular model for studying immune responses (Panda and Ravindran 2013). Further fields of research where PBMCs are used are immunopathology, immune therapy strategies, as well as various diseases such as cancer (Mosallaei et al. 2022; Zhou et al. 2015).

A further type of cells used for some experiments in this thesis are the mouse bone marrow-derived macrophages (BMDMs). These cells make macrophage-related research possible and are therefore used in numerous studies (Marim et al. 2010). As the name states, the macrophages are derived from the bone marrow (Barrett et al. 2015). These cells are able to differentiate into mature macrophages in the presence of specific signaling molecules such as the macrophage colony-stimulating factor (M-CSF) (Weischenfeldt and Porse 2008)

## 1.2 Toll-like receptor 4 signal transduction

In order to better understand the experiments that were performed in this thesis and the complex process of IL-1 $\beta$  secretion and inhibition, figures are added and completed according to the chapter that is viewed. The first figure (Figure 1) depicts a cell with a receptor called toll-like receptor 4 (TLR4), a first signal shown to be lipopolysaccharide (LPS) and a signal transduction including transcription factors nuclear factor  $\kappa$ B (NF- $\kappa$ B) or activator protein 1 (AP-1) that induce the expression of pro-interleukin-1 $\beta$  (pro-IL-1 $\beta$ ) and pro-interleukin-18 (pro-IL-18). This process will be described in detail in the following passages.

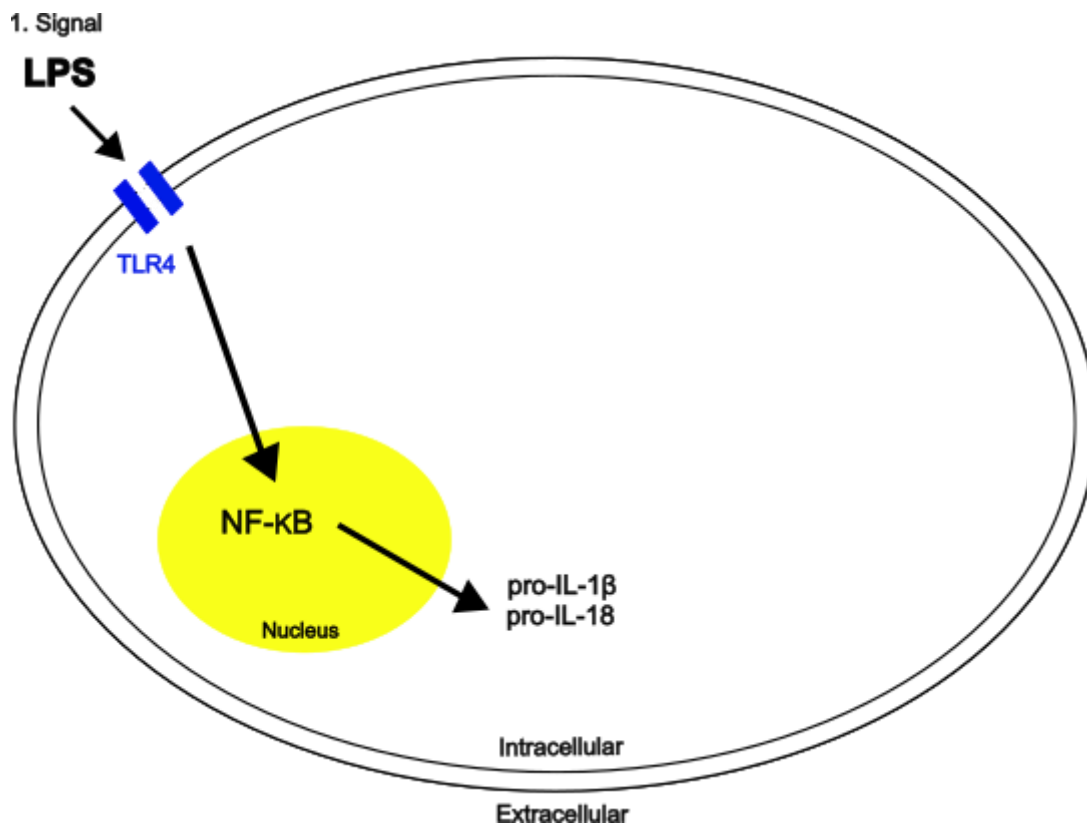


**Figure 1. Schematic overview of the first danger signal pathway.** For the release of mature interleukin-1 $\beta$  (IL-1 $\beta$ ) and interleukin-18 (IL-18), two signals are needed (not shown in the figure). The first danger signal lipopolysaccharide (LPS) leads to the activation of the toll-like receptor 4 (TLR4) and induces the expression of the precursor protein pro-IL-1 $\beta$  and pro-IL-18 through activation of the transcription factor nuclear factor  $\kappa$ B (NF- $\kappa$ B).

The human TLR4 is a transmembrane protein which is part of a family of 12 TLRs that belong to the PRRs (Botos et al. 2011; Fitzgerald and Kagan 2020). The PRRs initiate an inflammatory response against pathogens by activating antimicrobial genes (Pasare and Medzhitov 2004). TLRs are among one of the first of the PRRs to be identified in mammals and are best characterized (Sameer and Nissar 2021). They are expressed in innate immune cells like dendritic cells, monocytes or macrophages and a number of other cells (Kawasaki and Kawai 2014; Kawai and Akira 2010). They enable these to recognize a pathogen as mentioned in the previous chapter (Kawasaki and Kawai 2014; Kawai and Akira 2010). There are different localizations known for the TLRs (Takeda and Akira 2004). First being in the membrane of the cell and second intracellular, being on membranes of different cell compartments (Takeda and Akira 2004). The TLRs on the membrane of a cell have a similar structure that is made up of an extracellular, a transmembrane and an intracellular region (Takeda and Akira 2004). The extracellular region contains 18-25 leucine rich copies (LRRs) (Takeda and Akira 2004; Iwasaki and Medzhitov 2004). In the cytosolic side of the membrane, a Toll-IL receptor (TIR) domain is found which interacts with other TIR domains in other signaling molecules (Takeda and Akira 2004; Iwasaki and Medzhitov 2004).

The molecular highly conserved “patterns” of pathogens that are being recognized via the PRRs or specifically speaking the TLRs are called pathogen-associated molecular patterns (PAMPs) and are foreign to the body (Janeway 1989). PAMPs are mostly thought to be polysaccharides, glycolipids, lipoproteins, nucleic acids of the pathogen as well as LPS from the cell wall of Gram-negative bacteria. (Janeway 1989; Iwasaki and Medzhitov 2015). Bacterial LPS is recognized by TLR4, which can be seen in figure 1 and is therefore relevant for this thesis (Iwasaki and Medzhitov 2015). Not only TLR4 but further co-receptors like lymphocyte antigen 96 and the cluster of differentiation 14 (CD14) are needed to activate the intracellular signal transduction (Medzhitov 2001). This leads to a recruitment of adapter proteins like myeloid differentiation primary response 88 (MyD88) or TIR-domain-containing adapter-inducing interferon- $\beta$  (TRIF) which then again leads to an activation of NF- $\kappa$ B, interferon regulatory factor 3 (IRF3) and AP-1 (Kawasaki and Kawai 2014; Vaure and Liu 2014). This results in a higher transcription rate of the inflammatory cytokine precursor pro-IL-1 $\beta$  and pro-IL-18 as well as the expression of components of the multiprotein complex called the NLRP3-

inflammasome, that will be explained in the chapter 1.4 (Janeway and Medzhitov 2002; Kawasaki and Kawai 2014; Bauernfeind et al. 2009; Martinon et al. 2009).

Mononuclear phagocytes are also able to recognize damage-associated molecular patterns (DAMPs) via TLRs or several other receptors, which are endogenous and released on damage (Feldman et al. 2015; Di Virgilio et al. 2017). Typical DAMPs include extracellular adenosine triphosphate (ATP), free deoxyribonucleic acid (DNA) as well as components of the extracellular matrix (Martinon et al. 2009; Tsan and Gao 2004; Bianchi 2007; Matzinger 1994; Gong et al. 2020).

The importance of the immune system in responding appropriately is profound. It must be sensitive enough to respond to immediate danger, however also rigorously controlled not to induce an overreaction. Charles Alderson Janeway first described a model where PAMPs are recognized by PRRs in 1989. Then in 1994 Polly Matzinger added a so-called “danger model” claiming there must be additional endogenous DAMPs. Both models result in the conclusion that both PAMPs and DAMPs have the capability to activate the immune system. (Martinon et al. 2009; Gong et al. 2020). Two signals however are described to be relevant in the synthesis, maturation and release of IL-1 $\beta$  (Martinon et al. 2009). A typical first signal being LPS (see Figure 1) and a typical second signal being ATP released by damaged cells (Martinon et al. 2009). The pathway of the second signal will be reviewed in the next chapter.

### **1.3 P2X7 and P2X4 receptors**

This chapter and the next (see 1.4) put light on a second signal pathway, that leads to the activation of the NLRP3-inflammasome and ultimately to the cleavage of pro-IL-1 $\beta$  and pro-IL-18 into mature IL-1 $\beta$  and IL-18 that can then be secreted. The first part of the signal pathway includes the P2X7 receptor, which is the main emphasis of this thesis. The involvement of the P2X4 receptor is tested in one experiment and therefore only briefly outlined in this chapter.

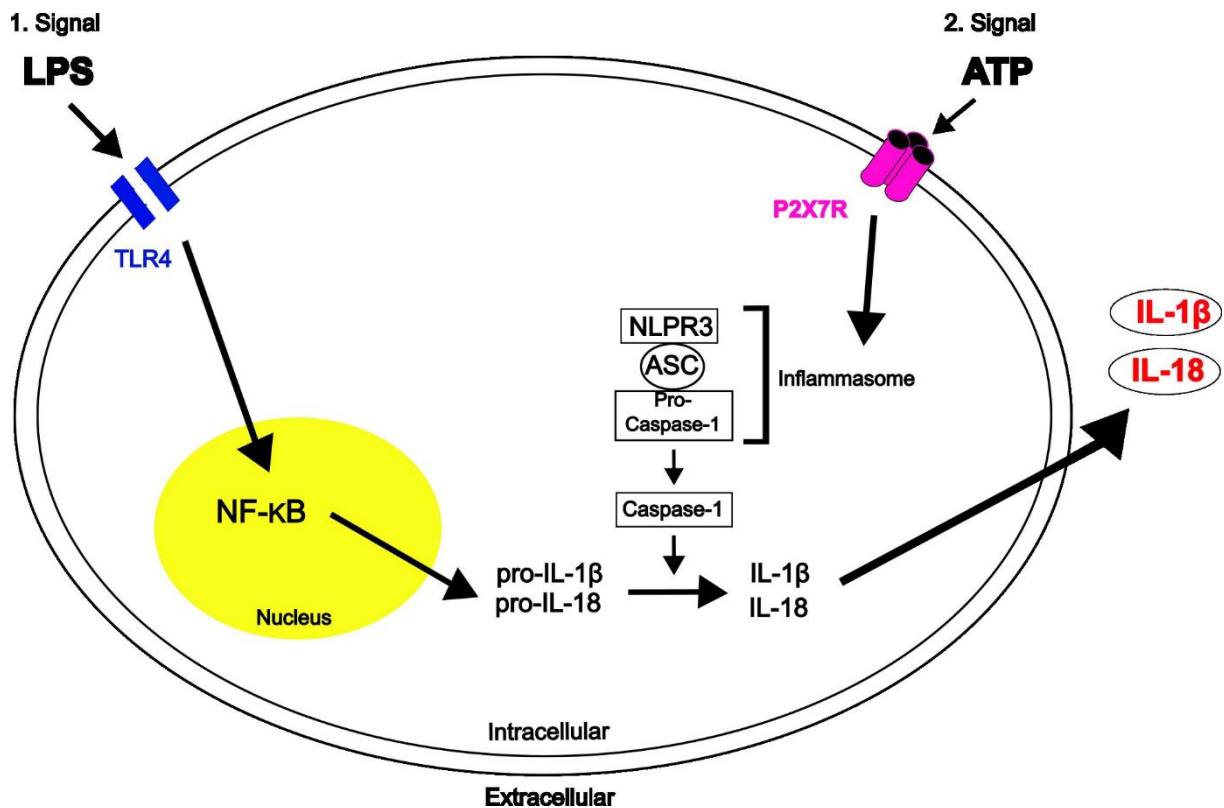


**Figure 2. Schematic overview of the first and second signal pathway.** For the release of mature IL-1 $\beta$  and IL-18, two signals are needed. The first danger signal lipopolysaccharide (LPS) leads to the activation of the toll-like receptor 4 (TLR4) and induces the expression of the precursor protein pro-IL-1 $\beta$  through activation of the transcription factor nuclear factor  $\kappa$ B (NF- $\kappa$ B). The second signal extracellular ATP activates the P2X7 receptor and leads to the assembling of the NLRP3-inflammasome, consisting of NLPR3, apoptosis-associated speck like protein (ASC) and pro-caspase-1. This, activates caspase-1 which induces the cleavage of pro-IL-1 $\beta$  and pro-IL-18 to mature IL-1 $\beta$  and IL-18, that can then be released.

The P2 receptor superfamily is divided into P2X and P2Y receptors. Both the P2X7 and the P2X4 receptors belong to the P2X receptor subfamily, comprising of 7 isoforms (Jarvis and Khakh 2009; Adinolfi et al. 2018). All P2X receptors have a similar structure being a trimeric ion channel consisting of two transmembrane domains with an extended C-terminus, one extracellular loop and intracellular amino and carboxyl termini (North 2002). The shape of the receptors has also been described as “dolphin-like”, with ten disulfide-bonding cysteine residues in the extracellular loop region that play a role in the

ligand-binding formation and channel gating (Ennion and Evans 2001; Kawano et al. 2012a; Rokic et al. 2010; Kawate et al. 2009)

P2X receptors are found in various different tissues and most cells of the human being such as the nervous system, heart, skeletal and smooth muscle tissue, blood platelets as well as most immune cells (Adinolfi et al. 2018). Furthermore, the P2X receptors are ATP-gated cation channels (Kawate et al. 2011). The ion-permeable pores allow cations like  $\text{Na}^+$  or  $\text{Ca}^{2+}$  to pass, upon the binding of ATP (Kawate et al. 2011). However, nicotine-adenine-dinucleotide ( $\text{NAD}^+$ ) has also shown to activate some P2X receptors (Seman et al. 2003). The result of the activation of the P2X receptors in mononuclear phagocytes for example is the inflammasome activation, chemokine and cytokine secretion and pyroptosis (Di Virgilio et al. 2017).

In this thesis, the **P2X7 receptor** plays an essential role, since it acts as the receptor for the second signal ATP, as mentioned in 1.2, and results in the formation of the NLRP3-inflammasome (Martinon et al. 2009). The P2X7 is the best studied receptor of its kind considering the immunological function (Adinolfi et al. 2018). Furthermore, the P2X7 receptor has a high expression in immune cells like monocytes (Adinolfi et al. 2018). Studies have shown, that the P2X7 receptor has a comparably low affinity to ATP, however a high one to the ATP derivate 3'-O-(4-benzoyl) benzoyl ATP (BzATP) (Adinolfi et al. 2018). Therefore, BzATP was used in most experiments conducted for this thesis. The activation of the P2X7 receptor leads to an influx of  $\text{Na}^+$  and  $\text{Ca}^{2+}$  and an efflux of  $\text{K}^+$  (Cekic and Linden 2016). This reduction of  $\text{K}^+$  in the cell then leads to the activation of the NLRP3-inflammasome, which results in the secretion of interleukins, amongst others IL-1 $\beta$  and IL-18 (Cekic and Linden 2016). The formation and activation of the NLRP3-inflammasome are mentioned in the next chapter 1.4.

Numerous pathomechanisms show the important role of the P2X7 receptor (Adinolfi et al. 2018). For example, the presence of the receptor in microglia is thought to have an influence on the pathogenesis of the Alzheimer's disease and multiple sclerosis (Francistiová et al. 2020; Amadio et al. 2017). Furthermore, the involvement of the P2X7 receptor in diseases like Lupus erythematosus and rheumatoid arthritis as well as further chronic inflammatory diseases is being discussed (Adinolfi et al. 2018).

The **P2X4 receptor** is expressed mostly in cells of the immune system like mast cells or macrophages, peripheral endothelial cells and in cells of the central nervous system

(Stokes et al. 2017; Suurväli et al. 2017). It is found on the cell membrane and in lysosomal compartments to which the P2X4 receptor is targeted through a dileucine-type motif within the N-terminus and a tyrosine-based endocytic motif within the C-terminus (Boumechache et al. 2009; Qureshi et al. 2007). Upon extracellular signals, such as stimulation for phagocytosis or lysosome exocytosis, the receptor is brought to the cell surface (Qureshi et al. 2007). The motifs mentioned above, control the internalization and recycling of the receptor (Bobanovic et al. 2002; Toulmé et al. 2006). A disruption of these motifs resulted in an increase of the expression of the P2X4 receptor on the cell surface (Xu et al. 2014).

In immune cells, the activation of the P2X4 receptor results in the influx of cations, mostly  $\text{Ca}^{2+}$ , leading to a cell membrane depolarization and signal transduction that results in various  $\text{Ca}^{2+}$ -sensitive intracellular processes, such as the release of prostaglandin E2 from macrophages or brain-derived neurotrophic factor (BDNF) from microglia (Khakh and North 2012; Trang et al. 2009; Baroja-Mazo et al. 2013). Furthermore, the inflammasome is activated via the P2X4 receptor upon injury (Ulmann et al. 2010; Rivero et al. 2012). P2X4 receptors expressed on microglia have shown to play a role in neuroinflammatory responses and chronic pain (Ulmann et al. 2010; Trang et al. 2009). P2X4 receptor expression and function is thought to be associated with the transmission of inflammatory and neuropathic pain (Bernier et al. 2018), cardiovascular disease (Bragança and Correia-de-Sá 2020) and alcohol abuse disorders (Franklin et al. 2014).

Various studies show, that the P2X7 and P2X4 receptors interact with one another (Guo et al. 2007). P2X7 and P2X4 receptor subunits form a heteromeric channel and show ATP-activated currents in ciliated airway epithelia, salivary epithelia and further tissues (Guo et al. 2007; Ma et al. 2006; Casas-Pruneda et al. 2009). Furthermore, both receptors are involved in the initial step of T-cell activation as well as P2X7 receptor dependent cell death (Kawano et al. 2012b). However, the interaction of both receptors has not yet been fully understood.

#### **1.4 NLRP3-inflammasome**

The activation and formation of the NLRP3-inflammasome can be the result of the signal transduction following the P2X7 receptor activation mentioned in 1.3. Figure 2 shows

some of the steps mentioned in this chapter that ultimately lead to the cleavage into mature IL-1 $\beta$  and IL-18.

Inflammasomes are multiprotein complexes that are found in the cytosol of a cell (Broz and Dixit 2016; Mariathasan et al. 2004). They are part of the innate immune system and are responsible for the activation of immune responses like the cleavage of interleukins (Mariathasan et al. 2004; Broz and Dixit 2016).

The NLRP3-inflammasome is a subset of the Nod-like receptor (NLR) family and is the best studied inflammasome (Vanaja et al. 2015). It plays a substantial role in the activation of the effector protein caspase-1 and is therefore essential for the trauma- and pathogen-associated IL-1 $\beta$  and IL-18 maturation (Lang et al. 2018; Yang et al. 2019). This makes the NLRP3-inflammasome the key inflammasome for this thesis.

It is made up of at least three different proteins (Martinon et al. 2002). First being the NLRP3 with its pyrin-domain at the N-terminus that distinguishes the NLRP3-inflammasome from the other NLR inflammasomes (Martinon et al. 2002; Srinivasula et al. 2002). Then the ASC and the procaspase-1 (Martinon et al. 2002). The pyrin-domain promotes the assembly of the inflammasome and the ASC has the function of recruiting procaspase-1 (Srinivasula et al. 2002). The inactive procaspase-1 is recruited by the caspase-recruitment domain (CARD) which binds to the pyrin domain of the NLRP3-inflammasome via ASC, creating the active caspase-1 by autocatalysis (Lamkanfi and Dixit 2014; Mariathasan et al. 2006). Caspase-1 then cleaves pro-IL-1 $\beta$  and pro-IL-18 to the active forms being IL-1 $\beta$  and IL-18 (Li et al. 2020).

The NLRP3-inflammasome is typically formed upon two signals (Dinarello 2009). The first one being LPS, or other PAMPs or DAMPs, which lead to a signal transduction via activation of the transcription factor NF- $\kappa$ B resulting in the transcription of the NLRP3-inflammasome protein components (Dinarello 2009) (see Figure 2). The second signal being a danger signal such as extracellular ATP that binds to the P2X7 receptor and leads to the formation of the NLRP3-inflammasome (Dinarello 2009; Stoffels 2015; Dinarello 2018) (see Figure 2). ATP can be released by injured cells or cells exposed to stress, also being mechanical stress (Grierson and Meldolesi 1995; Rathinam et al. 2012). Likewise, ATP and further danger signals have shown to induce a K<sup>+</sup>-efflux, reducing the cytosolic K<sup>+</sup>-concentration (Perregaux and Gabel 1994; Lang et al. 2018; Kahlenberg and Dubyak

2004; Pétrilli et al. 2007). It is thought that the NLRP3-inflammasome detects danger signals or cell injury upon a change in  $K^+$ -concentration in the cytosol (Pétrilli et al. 2007).

This is also seen with the bacterial exotoxin nigericin, that causes pores in the cell membrane, through which an ionic current, independent of the P2X7 receptor, is present (Greaney et al. 2015). The ionic current results in a reduction of intracellular  $K^+$  and also activates the NLRP3-inflammasome (Greaney et al. 2015). Further substances and processes can also act as a second signal including double-stranded ribonucleic acid (RNA) and lysosome damage (Li et al. 2020).

## 1.5 Interleukin-1 $\beta$ and Interleukin-18

IL-1 $\beta$  and IL-18 are secreted following various different steps mentioned in the previous chapters (see Figure 2). This thesis mainly considers the IL-1 $\beta$  cytokine. IL-1 $\beta$  is the substance quantitatively measured in the supernatants of the cells in most of the experiments performed. Therefore, the importance of this cytokine is emphasized at this point. IL-18 is only briefly mentioned at the end since it is not of high relevance for this thesis.

**IL-1 $\beta$**  is a pro-inflammatory inflammasome-dependent cytokine, that belongs to the IL-family (Lee et al. 2016). Apart from the  $\beta$  version, an  $\alpha$  version is known, which belongs to the same family as well as interleukin-receptor antagonist (IL-1Ra), IL-18 and 7 further cytokines (Dinarello 2018a; Garlanda et al. 2013). Interleukin-1 $\alpha$  (IL-1 $\alpha$ ) and IL-1 $\beta$  both bind to the interleukin-1 receptor (IL-1R) and mediate a similar response (Singh et al. 2019). Meaning both interleukins play an important role in inflammatory processes, however IL-1 $\beta$  has an effect primarily systemically and IL-1 $\alpha$  more locally since it is secreted by tissue macrophages (Galozzi et al. 2021). There are 10 receptors that belong to the interleukin-1-receptor (IL-1R) family, IL-1 $\beta$  however binds to interleukin-1 receptor 1 (IL-1R1) and interleukin-1 receptor 2 (IL-1R2) directly and interleukin-1 receptor 3 (IL-1R3) acts as a coreceptor, that is important for the signaling function (Boraschi et al. 2018). IL-1Ra is a natural IL-1R antagonist, inhibiting an interaction between IL-1 $\beta$  and IL-1R (Ren and Torres 2009).

IL-1 $\beta$  is produced by cells from the innate and acquired immune system such as activated monocytes, macrophages as well as natural killer cells, neutrophilic granulocytes and B-

lymphocytes (Dinarello et al. 2012; Stoffels et al. 2015). IL-1 $\beta$  is made from an inactive form called pro-IL-1 $\beta$  via proteolytic cleavage by the enzyme caspase-1, see chapter 1.4 (March et al. 1985; Kostura et al. 1989; Garlanda et al. 2013).

When IL-1 $\beta$  is released, numerous effects are seen, such as the release of IL-2 and IL-6, as well as granulocyte-colony stimulating factor (G-CSF), tumor necrosis factor  $\alpha$  (TNF $\alpha$ ) and chemokines which additionally stimulate the bone marrow, releasing neutrophilic granulocytes and thrombocytes (Crown et al. 1993; Garlanda et al. 2013). Furthermore, an upregulation of the gene expression as well as the synthesis of cyclooxygenase-2 (COX-2) and the inducible NO-synthase is seen. This results in the increased release of NO and prostaglandin E<sub>2</sub> (Busse and Mülsch 1990; Barberà-Cremades et al. 2012). NO leads to vasodilation and hypotension (Busse and Mülsch 1990). The elevated level of prostaglandin E<sub>2</sub> in the brain results in an upregulation of the nominal temperature, resulting in a fever (Barberà-Cremades et al. 2012).

IL-1 $\beta$  on the one hand has the important role of defending against infection (Garlanda et al. 2013). On the other hand, the dysregulated release can lead to systemic diseases such as gout, rheumatic diseases, sepsis as well as chronic inflammatory bowel diseases (Ren and Torres 2009; Dinarello et al. 2012; Ozaki et al. 2015; Bank et al. 2019; Geyer and Müller-Ladner 2010; Li et al. 2016). Therefore, the release of IL-1 $\beta$  needs to be strictly regulated (Dinarello 2018a). As mentioned in the previous chapters, only after having recognized two potential danger signals IL-1 $\beta$  is released, giving the IL-1 $\beta$  secretion a control mechanism (Stoffels et al. 2015; Dinarello 2009). When the IL-1 $\beta$  producing cells are confronted with a danger signal, pro-IL-1 $\beta$  is produced and accumulates in the cytosol (Dinarello 2018a). For the maturation of pro-IL-1 $\beta$ , a second danger signal, is often needed, which leads to the activation of the NLRP3-inflammasome (see Figure 2) (Dinarello 2018a). Caspase-1 then, as mentioned before, leads to the proteolysis of pro-IL-1 $\beta$  to mature IL-1 $\beta$  that can then be secreted, however the exact secretion process is controversial and still being discussed (Lopez-Castejon and Brough 2011).

A further regulatory component of the IL-1 $\beta$  release is the IL-1R antagonist (Dinarello et al. 2012). Different medicines targeting IL-1 $\beta$  dysregulated diseases have been developed since 1993. Anakinra for example is a IL-1Ra and therefore prevents the activity of IL-1 $\alpha$  and IL-1 $\beta$  and is used for different autoinflammatory diseases (Ramírez and Cañete 2018).

**IL-18** has many similarities to IL-1 $\beta$ . First, it belongs to the same IL-family and is also a pro-inflammatory cytokine that plays a crucial role in regulating the immune system (Gracie et al. 1999). IL-18, as well as IL-1 $\beta$ , is synthesized as an inactive precursor, that is cleaved by caspase-1 into the active IL-18 form (Gu et al. 1997). Therefore, the NLRP3-inflammasome is also relevant for IL-18 (Gu et al. 1997). A lot of cells have the capability to produce IL-18 in response to infection, inflammation or cellular stress, however monocytes and macrophages are mainly known to do so (Yasuda et al. 2019).

Furthermore, IL-18 can modulate the acquired and the innate immune system (Wawrocki et al. 2016). It has shown to promote and suppress inflammation, making it a complex regulator of the immune response (Gracie et al. 1999; Wawrocki et al. 2016). The dysregulation of the IL-18 release can, as with IL-1 $\beta$ , be implicated in a variety of immune-related diseases, including infectious diseases, cancer or autoimmune disorders, like rheumatoid arthritis (Baker et al. 2019). IL-18 signals through the receptor interleukin-18 receptor (IL-18R), which is expressed on various immune cells, including T-cells and monocytes (Wiley and Winkles 2003). Once IL-18 binds to the receptor, it activates a signal cascade that results in the production of other cytokines, such as interferon- $\gamma$  (INF- $\gamma$ ) and the activation of immune cells (Wiley and Winkles 2003). Research on IL-18 is ongoing, therefore a better understanding may lead to the development of new therapies for a range of diseases.

## **1.6 Cholinergic system**

The previous chapters have focused on the maturation and the signal cascades involved in the maturation and release of IL-1 $\beta$ . In the following chapter, one of the inhibition mechanisms of the ATP-dependent maturation and release of IL-1 $\beta$  will be viewed, being the cholinergic system. In figure 3, the nicotinic acetylcholine receptor (nAChR) with its subunits is shown as a pentamer. On activation of the nAChR via for example the agonist

acetylcholine (ACh), the P2X7 receptor is blocked and the IL-1 $\beta$  secretion inhibited. All steps in detail will be looked at in the following passages.

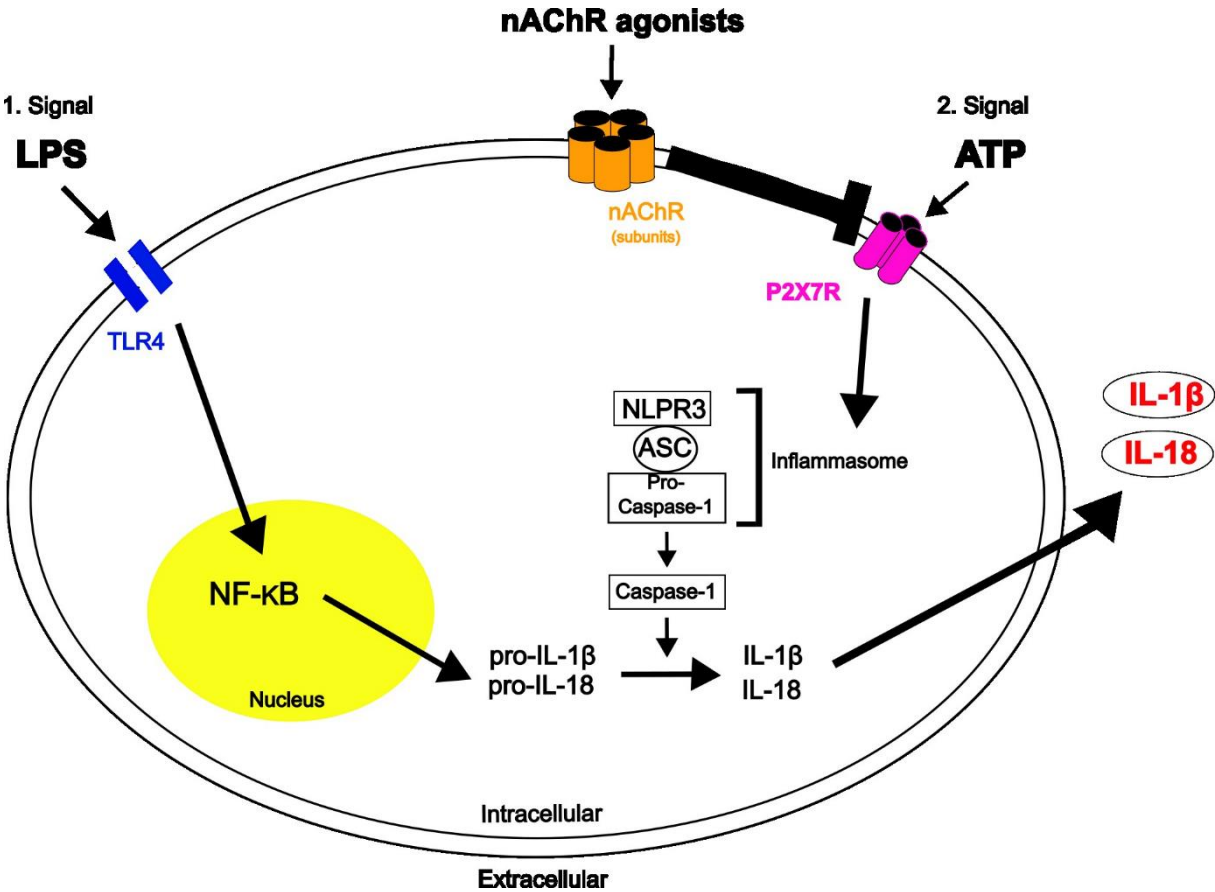


**Figure 3. Schematic overview of the cholinergic inhibition of the adenosine triphosphate (ATP)-mediated interleukin-1 $\beta$  (IL-1 $\beta$ ) and interleukin-18 (IL-18) release.** For the release of mature IL-1 $\beta$  and IL-18, two signals are needed. The first danger signal lipopolysaccharide (LPS) leads to the activation of the toll-like receptor 4 (TLR4) and induces the expression of the precursor protein pro-IL-1 $\beta$  through activation of the transcription factor nuclear factor  $\kappa$ B (NF- $\kappa$ B). The second signal extracellular ATP activates the P2X7 receptor and leads to the assembling of the NLRP3-inflammasome, consisting of NLRP3, apoptosis-associated speck like protein (ASC) and pro-caspase-1. This, activates caspase-1 which induces the cleavage of pro-IL-1 $\beta$  and pro-IL-18 to mature IL-1 $\beta$  and IL-18, that can then be released. The activation of the nicotinic acetylcholine receptor (nAChR) with its subunits  $\alpha$ 7,  $\alpha$ 9/ $\alpha$ 10 leads to an inhibition of the ATP-sensitive P2X7 receptor. Hence, the maturation of IL-1 $\beta$  and IL-18 is inhibited.

ACh is one of the oldest identified neurotransmitters (Tansey 2006). In the early 1900s, a substance, later identified as being ACh, was shown to reduce heart muscle tone and stimulate the smooth muscle of the intestine (Tansey 2006). Today, ACh is not only known to be a neurotransmitter, but also an immune system modulator (Olofsson et al. 2012; Cox et al. 2020). Therefore, it is not only found in neuronal cells but also released by non-neuronal cells such as lymphocytes and endothelial cells (Kawashima et al. 2015). ACh of neuronal origin, on the one hand, showed an anti-inflammatory effect in macrophages, by inhibiting the release of TNF $\alpha$  (Borovikova et al. 2000). On the other hand, recent studies have shown that non-neuronal ACh also plays an important role in the regulation of the immune system (Gwilt et al. 2007; Fujii et al. 2017; Borovikova et al. 2000). Furthermore, muscarinic and nicotinic ACh receptors were first found on immune cells in the 1970s, indicating a cholinergic system independent of the nervous system (Kawashima and Fujii 2000; Neumann et al. 2007). Research today shows, that nicotinic ACh receptors (nAChRs) are found in the central and peripheral nervous system, the immune system as well as in muscle tissue and others (Fujii et al. 2017). It is made up of 5 subunits arranged circularly creating an intramembrane channel (Fujii et al. 2017). Depending on the tissue, the constellation of subunits varies (Cascio 2004). It can either consist of heteromeric or homomeric subunits (Cascio 2004). The known subtypes are:  $\alpha$  ( $\alpha$ 1-10),  $\beta$  ( $\beta$ 1-4),  $\gamma$ ,  $\delta$  and  $\epsilon$  (Fujii et al. 2017). In immune cells the receptor can be made up of the subunits  $\alpha$ 7,  $\alpha$ 9/10, which is important for this thesis (Hecker et al. 2015; Zoli et al. 2018).

Further studies have shown that the nAChR and the P2X7 receptor can interact, the exact mechanism however remains unknown (Di et al. 2018; Richter et al. 2016). The activation of the neuronal ionotropic nAChR leads to an increase in permeability for specific cations like mainly Ca<sup>2+</sup> which leads to a cell membrane depolarization following intracellular signaling pathways (Albuquerque et al. 2009). However, in non-neuronal nAChRs an ionotropic function has not been seen, a metabotropic function is rather assumed (Hecker et al. 2015; Richter et al. 2018; Zakrzewicz et al. 2017). This metabotropic activation then leads to an inhibition of the P2X7 receptor, which then is not able to react to ATP in an ionotropic manner (Hecker et al. 2015; Richter et al. 2016).

Recent studies lead to the conclusion that further substances having a choline group like phosphocholine (PC), phosphatidylcholine, or are PC-modified, have a similar anti-inflammatory effect to ACh, however do not show an ionotropic effect at conventional nAChRs (Hecker et al. 2015; Richter et al. 2016). Further cholinergic agonists are C-reactive protein (CRP), dipalmitoylphosphatidylcholine (DPPC) and glycerophosphocholine (GPC) (Hecker et al. 2015; Richter et al. 2016). These agonists bind to the nAChR and lead to an inhibition of the BzATP-dependent NLRP3-inflammasome activation and therefore lead to an inhibition of the IL-1 $\beta$  release (Hecker et al. 2015; Richter et al. 2016; Backhaus et al. 2017). This was seen in different experiments. First, the primary danger signal being LPS was added to the cells, which induced the intracellular concentration of pro-IL-1 $\beta$  (Hecker et al. 2015; Richter et al. 2016). After the addition of BzATP, being the second stimulus, a higher concentration of IL-1 $\beta$  was measured in the cell supernatant (Hecker et al. 2015; Richter et al. 2016). However, after the addition of ACh, the IL-1 $\beta$  concentration was reduced in the cell supernatant (Hecker et al. 2015; Richter et al. 2016).

ACh and PC both unfold their effect via all 3 subunits  $\alpha 7$ ,  $\alpha 9$  and  $\alpha 10$  of the nAChR. DPPC and GPC for example depend on  $\alpha 9$  and  $\alpha 10$  nAChRs but can act independently of the subunit  $\alpha 7$  (Backhaus et al. 2017; Hecker et al. 2015; Zakrzewicz et al. 2017). In order to understand on which subunit a substance exerts its effect, the conopeptide ArIB, as an antagonist for the subunit  $\alpha 7$ , as well as the conopeptide RgIA4 as an antagonist for the subunits  $\alpha 9/\alpha 10$ , have been used in the past research and will be used for the experiments in this thesis (Grau et al. 2018). The experiments are performed on cells such as human peripheral blood mononuclear cells (hPBMCs), mouse peripheral blood mononuclear cells (mPBMCs) and mouse BMDMs. Additionally, gene-deficient free fatty acid receptor 2 (FFA2) mice are used for the experiments and reporter mice for the staining.

This cholinergic inhibition mechanism is used by invading pathogens (Grabitzki et al. 2008). Some bacteria and parasites such as protozoa secrete PC-modified macromolecules (Grabitzki et al. 2008). Furthermore, some pathogens use PC-modified cell membrane components from the host (Grabitzki et al. 2008). By using this PC group, the pathogens can inhibit and modify the immune system, since the cholinergic substance inhibits the IL-1 $\beta$  secretion in monocytes (Grabitzki et al. 2008). This enables the

pathogens to reduce inflammation and therefore escape an immune response making an intrusion easier (Grabitzki and Lochnit 2009).

### **1.7 Short-chain fatty acids (SCFAs)**

A fatty acid is a carboxylic acid with an aliphatic chain (Layden et al. 2013). It can be saturated or unsaturated and is organic (Layden et al. 2013). Different classification methods are used (Layden et al. 2013). In this thesis, the number of carbon atoms determines the classification. If the aliphatic tail has 5 carbon atoms or less, it is called a SCFA (Cifuentes 2013). At 6-12 carbon atoms the fatty acid would belong to the medium group (Layden et al. 2013). 13-21 carbon atoms are called long-chain fatty acids (Layden et al. 2013). 22 or more carbon atoms belong to the very long chain fatty acids (Moss et al. 1995; Layden et al. 2013) SCFAs are typically saturated (Cifuentes 2013). The three most common SCFAs are: acetate, butyrate and propionate, which are present in the human gut (Wong et al. 2006). The molar ratio they are found in is 60:20:20, respectively, however differences may occur (Cummings 1981).

SCFAs are the result of intestinal microbial fermentation of indigestible foods (Brody 1999). When a human being eats dietary fiber or resistant starches like complex carbohydrates that cannot be fully broken down by digestive enzymes and are resistant to hydrolysis, the components reach the colon for fermentation (Wong et al. 2006). Primarily in the proximal colon, the fiber, being a substrate, is fermented by specific anaerobic bacteria of the genus *Bacteroides*, *Clostridium*, *Lactobacillus* and others (Wong et al. 2006). The result of the fermentation process are the SCFAs, gases such as CO<sub>2</sub>, CH<sub>4</sub> and H<sub>2</sub> as well as heat (Topping and Clifton 2001). The rate and amount of SCFAs produced is determined by various different factors (Roberfroid 2007). One being the amount and species of microflora present in the colon (Roberfroid 2007). Then, the origin of the fiber and the time needed to pass through the intestine (Roberfroid 2007; Cook 1998; Agrenzio and Southworth 1975). The substrates transiting the intestine may also have an influence on the population and species of bacteria in the gut (Savage 1986).

The absorption of the SCFAs is very efficient (McNeil et al. 1978). Only about 5-10% are excreted (McNeil et al. 1978). Thus, the SCFAs are absorbed into the colonocytes, which are cells lining the colon, via anion exchange or diffusion of protonated SCFAs

(Besten et al. 2013; Birt et al. 2013). Furthermore, the SCFAs are used as an energy source by the colonocytes or enter the bloodstream via the portal vein and then are used as an energy source by other organs like the liver or muscles (Wong et al. 2006; Besten et al. 2013; Birt et al. 2013).

The functions of SCFAs are broad and generally crucial for gastrointestinal health (Canfora et al. 2015). Therefore, alterations in the composition and quantity of the microflora in the gut, consequently leads to a change in the concentration of the production of SCFAs (Maslowski et al. 2009). This has thought to lead to the development of illness such as inflammatory bowel disease (IBD), colon cancer, obesity and diabetes mellitus type 1 and 2 (Maslowski et al. 2009; Filippo et al. 2010). SCFAs are known to be regulators in proliferation, gene expression and differentiation (Corrêa-Oliveira et al. 2016). Furthermore, they have an influence on the pH level as well as cell volume (Cook 1998). Therefore, they indirectly have an impact on the composition of the microflora present in the colon, since depending on the pH level different bacteria are found (Roberfroid 2007; Vince et al. 1978; Jenkins et al. 1987). A further function is the ability of SCFAs to affect the production of lipids and vitamins (Byrne et al. 2015). Recent studies show that SCFAs have an impact on cardiometabolic health and appetite, as well as mental health and mood (Mueller et al. 2020; Merchak and Gaultier 2020). They are also thought to lower blood pressure in experimental animals (Marques et al. 2017). A further relevant function of SCFAs is its involvement in immune responses (Ramos et al. 2002; Bailón et al. 2010). Fatty acids can induce apoptosis in a variety of immune cells (Ramos et al. 2002; Bailón et al. 2010).

The first discovery in 1813, that a so-called “acide grass” may exist, was made by a Frenchman called Michel Eugène Chevreul (Chevreul 1813). In the early 20th century, a man called Maurice Hanriot identified fatty acids in horse feces (Hanriot 1911). After further decades of research, in the 1960s, the Japanese men Joij Suzuki and Shigeru Mitsuoka studied the effects of SCFA on gut health and the microbiome. Today, the research on the role of SCFAs in humans’ health and disease, as well as the potential as a therapeutic target for a variety of conditions is ongoing. Therefore, in this thesis, experiments on the effect of SCFAs in the secretion of IL-1 $\beta$  were conducted.

**Acetate** chemically consists of 2 carbon atoms (C<sub>2</sub>) and is therefore the shortest of the 3 SCFAs mentioned in this thesis (Brody 1999; Martin-Gallausiaux et al. 2021). It is also

the principal SCFA in the colon (Brody 1999). Acetate does primarily not stay in the colon for metabolization, but is easily absorbed, predominantly enters the portal vein and is primarily transported to the liver (Canfora et al. 2015). Therefore, acetate is the main SCFA in the human blood and is used to monitor colonic function (Cook 1998). Organs with cells that have the enzyme acetyl-CoA synthetase are able to use acetate as an energy source for lipogenesis (Canfora et al. 2015). Furthermore, acetate is also used in the cholesterol synthesis (Wolever et al. 1989).

Acetate has shown to be involved in metabolic regulation (Martin-Gallausiaux et al. 2021). It is known that acetate has an influence on the lipid metabolism and glucose homeostasis (Canfora et al. 2015). Therefore, recent studies suggest that acetate plays a role in body weight control and insulin sensitivity (Hernández et al. 2019; Tripolt et al. 2013).

Another important function recently discovered, is the role of acetate in neuroinflammation, which itself is associated to the Alzheimer's disease (Liu et al. 2020). This fatty acid is able to pass the blood brain barrier and has shown to have an anti-inflammatory effect on the brain (Liu et al. 2020). In studies performed on the mouse, first indications were seen, that acetate can inhibit the activation of microglia and therefore the production of pro-inflammatory cytokines (Liu et al. 2020).

The anti-inflammatory effect is not only seen in the brain but also in the gut, where acetate promotes the production of anti-inflammatory cytokines (Deleu et al. 2023). Acetate can also induce the growth of beneficial bacteria and inhibit the growth of pathogenic bacteria in the colon (Martin-Gallausiaux et al. 2021; Deleu et al. 2023). Moreover, the fatty acid is able to enhance the barrier function of the colon, that helps reduce the risk of permeability-associated diseases such as food allergies (Roberfroid 2007; Deleu et al. 2023). A broad number of studies have been done and still being performed on the functions of acetate as well as the other SCFAs. Only some will be mentioned in this thesis.

**Butyrate** is the SCFA consisting of 3 carbon atoms (C3) (Brody 1999; Martin-Gallausiaux et al. 2021). The colonocytes, which are epithelial cells of the colon, use butyrate as the favored energy source to create ATP, even compared to glucose supplied by the blood (Fleming and Floch 1986). Therefore, butyrate is metabolized by the

colonocyte to a high percentage: 70% to 90%, compared to the other SCFAs (Cook 1998; Martin-Gallausiaux et al. 2021).

This fatty acid also plays a role in the regulation of cell proliferation and differentiation, giving it a very important function in the health of the colon (Roberfroid 2007; Topping and Clifton 2001; Cook 1998). Butyrate has shown a stronger antiproliferative effect compared to acetate and propionate (Bornet et al. 2002). In animals and cell line studies, a preventive effect on colon cancer and also the development of adenomas has been observed (Bornet et al. 2002; Hague et al. 1995). The exact mechanism of the inhibitory effect considering the cell proliferation has not yet been fully understood. There are studies showing that butyrate leads to an induction of ICAM-1 messenger RNA (mRNA) and p21<sup>WAF1/Cip1</sup> levels which then leads to a cell cycle arrest at stage G1, resulting in a cell proliferation inhibition (Scheppach and Weiler 2004). This arrest at G1 may allow DNA checkpoint-mediated repair of possible mutations (Scheppach and Weiler 2004; Archer et al. 1998). Furthermore, butyrate inhibits the histone deacetylase, inducing apoptosis and also leading to a different confirmation of the DNA, enabling possible DNA damage to be repaired by repair enzymes (Sealy 1978; Grunstein 1997). The so-called butyrate paradox describes that butyrate on the one hand leads to cell stimulation in colonocytes and on the other hand has the ability of suppressing the proliferation of adenocarcinoma cells in the colon (Lupton 2004). The paradox can occur due to different factors, such as the amount and source of butyrate administered as well as at what stage of cancer butyrate is given (Lupton 2004).

Butyrate has a similar anti-inflammatory effect in the gut, compared to acetate mentioned above (Martin-Gallausiaux et al. 2021; Tedelind et al. 2007). Not only does butyrate reduce inflammation in the colon, it also does so in other parts of the body, primarily by promoting the production of anti-inflammatory cytokines and therefore inhibiting the production of pro-inflammatory cytokines (Tedelind et al. 2007).

Another similarity seen in all SCFAs, but especially in acetate and butyrate is the function to strengthen the intestinal barrier (Peng et al. 2009; Bach et al. 2018). This is done for example by increasing the production of mucus and also the production of tight junction proteins (Bach et al. 2018; Peng et al. 2009). The barrier in the intestine is important to prevent specific substances from entering the blood stream (Peng et al. 2009). Therefore,

the function of strengthening this barrier stops harmful substances passing, preventing specific diseases of the gut (Peng et al. 2009).

**Propionate** is the longest SCFA used for experiments in this thesis. It consists of 4 carbon atoms (C4) (Martin-Gallausiaux et al. 2021; Brody 1999). There are 2 main ways of production (Hosseini et al. 2011). First being the formation of succinate that is then decarboxylated (Hosseini et al. 2011). The second is called the “acrylate pathway”, here propionate is produced from lactate or acrylate (Cummings 1981; Hosseini et al. 2011). Research shows that propionate is better absorbed in the colon than acetate is (Dawson et al. 1964; Wong et al. 2006). Furthermore, propionate is extracted to a higher percentage by the liver than acetate, during one single pass (Peters et al. 1992; Wong et al. 2006). Propionate is used as a substrate for gluconeogenesis in the liver, however studies also report the opposite effect (Baird et al. 1980; Verbrugghe et al. 2012). Propionate also inhibits gluconeogenesis (Baird et al. 1980; Verbrugghe et al. 2012). The exact mechanism in this area remains unknown. In various studies propionate shows a lipid lowering effect (Venter et al. 1990). It is thought, that the higher production of propionate through fermentation leads to an inhibition of the hepatic cholesterol synthesis (Venter et al. 1990).

On the one hand, both butyrate and propionate have an anti-inflammatory effect (Filippone et al. 2020). They lead to a reduction of chemokine production in immune cells which therefore suppresses the recruitment of immune cells such as monocytes and neutrophils (Filippone et al. 2020). On the other hand, however research shows that SCFAs are able to induce the migration of immune cells to the site of infection (Vinolo et al. 2009; Niedermann et al. 1997). This opposing observation has not yet been fully understood.

Recent studies performed only with propionate show the influence of this SCFA on appetite and metabolism (Chambers et al. 2015). Propionate stimulated the release of glucagon-like peptide-1 (GLP-1) and peptide YY (PYY) in human colonic cells (Chambers et al. 2015). These hormones are known to play a role in appetite regulation and glucose homeostasis (Chambers et al. 2015). The study shows a reduced weight gain in overweight human adults (Chambers et al. 2015). Propionate has also shown to improve insulin sensitivity, therefore a possible treatment in diseases like diabetes type 2 is plausible (Chambers et al. 2015).

A further effect propionate has shown on the human body is the reduction of cholesterol levels in the blood, as well as a reduction of the blood pressure (Tang et al. 2013). These factors have a positive influence on cardiovascular health (Tang et al. 2013).

Similar to both other SCFAs, propionate has an important role in regulating immune functions (Gonçalves et al. 2018). This immunomodulatory effect may help to prevent or treat autoimmune diseases (Gonçalves et al. 2018). Propionate has shown to influence the promotion of regulatory T-cells (Treg) which helps reduce the extreme immune responses and therefore prevent autoimmune disease (Arpaia et al. 2013). Further important functions, such as the regulation of cytokine production, maintenance of the gut barrier and the regulation of immune cell migration are attributed to propionate, which will not be discussed in more detail at this point (Peng et al. 2009; Gonçalves et al. 2018).

## 1.8 FFA2/FFA3

After having gone through the function of the SCFAs generally and each SCFA specifically, this chapter will look at the fatty acid receptors. The exact signal transduction is not yet fully understood. In the experiments of this thesis, the role of the SCFAs on the IL-1 $\beta$  secretion via FFA2 and free fatty acid receptor 3 (FFA3) in hPBMCs and mPBMCs as well as mouse BMDMs will be looked at.

FFA2 and FFA3 belong to a big family of G-protein coupled receptors (GPRs) and are also known as GPR43 and GPR41 (Ximenes et al. 2007). The receptors are encoded by the *FFAR2* and *FFAR3* genes (Sawzdargo et al. 1997). When the receptors were first discovered, they were named “orphan receptors” since it was not yet known what ligands activate the receptors (Pierce et al. 2002). However, both receptors display a structure that is typical for GPRs (Hara et al. 2013; Brown et al. 2003). An N-terminus with cysteine residues is found on the extracellular side of the membrane, which is important for the binding of ligands (Brown et al. 2003). Intracellularly, a C-terminus with regulatory domains is found, that shows importance in downstream signaling pathways (Brown et al. 2003; Ulven 2012). The most typical structure known for FFA2 and FFA3 is the 7 transmembrane  $\alpha$ -helical bundle (Hara et al. 2013; Brown et al. 2003; Ulven 2012).

FFA2 and FFA3 are expressed on various different cells throughout the body, however FFA3 seems to be more widely spread (Maslowski et al. 2009). They are found on for

example immune cells such as monocytes, enteroendocrine cells and enterocytes (Maslowski et al. 2009). The highest expression of FFA2 is found on monocytes and neutrophils (Maslowski et al. 2009; Tolhurst et al. 2012). However, the measurement of the expression level is based on mRNA measurements, therefore the values may not correlate with the actual protein expression (Tolhurst et al. 2012; Maslowski et al. 2009; Kimura et al. 2013). The expression of FFA2 has seen to change in response to for example inflammation (Ang et al. 2015). In monocytes, treatment with LPS or TNF $\alpha$  can lead to an upregulation of FFA2 expression (Ang et al. 2015). The ligands for FFA2 and FFA3 are SCFAs (Brown et al. 2003). This discovery was made by 3 different research groups simultaneously in 2003. Though further studies show that FFA2 is activated more by acetate and propionate and FFA3 on the other hand is activated most by butyrate and propionate (Brown et al. 2003).

After the binding of SCFAs, the FFA2 and/or FFA3 are activated (Brown et al. 2003). A complex signal cascade follows this activation (Brown et al. 2003). Until today, the exact signaling pathway remains partly unknown. However, in the following, only a few discovered steps will be mentioned (Le Poul et al. 2003). Starting with the activation of guanine nucleotide binding proteins (G-proteins) (Le Poul et al. 2003; Katritch et al. 2013). It is thought, that the signal pathway of FFA2 and FFA3 may differ, resulting in the activation of different G-proteins (Katritch et al. 2013). For example, the G $\alpha_{i/o}$  and G $\alpha_{q/11}$  pathway (Le Poul et al. 2003; Katritch et al. 2013). FFA2 is thought to be capable of dual signaling (Le Poul et al. 2003). The activation of the FFA3 leads to an inhibition of the adenylyl cyclase activity which reduces the production of cyclic AMP (cAMP) (Le Poul et al. 2003). The activation of one of the G-protein family (G $_q$ ) leads to the increase of intracellular Ca<sup>2+</sup> levels and the activation of the extracellular-signal regulated kinases (ERK1/2) cascade (Le Poul et al. 2003). Additionally, the FFA2/3 can lead to an activation of further intracellular signaling pathways such as those mediated via  $\beta$ -arrestin, which can lead to cellular processes like the migration of cells or the rearrangement of the cytoskeleton as well as inactivation of NF- $\kappa$ B and therefore a reduced expression of pro-inflammatory cytokines (Le Poul et al. 2003; Kimura et al. 2013; Lee et al. 2013; Ang et al. 2018). A potent FFA2 activator 4-chloro- $\alpha$ -(1-methylethyl)-N-2-thiazolylbenzeneacetamide (4-CMTB) is reported to activate the G $\alpha_{i/o}$  and G $\alpha_{q/11}$  pathway (Lee et al. 2008). Furthermore, studies show that the FFA2 and FFA3

are able to interact and form a heteromeric structure showing a signaling that differs from the homomeric form (Ang et al. 2018).

Receptor knockout mice as well as mice expressing the wild-type receptors and synthetic ligands have made it able to show the broad physiological function the two receptors display (Kim et al. 2014). As mentioned above, each SCFA shows various different functions (Martin-Gallausiaux et al. 2021). These can make an impact by activating the signaling pathways of the FFA2 and FFA3, that lead to the great amount of different physiological processes (Brown et al. 2003). FFA2 and FFA3 appear to play an important role in numerous health conditions (Ulven 2012; Tolhurst et al. 2012; Nøhr et al. 2013). Here, just a few are mentioned. Beginning with cellular functions like insulin secretion, the glucose metabolism and reaching systemic functions such as appetite regulation, diabetes, asthma, hypertension, modulation of inflammatory responses, energy metabolism or gut motility and cancer (Kim et al. 2014; Ulven 2012; Tolhurst et al. 2012; Nøhr et al. 2013; Maslowski et al. 2009; Ang and Ding 2016). Most of these functions were primarily discovered through FFA2 or FFA3 deficient mice (Maslowski et al. 2009). FFA2 deficient mice showed exacerbated inflammation in different experimental models for human diseases such as colitis, arthritis and asthma, probably due to the increased production of inflammatory mediators by FFA2 deficient immune cells (Maslowski et al. 2009). A similar dysregulation was seen in mice that were devoid of bacteria, in which the production of SCFAs was little to none (Maslowski et al. 2009).

After understanding the importance of FFA2 as well as FFA3 and the influence of SCFAs on various diseases and functions, the therapeutic potential has become interesting in relation to specific diseases (Maslowski et al. 2009; Ulven 2012). FFA2 and FFA3 have therefore become a potential therapeutic target (Ulven 2012). There are several possibilities of targeting the receptors (Ulven 2012). For example, the consumption of fiber rich food or a future possibility is seen in synthetic agonists (Ulven 2012). However, experiments have already been performed using synthetic agonists in patients suffering from ulcerative colitis, but have failed to provide a clinical benefit (Namour et al. 2016). This trial showed, that multiple factors play a role in the interplay between disease and the possible therapeutic target (Namour et al. 2016). Therefore, the complex role of FFA2 and FFA3 still remains not fully understood.

## 1.9 Hypothesis

SCFAs have shown to have a significant systematic impact on physiological processes in the human body via FFA2 and/or FFA3. These functions range from strengthening the gut barrier to functions like the regulation of glucose homeostasis (Peng et al. 2009; Chambers et al. 2015). The profound influence of SCFAs on inflammation has become of interest. In past studies, a cholinergic inhibition mechanism of the ATP-induced IL-1 $\beta$  release via for example PC-modified macromolecules has been discovered (Hecker et al. 2015; Richter et al. 2016). In this present work, I use hPBMCs, mPBMCs and mouse BMDMs as well as PBMCs from FFA2 gene-deficient mice to test the following main hypothesis: the SCFAs lead to an inhibition of the ATP-induced IL-1 $\beta$  release via the activation of the cholinergic system (see figure 4).

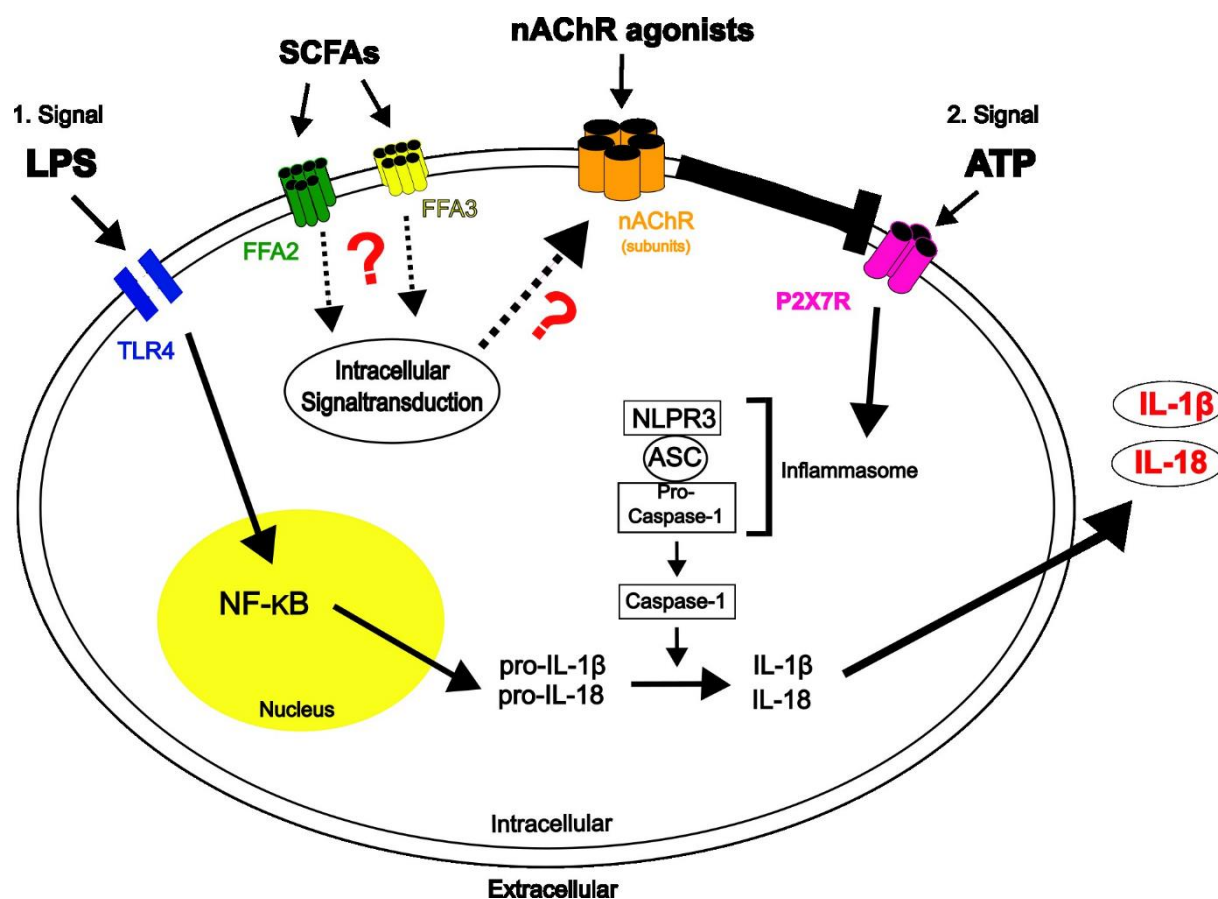


**Figure 4.** Schematic overview of the short-chain fatty acid (SCFA)-induced inhibition mechanism of the adenosine triphosphate (ATP)-mediated interleukin-1 $\beta$  (IL-1 $\beta$ ) and interleukin-18 (IL-18) release. For the release of mature IL-1 $\beta$  and IL-18,

two signals are needed. The first danger signal lipopolysaccharide (LPS) leads to the activation of the toll-like receptor 4 (TLR4) and induces the expression of the precursor protein pro-IL-1 $\beta$  through activation of the transcription factor nuclear factor  $\kappa$ B (NF- $\kappa$ B). The second signal extracellular ATP activates the P2X7 receptor and leads to the assembling of the NLRP3-inflammasome, consisting of NLRP3, apoptosis-associated speck like protein (ASC) and pro-caspase-1. This, activates caspase-1 which induces the cleavage of pro-IL-1 $\beta$  and pro-IL-18 to mature IL-1 $\beta$  and IL-18, that can then be released. In the following, the hypothesis of this thesis is displayed. This signal path is inhibited by SCFAs that lead to an intracellular signal transduction via free fatty acid receptor 2 and 3 (FFA2, FFA3) and guanin nucleotide binding proteins (G<sub>q</sub>, G<sub>i</sub>). This leads to an activation of the nicotinic acetylcholine receptor (nAChR) with its subunits  $\alpha$ 7,  $\alpha$ 9/ $\alpha$ 10 and therefore, an inhibition of the ATP-sensitive P2X7 receptor. Hence, the maturation of IL-1 $\beta$  and IL-18 is inhibited. Modified according to (Siebers et al. 2018; Dinarello 2009; Hecker et al. 2015; Richter et al. 2016; Zakrzewicz et al. 2017; Backhaus et al. 2017; Grau et al. 2018).

## 2. Materials and Methods

### 2.1 Materials and Chemicals

2.1.1 Reagents	Manufacturer
4-CMTB (4-chloro- $\alpha$ -(1-methylethyl)-N-2-thiazolylbenzeneacetamide)	Tocris Bioscience, Tocris House, Bristol, UK #4642
5-BDBD (5-(3-Bromophenyl)-1,3-dihydro-2H-Benzofuro[3,2-e]-1,4-diazepin-2)	Tocris Bioscience #3579
A 438079 hydrochloride	Bio-Techne/ Tocris, Minneapolis, MN, USA #2972
Acetate (sodium acetate trihydrate, Emsure <sup>®</sup> )	Merck #1.06267.0500
Agarose (UltraPure <sup>™</sup> )	Invitrogen <sup>™</sup> , Thermo Fisher Scientific, Waltham, MA, USA #16500-100
Aqua dest. (Aqua destillata)	B. Braun, Melsungen, Germany
Aqueous mounting medium; Fluoromount <sup>™</sup>	Sigma-Aldrich Chemie #F4680
AR420626	Tocris Bioscience #6163
ArIB	J. Michael McIntosh, Salt Lake City, UT, USA Provided in the context of a cooperation.
ATP (Adenosine triphosphate)	Sigma-Aldrich Chemie #A2383
BSA (Bovine serum albumin)	Sigma-Aldrich Chemie #A9418
Butyrate (sodium butyrate)	Merck #8.20236.0250
BzATP (2'(3')-O-(4-Benzoylbenzoyl) adenosine 5'-triphosphate triethylammonium salt)	Jena BioScience, Jena, Germany #NU-1620-5
Chloroform	Merck #67663

DAB (3,3'-Diaminobenzidinetetrahydrochloride)	Sigma-Aldrich Chemie #SLBF8928V
DMSO (Dimethyl sulfoxide)	Sigma-Aldrich Chemie #D5879
DNA loading dye	Thermo Scientific, Schwerte, Germany #R0611
Ethanol	Merck #32205
<u>Ethylenediamine tetraacetic acid</u> (EDTA)	Carl Roth, Karlsruhe, Germany #6381-92-6
Fast Blue BB salt	Sigma-Aldrich Chemie #5486-84-0
FCS (Fetal bovine serum)	Cell Concepts, Umkirch, Germany #S-EUR30-I
Ficoll Paque (Leukosep™ tube) 50 ml	Greiner Bio-One, Frickenhausen, Germany #227288
GelRed™ Nucleic Acid Gel Stain	Biotium, Fremont, CA, USA #41003
GeneRuler 100bpPlus DNA Ladder	Thermo Scientific, Schwerte, Deutschland #SM0323
Glycergel	Dako, Glostrup, Denmark #11206547
H <sub>2</sub> O <sub>2</sub> (Hydrogen peroxide 30%)	Merck #107209
Haematoxylin	Merck #15938
HCl (Hydrochloric acid)	Merck #H1758
Heparin-Natrium-25000-ratiopharm®	Ratiopharm®, Ulm, Germany
High purity HPLC (high performance liquid chromatography) water	Merck #1.15333.1009
HRP (Horseradish peroxidase)	Merck #9003-99-0
INF-γ (Recombinant mouse interferon-γ)	Merck # IF005

Isoflurane	Sigma-Aldrich Chemie #26675-46-7
Isopropanol	Sigma-Aldrich Chemie, Steinheim, Germany #33539
KAl(SO <sub>4</sub> ) <sub>2</sub> (potassium alum)	Merck, Darmstadt, Germany #1042
KCl (potassium chloride)	Merck #7447-40-7
KH <sub>2</sub> PO <sub>4</sub> (Monopotassium phosphate)	Sigma-Aldrich Chemie #7758-11-4
Levamisole	Sigma-Aldrich Chemie #16595-80-5
LPS (Lipolysaccharide from E. coli O26:B6)	Sigma-Aldrich Chemie #L2654
MAM (Monocyte attachment medium)	PromoCell, Heidelberg, Germany #C-28051
M-CSF (Macrophage colony-stimulating factor human 10 ng/ml)	Sigma-Aldrich Chemie #SRP3110
Na <sub>2</sub> HPO <sub>4</sub> (Disodium phosphate)	Sigma-Aldrich Chemie #7558-79-4
NaCl (sodium chloride)	Sigma-Aldrich Chemie #31434
NaH <sub>2</sub> PO <sub>4</sub> (Monosodium phosphate)	Sigma-Aldrich Chemie #7558-80-7
NaIO <sub>3</sub> (sodium iodate)	Merck #6525
NaN <sub>3</sub> (sodium azide)	Merck #26628-22-8
NaOH (sodium hydroxide)	Merck #1310-73-2
Naphtol-AS-MX phosphate powder	Sigma-Aldrich Chemie #1596-56-1
N-Dimethylformamide (C <sub>3</sub> H <sub>7</sub> NO)	Sigma-Aldrich Chemie #68-12-2
Nigericin sodium salt	Sigma-Aldrich Chemie #N7143
NMS (Normal mouse serum)	Sigma-Aldrich Chemie #M5905
Paraffin	Merck #8002-74-2

Paraformaldehyde	Sigma-Aldrich Chemie #3052-5-89-4
PBS (Dulbecco's phosphate buffered saline)	Sigma-Aldrich Chemie #D8537
PenStrep (Penicillin Streptomycin solution)	Gibco™, Thermo Fisher Scientific, Waltham, Massachusetts, USA #15140-122
Percoll™	GE Healthcare Bio-Sciences AB, Uppsala, Sweden #17-0891-02
Propionate (sodium propionate)	Sigma-Aldrich Chemie #P1880-500G
Protease (from Streptomyces griseus)	Sigma-Aldrich Chemie #P5147
RCB (Red blood cell lysis buffer)	BioLegend®, San Diego, CA, USA #420301
RgIA4	J. Michael McIntosh, Salt Lake City, UT, USA Provided in the context of a cooperation.
RNase-free water	Qiagen, Hilden, Germany #129112
RPMI-1640 medium (Roswell Park Memorial Institute), with L-glutamine and sodium bicarbonate	Sigma-Aldrich Chemie #R8758
RPMI-1640 medium; HyClone RPMI-1640 medium	GE Healthcare Life Sciences HyClone Laboratories, South Logan, UT, USA #SH30027.01
TAE buffer (50x) Rotiphorese®	Carl Roth #CL86.1
Tris	Carl Roth #48552
Trypan blue solution	Sigma-Aldrich Chemie #T8154

Tuerk´s solution (= Acetic acid gentian violet solution)	Merck #1.09277.0100
Tween® 20	Merck #9005-64-5
Xylol	Merck #1330-20-7
β-Mercaptoethanol	Merck #60242

### 2.1.2 Antibodies

<b>Antigen</b>	<b>Host</b>	<b>Clonality</b>	<b>Labelling</b>	<b>Provider</b>
Rat immunoglobulin	Rabbit	Polyclonal	HRP	Dako North America, CA, USA #00082901
Red fluorescent protein (RFP)	Rabbit	Polyclonal	---	Rockland Immunochemicals, Limerick, PA, USA #600-401-379
F4/80, mouse	Rat	Monoclonal	---	Bio-Rad, Serotec, Dreieich, Germany #MCA497RT
Rabbit immunoglobulin	Swine	Polyclonal	Alkaline phosphatase (AP)	Dako North America, CA, USA #00079673
Rabbit immunoglobulin	Goat	Polyclonal	HRP + Envision®+	Dako North America, CA, USA #10076144

## 2.1.3 Kits

## Manufacturer

CytoTox96® Non-Radioactive Cytotoxicity Assay (LDH-Kit)	Promega #G1780
ELISA (Enzyme-linked Immunosorbent Assay) Human IL-1 beta/IL-1F2 DuoSet	R&D Systems, Minneapolis, MN, USA #DY201
ELISA Mouse Quantikine®; Mouse IL-1β/IL-1F2	R&D Systems #MLB00C
MinElute® Gel Extraction Kit	Qiagen #28604
QuantiTect® Reverse Transcription Kit	Qiagen #205311
RNeasy® Lipid Tissue Mini Kit	Qiagen #74804
RNeasy® Plus Mini Kit	Qiagen #74134
SsoAdvanced™ Universal SYBR® Supermix	Bio-Rad Laboratories, Inc. Watford, UK #1725270

## 2.1.4 Consumables

## Manufacturer

12-well plate	Corning Incorporated Costar, Amsterdam, The Netherlands #CLS3512
24-well plate	Greiner Bio-One #662160
26 G x 1/2 needle	BD Microlance™, Becton, Dickinson and Company, Louth, Ireland #303800
27 G x 3/4 needle	BD Microlance™ #302200
8-well cellview chamber	Sarstedt, Nümbrecht, Germany #94.6140.802
96-well plate	Greiner Bio-One #655180

Adhesive seal sheets	Thermo Scientific, Waltham, MA, USA #AB-1170
Butterfly needle; Safety-Multifly <sup>®</sup> , 21 G 200 mm	Sarstedt #85.1638.235
Chamber (Electrophoresis mold and comb)	Thermo Scientific International, Walldorf, Germany
Cuvette	Carl Roth #2292.2
Embedding cassette	Merck #H0542
Eppendorf tube 1.5 ml; Micro tube 1.5 ml	Sarstedt #72.690.001
Eppendorf tube 2.0 ml; Safe-Lock tubes 2.0 ml	Eppendorf #0030 102.094
Erlenmeyer flask	Fischer Scientific, Schwerte, Germany #10374661
Falcon <sup>®</sup> tubes (Polypropylene tubes); 12 ml, Cellstar <sup>®</sup>	Greiner Bio-One International GmbH, Kremsmuenster, Austria #164161
Falcon <sup>®</sup> tubes (Polypropylene tubes); 15 ml, Cellstar <sup>®</sup>	Greiner Bio-One International #188271
Falcon <sup>®</sup> tubes (Polypropylene tubes); 50 ml, Cellstar <sup>®</sup>	Greiner Bio-One International #227261
Heating plate Leica HI 1220	Leica Biosystems, Nussloch, Germany
Ice cooler Tissue Tek <sup>®</sup>	Sakura <sup>®</sup> Finelek, Umkirchen, Germany
Magnetic stirrer IKA <sup>®</sup> C-MAG MS10	IKA <sup>®</sup> -Works, Wilmington, USA #0003582600
Microscope slides	Fisher Scientific #13192131

Multipipette; Eppendorf Reference <sup>®</sup> 2.8, 10-100 µl	Eppendorf, Hamburg, Germany #4926000050
Multipipette; Eppendorf Reference <sup>®</sup> 2.8, 30-300 µl	Eppendorf #4926000034
Petri dish; Tissue culture dish	Sarstedt #83.1802.002
Pipette 5 ml	Greiner Bio-One International #606107
Pipette 10 ml	Greiner Bio-One International #607180
Pipette 25 ml	Greiner Bio-One International #760180
Pipette tips 10; Filtertip (sterile), 0.1-10 µl	Nerbe plus, Winsen, Germany #07-613-8300
Pipette tips 100; Filtertip (sterile), 0-100 µl	Nerbe plus #07-642-8300
Pipette tips 1000; Filtertip (sterile), 100-1.250 µl	Nerbe plus #07-695-8300
Pipette tips 100-1000 µl (not sterile)	Greiner Bio-One International #686290
Pipette tips 200 µl (not sterile)	Sarstedt #70.760.012
Pipette tips; epT.I.P.S. <sup>®</sup> Standard, 30-300 µl	Eppendorf #0030000897
Pipette; Eppendorf Reference <sup>®</sup> 2, 0.5-10 µl	Eppendorf #4924000010
Pipette; Eppendorf Reference <sup>®</sup> 2, 10-100 µl	Eppendorf #4924000053
	Eppendorf #4924000088

Pipette; Eppendorf Reference <sup>®</sup> 2, 100-1000 µl	
Pre-wet sterile 40 µm mesh (Cell Strainer)	BD Biosciences Europe, Erembodegem, Belgium #352340
RT-PCR (Real-time PCR ) 96-well plate	Thermo Fisher Scientific #AB0600
Sterile plunger 10 ml, Luer Lock Solo; Omnifix <sup>®</sup>	B. Braun #4617100V
Sterile scalpel; Sterile surgical blades	B. Braun
Sterile scissors	Peha-instrument, Paul Hartmann AG, Heidenheim, Germany
Syringe 5 ml; Injekt <sup>®</sup> 5 ml, 2-part disposable syringe	B. Braun #4606051V
Syringe 10 ml; Injekt <sup>®</sup> 10 ml, 2-part disposable syringe	B. Braun #4606108V
Syringe 20 ml; Injekt <sup>®</sup> 20 ml, 2-part disposable syringe	B. Braun #4606205V
Syringe cap, Combi-stopper	B. Braun #4495101R
Tissue flotation bath	Fisher Scientific #22-047-771

### 2.1.5 Equipment

### Manufacturer

AT Kamera Axiocam 305 color	Carl Zeiss Microscopy GmbH, Jena, Germany
Ball mill MM 500 Vario + steel ball	Retsch Lab Equipment, Haan, Germany
Centrifuge Mirko 220R	Hettich Lab Technik, Tuttlingen, Germany
Centrifuge Rotina 420R	Hettich Lab Technik, Tuttlingen, Germany

Counting chamber Neubauer, depth 0.1 mm, 0.0025 mm <sup>2</sup>	Laboroptik, Friedrichsdorf, Germany
Fume hood class II	Thermo Fisher Scientific
Incubator; Heracell 240i CO <sub>2</sub> - Inkubator  Incubator, Heracell vios 160i CO <sub>2</sub> - Inkubator	Thermo Fisher Scientific  Thermo Fisher Scientific
Microplate reader (Extinction plate reader); Fluostar Optima <sup>®</sup>	BMG Labtech, Ortenberg, Germany
Microscope Laborlux D	Leica Mikrosystem, Wetzlar, Germany
Microtome Microm cool-cut HM3553	Thermo Scientific Microm International GmbH, Walldorf, Germany
Microwave LG Intellowave	LG Electronics, Seoul, South Korea #MS-202VUT
NanoDrop <sup>™</sup> 1000 spectrophotometer	Peqlab Biotechnologie, Erlangen, Germany
Power source EV211	Consort, Hertestraat, Belgium
Safety workbench (Biological Safety Cabinet Class II)	MSC-Advantage <sup>™</sup> , Thermo Scientific #51028225  ENA II, Nuaire, Plymouth, MN, USA #NU S437 500E
Scale AE100	Mettler-Toledo, Columbus, OH, USA
StepOnePlus <sup>™</sup> Real-time PCR-System	Applied Biosystems, Carlsbad, CA, USA #4376598
Thermal Cycler G-Storm GS482	AlphaMetrix Biotech, Roedermark, Germany
Ultrasonic cleaner Sonorex Super RK102H	Sonorex, Bandelin, Berlin, Germany

Ultrasonic cleaner	VWR International, Radnor, PA, USA #142-6044
UV-light table (E3000 UV Transillumination)	Benchmark Scientific, NJ, USA
Vortex	Vortex Mixer REAX 2000, Heidolph, Schwabach, Germany
Water bath	Koettermann, Uetze, Germany

#### 2.1.6 Software

#### Manufacturer

AlphaDigiDoc 1201 Software	Alpha Innotech (ait-deutschland GmbH), Kasendorf, Germany
Microsoft Word and Excel	Microsoft, Redmond, WA, USA
SPSS (Statistical Package for the Social Sciences) statistics 29	IBM (International Business Machines), Munich, Germany
StepOne Software v2.3	Thermo Fisher Scientific, Waltham, MA, USA

## **2.2 Methods**

### **2.2.1 Human blood experiments**

The study was approved by the ethics committee of the medical faculty Giessen, Germany (No. 90/18) and performed in accordance with the Helsinki Declaration. Each volunteer gave written informed consent. Blood was drawn under surveillance of a doctor from healthy, non-smoking male and female adult volunteers using sterile instruments.

#### **2.2.1.1 hPBMCs**

Using a sterile pre-prepared heparin-filled syringe with a heparin concentration of 5.000 U/ml (35 µl heparin /15 ml blood), blood was drawn from a cubital vein.

Shortly before usage, the Ficoll Paque (Leukosep™) was put in a centrifuge at 19°C, 500 g and spun for 8 min. The heparin-blood mixture was transferred to a 50 ml Falcon tube in the safety workbench and diluted with a 1:2 concentration mix of Dulbecco's phosphate buffered saline (PBS) and bovine serum albumin (BSA) at a concentration of 0.1%, to the volume of 50 ml. 5 ng/ml LPS was then added to the blood-PBS-BSA mixture. This process is called "pulsing".

25 ml of the blood-PBS-BSA mixture was slowly poured onto the Ficoll Paque using a 10 ml pipette and then centrifuged at 19°C, 800 g for 25 min, without a break being applied. After having discarded approximately 10-12 ml of the top layer, the white ring also called the interphase, which is located just above the Ficoll Paque, was removed completely and transferred to another Falcon tube without disturbing the lower layers. The interphase was then filled up to the 45 ml mark with PBS/BSA and centrifuged at 19°C, 500 g for 8 min. The resulting supernatant was discarded and the pellet generated washed twice with 25 ml of PBS/BSA at 19°C, 500 g for 8 min. The supernatant was discarded and the pellet was taken up in 10 ml of monocyte attachment medium (MAM) counted in a 1:10 dilution with Tuerk's solution in a counting chamber and seeded out in a 24-well plate in a concentration of  $0.5 \times 10^6$  cells/500 µl per well.

Following the 3 h incubation time at 37°C and 5% CO<sub>2</sub>, the plate was inverted to discard the MAM and non-adhering cells and the MAM was replaced with RPMI-1649 medium.

After incubation, ATP or BzATP and substances like FFA2 and or FFA3 agonists were added according to the pipette chart and incubated for further 30 min. Then the whole plate was centrifuged at 4°C, 500 g for 8 min. 250 µl of cell free supernatant of each well was transferred to an Eppendorf tube and frozen at -20°C and the plate at -80°C for enzyme-linked immunosorbent assay (ELISA) and lactate dehydrogenase (LDH) measurements, respectively.

### **2.2.1.2 ELISA**

In this thesis a sandwich ELISA was used to measure concentrations of IL-1 $\beta$  in cell free cell culture supernatants in pg/ml. The ELISA was carried out according to the manufacturer's instructions "Human IL-1 beta/IL-1F2 DuoSet ELISA". The kit contains the following substances: Human IL-1  $\beta$  capture antibody, detection antibody, standard, Streptavidin-HRP, wash buffer, reagent diluent, substrate solution and stop solution.

Firstly, in order to generate a standard curve, a series of dilutions of a standard provided in the kit with a known concentration, were made. This was done across a range of concentrations, where the to be measured sample concentrations were expected.

In brief, the plate preparation was done the day before measurement when the capture antibody was diluted with PBS to the working concentration which was set at 4 µg/ml by the manufacturer. The 96-well plate was coated and then immediately sealed using an adhesive seal sheet and incubated overnight. After removing the liquid, 400 µl wash buffer was added and removed in a total amount of three washing steps. After the last wash, the plate was inverted and blotted using clean paper towels. 300 µl of reagent diluent was added to each well and incubated at room temperature for 1 h. After the plates had been washed three times, 100 µl of diluted or undiluted samples and standards were added per well, covered with an adhesive seal sheet and incubated for 2 h. A further three washing steps took place before adding 100 µl of the biotinylated detection antibody, diluted in reagent diluent and covered with a new adhesive seal sheet for further 2 h.

After three final washes 100 µl of the working dilution of Streptavidin-horseradish peroxidase (HRP) was added to each well and covered for 20 min at room temperature avoiding direct light. Following a further three washes, 100 µl of substrate solution was

then added to each well, then covered and incubated for 20 min at room temperature. 50 µl of stop solution was added to each well, mixed and then the optical density for each well was measured using a microplate reader set at 450 nm. This was compared with the extinction of the generated standard curve.

### **2.2.1.3 LDH**

LDH is an enzyme found in the cytoplasm of all cells of the human body. Its release occurs when cells are damaged and is therefore a good marker to account for viability. Total release in this matter means the maximum amount of LDH that is released by a specific amount of cells and is used as a standard value. The LDH measurements were only partly carried out according to the manufacturer's instructions "CytoTox96® Non-Radioactive Cytotoxicity Assay". The kit contains the following substances: lysis solution, substrate solution and stop solution.

The total release cells were previously frozen at -20°C and treated with lysis solution to ensure the death of all cells and membrane rupture. Then, a 96-well plate was set up with 50 µl cell culture supernatant and 50 µl plain medium serving as the negative control. Further 50 µl substrate solution was added to each well and incubated at room temperature for 30 min in the dark. To stop the reaction 50 µl of stop solution was added to each well making a total volume of 150 µl per well.

The extinction was measured using a microplate reader set at 490 nm.

## **2.2.2 Mouse experiments**

### **2.2.2.1 Animal experimentation approval**

Specified pathogen-free mice were obtained via Janvier Labs, Le Genest-Saint-Isle, France and were housed in our animal facility for about 2 weeks under a 12 h light/dark cycle and access to standard chow and water ad libitum. Experimental animals received humane care according to National Institutes of Health (NIH) "Guide for the Care and Use of Laboratory Animals". The protocol was registered and approved by the local authorities (Regierungspräsidium Giessen, Germany; reference no. 571\_M). C57BL/6 mice were sacrificed via isoflurane and neck fracture by Alexander Perniss, Institute of

Anatomy, Justus-Liebig University (JLU), Giessen. Furthermore, knockout mice were also kindly provided by Prof. Offermann, Max-Planck Institute, Bad Nauheim. After the scarification, blood was drawn according to the protocol (see 2.2.2.2) and/or bones collected (see 2.2.2.3).

### **2.2.2.2 mPBMCs**

Blood was drawn from the Vena cava using a syringe filled with 15  $\mu$ l heparin at a concentration of 25.000 IU/5 ml and 1 ml PBS + BSA at a concentration of 0.1%. The whole white blood cells were prepared for counting by using a 1:5 dilution with 40  $\mu$ l Tuerk's solution and 10  $\mu$ l of the drawn blood. A 5 min waiting period was needed for the erythrocytes to be lysed before the cells were counted. The blood solution was "pulsed" with 10 ng/ml LPS before it was transferred carefully to a Falcon containing 3 ml of 1.078 g/ml density gradient consisting of 1.4 ml 1.3 M NaCl, 7.8 ml 55.7% Percoll, 4.8 ml 34.3% high purity HPLC water (ddH<sub>2</sub>O) and 7  $\mu$ l 0.5 mM HCl.

MPBMCs were isolated by centrifugation at 18°C, 850 g for 30 min without a break being applied. The upper phase was carefully removed by pipetting with a safety zone to the interphase. Thereafter the interphase was transferred to a new Flacon containing 5 ml of PBS + BSA (0.1%) following a further centrifugation at 18°C, 800 g for 10 min. The supernatant was discarded, then a further 5 ml PBS + BSA were added. This was then centrifuged under the same conditions as before only this time at 500 g.

After discarding the supernatant, the pellet was resuspended in 400  $\mu$ l RPMI-1640 medium (Sigma-Aldrich) and then counted using a 1:5 dilution with Tuerk's solution. Using a 96-well plate the cells were seeded out with a density of  $1 \times 10^5$  cells/ 100  $\mu$ l medium incubated at 37°C and 5% CO<sub>2</sub> for 2 h. Thereafter, mPBMCs were purified by adherence selection. The plate was inverted to discard the medium and non-adherent cells and the medium was replaced by a fresh RPMI-1640 medium (Sigma-Aldrich). Substances were added according to the pipette chart. Then the plate was incubated at 37°C and 5% CO<sub>2</sub> for 30 min to then be centrifuged at 4°C at 500 g for 8 min. The cell free cell culture supernatants were transferred to Eppendorf tubes for ELISA and LDH measurements, respectively. All samples, including the ones remaining in the plate which are the medium control and the total release were frozen at -20°C.

### 2.2.2.3 Mouse BMDMs

In this project bone marrow cells were isolated from mouse hind limbs in order to differentiate the cells into BMDMs.

Firstly, the skin was carefully cut away. Then the hind limbs were removed without damaging the bones. The hind limbs were placed into 70% ethanol for approximately 1 min to disinfect the femur. After that, the bones were put into a 50 ml Falcon containing 15 ml PBS and PenStrep at a concentration of 50 U penicillin/ml and 50 µg streptomycin/ml. This was kept on ice until transferred to a safety workbench.

Under the safety workbench the bones were placed on a Petri dish and sprayed with 70% ethanol then carefully cleaned to remove muscle and other tissue. The ends of the femur were opened with sterile scissors. Using a 26G or 27G needle attached to a 5 ml syringe filled with RPMI-1640 medium (+ 10% FCS) (HyClone) and PenStrep the bone marrow was flushed into a sterile water pre-wet sterile 40 µm mesh set on a 50 ml Falcon. The bones turned white during the flushing procedure. The mesh was rinsed and gently rubbed with a sterile plunger of a 5 ml syringe, flushing the remaining cells out of the mesh into the Falcon. The cell suspension was centrifuged at 4°C, 520 g for 13 min. The supernatant was discarded and the red blood cells remaining in the pellet were lysed by adding 3 ml red blood cell lysis buffer (RCB) and incubated for 6 min. Before centrifugation for 10 min at 4°C and 520 g, 20 ml of PBS + PenStrep were added to stop the reaction.

After discarding the supernatant, the cells were resuspended in 5 ml RPMI-1640 medium (HyClone) and counted at a 1:20 dilution using the trypan blue solution. The cell number was adjusted to  $1 \times 10^6$  cells/ml medium in RPMI-1640 medium (HyClone) (+10% FCS and PenStrep at a concentration of 10.000 U/ml, 10 mg/ml).  $1 \times 10^6$  cells/ml supplemented with 10 ng/ml M-CSF were seeded out in a 12-well plate (Costar) for 3 days and were incubated in a humidified incubator at 37°C and 5% CO<sub>2</sub>, to allow bone marrow cells to differentiate to BMDMs.

On day 3, 1 ml of fresh RPMI-1640 medium (HyClone) (+10% FCS + PenStrep) was supplemented with the total concentration of 10 ng/ml M-CSF, 50 pg/ml LPS and 10 ng/ml INF-γ, added per well and then cultured for further 3 days.

On day 6 of cultivation 1 ml of the cell culture supernatant was discarded by pipetting. Cells were left untreated or primed with LPS (1 µg/ml) according to the pipette chart. In some experiments, SCFA or synthetic FFA agonists were added shortly before LPS. After 5 h of incubation, cells were treated with ATP (1 mM, 2 mM), BzATP (100 µM) or nigericin (50 µM) in the presence or absence of SCFAs and synthetic agonists for 40 min in a humidified incubator at 37°C and 5% CO<sub>2</sub>. Cell culture supernatant was harvested by centrifugation at 4°C, 500 g for 8 min then transferring 600 µl of the cell free culture supernatant to Eppendorf tubes. The total release and control medium stayed in the plate and both the Eppendorf tubes and plates were stored at -20°C to perform ELISA and LDH measurements (see 2.2.2.4), respectively.

#### **2.2.2.4 ELISA**

The mouse Quantikine® ELISA kit is, similar to the human ELISA as described in 2.2.1.3. It is a detection method used in this case for mouse IL-1β. The measurements were performed according to the manufacturer's instructions.

#### **2.2.2.5 Immunocytochemistry of BMDMs**

To verify that the isolated bone marrow cells were differentiated into BMDMs (see 2.2.2.3) immunohistochemical staining against F4/80, a well-known macrophage marker was used.

Bone marrow cells were isolated as described before (see 2.2.2.3) and seeded into 8-well cellview chambers (Sarstedt) at a density of  $0.125 \times 10^6$  cells/200 µl medium per well. Then the cells were differentiated into BMDMs according to the protocol described in 2.2.2.3.

After 6 days of cultivation, the RPMI-1640 medium (HyClone) and non-adherent cells were discarded by turning the chambers around and gently blotting them against clean towels. Cells were washed by adding 500 µl PBS then discarding the liquid by blotting the chamber against paper towels. Thereafter, 500 µl of cold 100% isopropanol was added and the cellview chambers were put on ice. After 10 min the isopropanol in the cellview

chambers was discarded by blotting the chamber against paper towels once again. H<sub>2</sub>O<sub>2</sub> was diluted in PBS to a 1% solution, added to the chambers and stored on ice for 30 min. After that the chambers were washed three times for 2 min using PBS. Free protein binding sites were blocked using a blocking solution containing: PBS + 1% BSA, 0.05% Tween<sup>®</sup> 20 and 5% NMS. The blockage solution was kept on the cells for 30 min at room temperature then removed.

The anti-F4/80 antibody which was diluted 1:200 with the blocking solution, was added and kept overnight at 4°C. After that the cells were washed three times with PBS + 0.05% Tween<sup>®</sup> 20.

The secondary antibody being a rabbit anti-rat immunoglobulins/HRP was diluted 1:200 with PBS containing 0.05% Tween<sup>®</sup> 20 and 5% normal mouse serum (NMS). This was incubated for 60 min at room temperature. The slide was washed three times with PBS + 0.05% Tween 20 before the tertiary detection reagent being a goat anti-rabbit immunoglobulin EnVision<sup>®</sup>+ System-HRP and 5% NMS was added. This was incubated for 30 min at room temperature following three washes with tris buffered saline (TBS).

- 10x TBS was made by adding 60.5 g Tris (final concentration: 55 mM) and 90 g NaCl both solved in 900 ml aqua dest.. By adding 25% HCl the pH was adjusted to 7.6. The solution was filled up to 1000 ml.

Then one tablet (10 mg) of 3,3'-Diaminobenzidinetetrahydrochloride (DAB) was solved in 20 ml TBS at a pH of 7.6. The solution was centrifuged at 19°C, 500 g for 1 min. After that, the solution was put in 1 ml aliquots. All aliquots except for two were stored and frozen at -20°C. A 1.15% dilution of H<sub>2</sub>O<sub>2</sub> was made using aqua dest.. Then 10 µl of the diluted H<sub>2</sub>O<sub>2</sub> was added to each of the two 1 ml aliquots. 500 µl of the DAB- H<sub>2</sub>O<sub>2</sub> solution was put in the chamber for 10 min and rinsed with PBS. The next day, a slight counter staining with 1:5 diluted hemalum using aqua dest. was added for 2 min.

- Hemalum was made by dissolving 1 g haematoxylin (final concentration: 3.3 mM), 0.2 g NaIO<sub>3</sub> (final concentration: 1 mM) and 50 g KAl(SO<sub>4</sub>)<sub>2</sub> (final concentration: 0.1 M) in 1000 ml aqua dest..

In the next step, the slides were blued in a cuvette for 5 min using tap water. Then, the slides were cover slipped with glycergel in the final step.

### **2.2.2.6 Mouse colon removal, fixation and F4/80/red fluorescent protein (RFP) double immunohistochemistry**

Mouse colon removal and fixation: The mice were sacrificed according to 2.2.2.1. After having cut open the abdomen using a sterile scalpel, 3-5 mm colon pieces were cut out and put into 4% dissociated paraformaldehyde in Sørensen´s buffer over night at 4°C.

- The 2x Sørensen´s buffer was previously prepared and consisted of 0.696 g  $\text{NaH}_2\text{PO}_4$  (final concentration: 58 mM) and 2.860 g  $\text{Na}_2\text{HPO}_4$  (final concentration: 0.2 M). After that, 100 ml aqua dest. was added.
- The 4% dissociated paraformaldehyde in Sørensen´s buffer was also prepared previously by adding 4 g paraformaldehyde to 50 ml aqua dest.. Using a safety vent, the solution was heated up to 60°C and continuously stirred using a magnetic stirrer. Then 2 drops (ca. 75  $\mu\text{l}$ ) 1 N NaOH were added until the solution turned clear. In the last step 50 ml 2x Sorensen´s buffer was added, the fixing solution was cooled off on ice and the pH checked. The pH should be in the range of 7.3-7.4.

The next day, the organs were transferred into Sørensen´s buffer for 24 h. On day 3 the organs were put in 50% isopropanol for 0.5-1 h then in 70% isopropanol for 2 h. The 70% isopropanol was then renewed twice in which the colon was stored in.

Next, the organs and the 70% isopropanol in which they were kept in, were transferred to embedding cassettes. These embedding cassettes were soaked in different solutions in different vessels for a specific duration at a specific temperature according to Table 1.

<b>Solution</b>	<b>Duration</b>	<b>Temperature</b>
96% isopropanol	1 h	Room temperature

100% isopropanol	1 h	Room temperature
100% isopropanol	1 h	Room temperature
30% xylol, 70% isopropanol	1h	Room temperature under the fume hood
70% xylol, 30% isopropanol	1 h	Room temperature under the fume hood
100% xylol	1 h	Room temperature under the fume hood
100% xylol	1 h	Room temperature under the fume hood
Paraffin	2 h	60°C
Paraffin	Over night	60°C

**Table 1: Embedding in paraffin** This table shows the ten different solutions in which the cassettes containing the organs are soaked in. The duration and temperature of each soaking stage is also shown.

The next day, after having left the organs in the heated paraffin overnight, the paraffin including the organs were poured into blocks and then to be cut after having cooled down.

Immunohistochemistry of colon sections: The colon embedded in paraffin was put on an ice cooler before being cut. Degased aqua dest. was poured into the tissue flotation bath in which it was heated. The colon was then cut using the microtome, in slices with a thickness of 5 µm. Then the sections were put on microscope slides and on a heating plate set at 40°C for 15 min. The slides were placed in an incubator overnight set at 60°C.

The following day, the slides were deparaffinized using so-called deparaffinization series. In the first step of the series the slides were put in 100% xylol 3x for each 10 min using a cuvette. After that, the slides were put in descending concentrations of isopropanol starting at 90% then continuing at 80%, 70% and 50%. The slides were put in each

concentration twice, each for 3 min. At the end of the deparaffinization series, the slides were placed in aqua dest. and then transferred to PBS.

- 10x PBS is made up of 80 g NaCl, 2 g KCl (final concentration: 32 mM), 14.24 g Na<sub>2</sub>HPO<sub>4</sub> (final concentration: 125 mM), 2 g KH<sub>2</sub>PO<sub>4</sub> (final concentration: 21 mM) which was dissolved in 800 ml aqua dest.. Then the pH was adjusted to 7.2 in 1x PBS by adding of 1 N HCl. The solution was filled up to 1 l.

Next, the slides were placed in a chamber which was lined with wet paper towels. Thereafter, the slides were pretreated with 50 µl protease solution on each colon slice for 15 min consisting of 1 mg protease and 2 ml of TBS. After the pretreatment with protease, the slides were rinsed off 3x with PBS using a pipette.

After this, the slides were put into a cuvette filled with PBS, 3x each for 2 min. Then, 6.6 ml of a 1.15% dilution of H<sub>2</sub>O<sub>2</sub> was added to 200 ml PBS and stored on ice. Then, enough of the solution was pipetted onto each colon section fully covering it for 30 min. After that the slides were rinsed again 3x with PBS using a pipette. Next, 50 µl of the blockade was added for 30 min consisting of 0.2 g BSA, 0.02 g NaN<sub>3</sub> and 20 ml PBS for 30 min and then shaken off. The anti-F4/80 antibody was diluted 1:12000 using the blockade and 5% NMS then was added and put on the slide overnight.

The next day, the slides were rinsed with PBS 3x using a pipette. Then the rabbit anti-rat immunoglobulin antibodies + HRP were diluted 1:200 using 5% NMS. Enough of the mixture was pipetted to each colon section covering it fully and remaining there for 60 min at room temperature. Then, the slides were rinsed with PBS 3x using a pipette. Next, the anti-rabbit immunoglobulin, EnVision+ System-HRP and 5% NMS were added to the colon sections covering them fully for 30 min. Using TBS the slides were rinsed 3x.

The next steps were done according to 2.2.2.5. Then, the slides were rinsed with PBS for 3x using a pipette. After that they were put into a cuvette filled with PBS, 3x each for 2 min. Next, the blockade was added again for 30 min. Antibodies to RFP were diluted with the blockade 1:5000 and 5% NMS was pipetted to the sections and left overnight in a humidified chamber in the fridge at 4°C.

The next day, the slides were rinsed 3x with PBS using a pipette. Then swine anti-rabbit immunoglobulin antibodies AP conjugated were diluted 1:50 using 5% NMS and left for 60 min. After that, the slides were rinsed 3x using 0.1 M Tris HCl buffer.

- The Tris buffer was made by adding 12.1g Tris base (final concentration: 125 mM) to 800 ml aqua dest.. HCl was used to adjust the pH to 8.2. The solution was filled up to 1 l.

1 mg of fast blue AP solved in 1 ml naphthol phosphate buffer and 1 mM levamisole was added to the specimen for 20 min.

- The naphthol phosphate buffer with 1 mM levamisole was made by solving 2 mg naphthol AS-MX-phosphate (final concentration: 27 mM) in 200 µl 99% n-dimethylformamide. 9.8 ml 0.1 M Tris HCl buffer (see above) and 2.4 mg levamisole (final concentration: 1 mM) were added.

Then the slides were rinsed 3x using PBS and in the last step the slides were cover slipped via aqueous mounting. Meaning the aqueous mounting medium was heated up and added to each specimen as well as a cover slip and the medium left to cool and harden.

### **2.2.3 Statistical analysis**

The statistical analysis for the data in this thesis was done using the IBM statistical program SPSS version 29. In the first step, the data sets were checked for occurrence by coincidence using the Friedmann-test. If the p-value given by the test was smaller than or as big as 0.05 it was assumed to be non-coincidental. In the next step, the data of two groups was analyzed to see whether they differed significantly from one another. To do so, the non-parametric Wilcoxon-test was used. If the test showed a p-value smaller than or as big as 0.05 it was assumed to be significantly different. These two statistical tests were used for all measured data.

To calculate the half maximal inhibitory concentrations ( $IC_{50}$ ), the regression model Weibull type 2 and the statistical program R (version: 3.6.1) were used. The figures were created using the vector graphics software called Inkscape (version: 1.3).

### 3. Results

#### 3.1 Synthetic FFA2/FFA3 agonists inhibit the ATP-induced IL-1 $\beta$ release in hPBMCs and require the activity of nAChRs

##### 3.1.1 The BzATP- or ATP-induced release of IL-1 $\beta$

The following experiments were performed on freshly isolated hPBMCs. The hPBMCs were isolated via density gradient centrifugation. The secretion of IL-1 $\beta$  by hPBMCs was induced by two stimuli. Firstly, hPBMCs were “pulsed” with 5 ng/ml LPS for 25 min during the process of hPBMC isolation to induce the expression of the bio inactive pro-IL-1 $\beta$ . After 3 h of culturing, non-adherent cells were removed. Thereafter, BzATP or ATP were added to induce IL-1 $\beta$  release. While in all experiments, in supernatants of LPS-pulsed cells, low amounts of IL-1 $\beta$  (23 pg/ml to 841 pg/ml; n = 28; Fig. 5) were detected, additional stimulation with BzATP (100  $\mu$ M) resulted in elevated IL-1 $\beta$  levels in the range of 407 to 5771 pg/ml (n = 28; p  $\geq$  0.05; Fig. 5-10). Similar results were found using 1 mM ATP (81 pg/ml to 1312 pg/ml; n = 14; p  $\geq$  0.05; Fig. 5, 6 B).

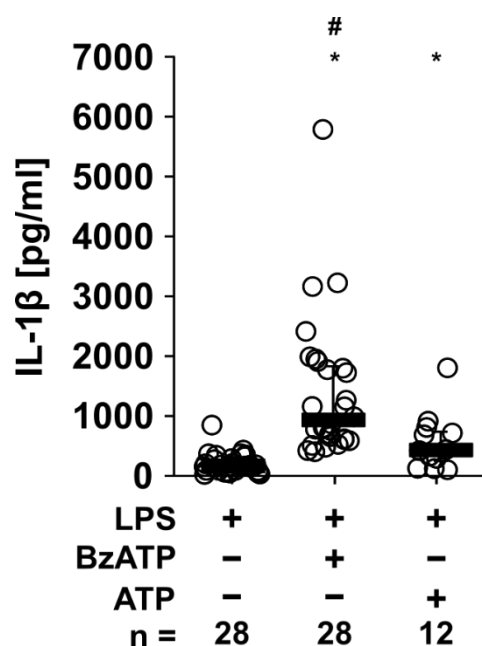


**Figure 5. The impact of BzATP (3'-O-(4-benzoyl) benzoyl ATP) or ATP on the secretion of IL-1 $\beta$ .** Human blood was freshly drawn from healthy volunteers. Peripheral blood mononuclear cells (hPBMCs) were “pulsed” with lipopolysaccharide (LPS; 5 ng/ml for 25 min) during the process of hPBMC isolation. After culturing for 3 h, non-

adherent cells were removed. The P2X7 receptor agonists BzATP (100  $\mu$ M) or ATP (1 mM) were added. The data depicted in this figure are a summary of the respective data shown in figures 2-6. Data are presented as individual data points, bars represent median, whiskers percentiles 25 and 75. Friedmann-test followed by Wilcoxon signed-rank test. \*  $p \leq 0.05$  significantly different from LPS-pulsed hPBMCs. #  $p \leq 0.05$  significantly different from samples where ATP was given to LPS-pulsed hPBMCs.

### **3.1.2 Involvement of P2X7 and P2X4 receptors in the BzATP- and ATP-induced secretion of IL-1 $\beta$**

To investigate whether the BzATP- or ATP-induced release of IL-1 $\beta$  depends on the P2X7 and/or P2X4 receptor activity the experiment was conducted on hPBMCs. While in supernatants of LPS-pulsed cells low amounts of IL-1 $\beta$  (23 pg/ml to 427 pg/ml;  $n = 16$ ; not shown) were detected, additional stimulation with BzATP (100  $\mu$ M) resulted in elevated IL-1 $\beta$  levels in the range of 407 to 1986 pg/ml ( $n = 16$ ;  $p \geq 0.05$ ; Fig. 6 A). Similar results were found using 1 mM ATP (81 pg/ml to 1312 pg/ml;  $n = 14$ ;  $p \geq 0.05$ ; Fig. 6 B). In figure 6 the IL-1 $\beta$  concentration measured in supernatants of cells treated with LPS alone were deducted from all other values.

To test for an involvement of the P2X7 and the P2X4 receptor, the P2X7 receptor antagonist A438079 and the P2X4 receptor antagonist 5-BDBD (5-(3-Bromophenyl)-1,3-dihydro-2H-benzofuro[3,2-e]-1,4-diazepin-2-on) were used (Fig. 6). In both occasions either with BzATP being the second stimulus or ATP, the release of IL-1 $\beta$  was inhibited by A438079 (1  $\mu$ M – 50  $\mu$ M;  $p \geq 0.05$ ; Fig. 6). In contrast, the P2X4 receptor inhibitor 5-BDBD in the concentrations 10  $\mu$ M and 20  $\mu$ M only blunted the BzATP-induced release of IL-1 $\beta$  (Fig. 6 A), whereas no statistically significant impact on the ATP-induced release was found and a large variability of the results was seen (Fig. 6 B).

After the addition of P2X7 receptor antagonist A438079 without the addition of the second stimulus being BzATP or ATP, low amounts of IL-1 $\beta$  (117 pg/ml to 293 pg/ml;  $n = 5$ ; Fig. 6 B) were detected, which did not significantly differ from those released by cells pulsed with LPS. Similar IL-1 $\beta$  concentrations were seen, when the P2X4 receptor antagonist 5-BDBD was added to cells primed with LPS (55 pg/ml to 476 pg/ml;  $n = 8$ ).

The LDH activity measurements are shown in Table S1. The median of the LDH activity measured in the supernatants of both groups of cells stimulated with BzATP or ATP, is generally low, under 6.0%. However, in some experimental settings, the LDH activity is significantly higher. Cells stimulated with LPS and BzATP/ATP are significantly different compared to data of cells treated with only LPS. Furthermore, cells stimulated with LPS + BzATP and the addition of 5-BDBD (10  $\mu$ M, 20  $\mu$ M, 50  $\mu$ M) are significantly different compared to data of cells treated with LPS + BzATP. This statistically significant difference is also seen in the supernatants of cells stimulated with LPS + ATP and the addition of 5-BDBD (10  $\mu$ M, 50  $\mu$ M) compared with cells treated with only LPS + ATP. The number (n) varies between 4-16.

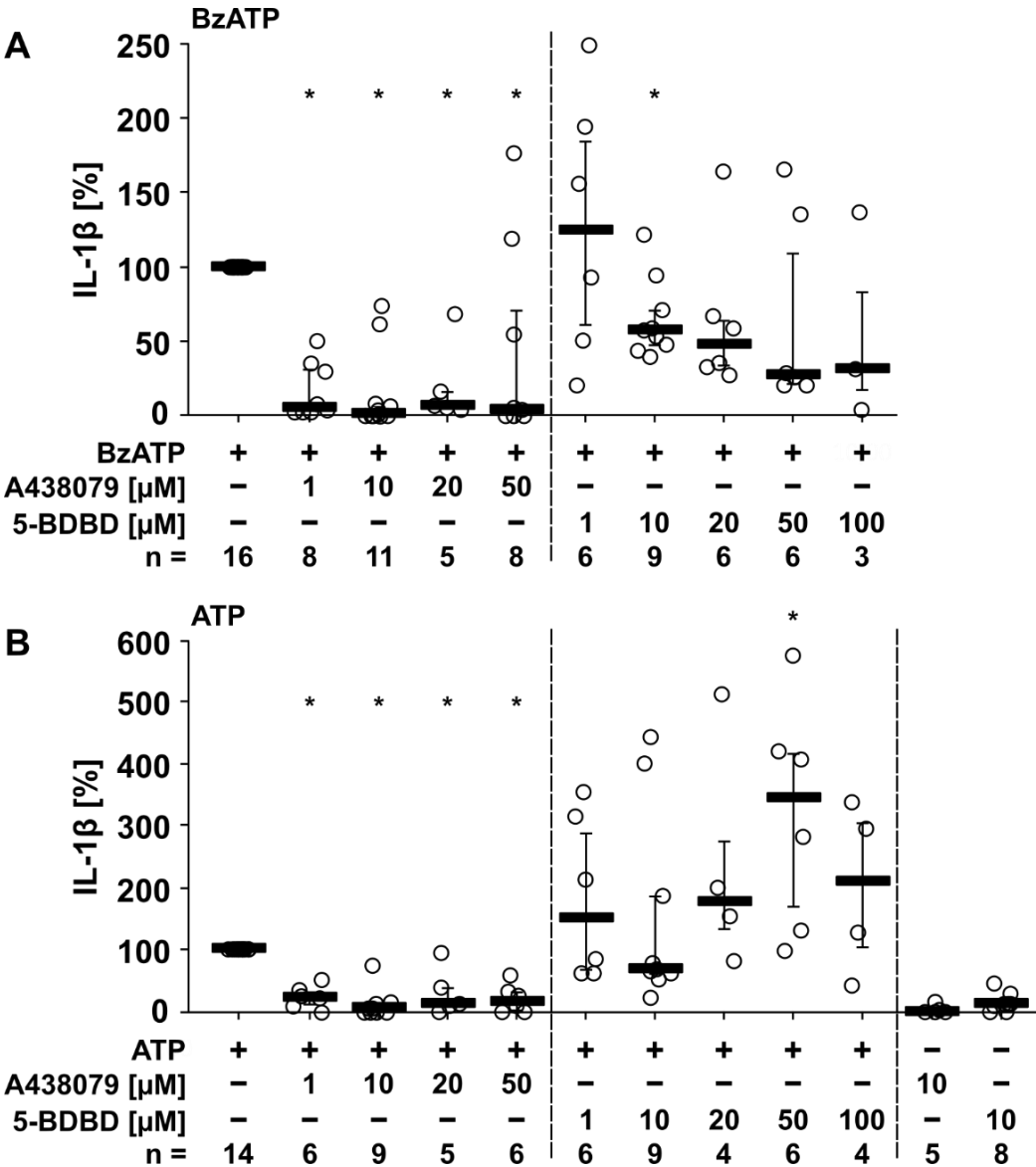


**Figure 6. The impact of P2X7 and P2X4 receptors on the BzATP (3'-O-(4-benzoyl) benzoyl ATP) and ATP-induced release of interleukin-1 $\beta$  (IL-1 $\beta$ ) by human peripheral blood mononuclear cells (hPBMCs).** Human blood was freshly drawn from healthy volunteers. HPBMCs were “pulsed” with lipopolysaccharide (LPS; 5 ng/ml for 25 min) during the process of hPBMC isolation. After culturing for 3 h, non-adherent cells were removed. **A)** The P2X7 receptor antagonist A438079 or the P2X4 receptor antagonist 5-BDBD (5-(3-bromophenyl)-1,3-dihydro-2H-benzofuro[3,2-e]-1,4-diazepin-2-one) were added in the absence and presence of the P2X7 receptor agonist BzATP (3'-O-(4-benzoyl) benzoyl ATP, 100  $\mu$ M). **B)** Similar experiments as described in A) were performed using ATP (1 mM). **A and B)** IL-1 $\beta$  was measured in cell culture supernatants by ELISA. The IL-1 $\beta$  concentration measured in supernatants of cells treated with LPS alone were deducted from all other values. The IL-1 $\beta$  concentration in experiments where pulsed hPBMCs were stimulated with BzATP/ATP alone was set to 100% and all other values were calculated accordingly. Data are presented as individual data points, bars represent median, whiskers percentiles 25 and 75. Friedmann-test followed by Wilcoxon signed-rank test. \*  $p \leq 0.05$  significantly different from samples where BzATP/ATP was given alone to LPS-pulsed hPBMCs.

### **3.1.3 Inhibition of IL-1 $\beta$ release via FFA2 agonist 4-CMTB**

The following experiments were performed on hPBMCs to test the hypothesis that the stimulation of the FFA2 downregulates the BzATP-induced IL-1 $\beta$  release. While in supernatants of LPS-pulsed cells low amounts of IL-1 $\beta$  (80 pg/ml to 345 pg/ml;  $n = 6$ ; not shown) were detected, additional stimulation with BzATP (100  $\mu$ M) resulted in elevated IL-1 $\beta$  levels in the range of 422 to 3158 pg/ml ( $n = 6$ ;  $p \geq 0.05$ ; Fig. 7).

The secretion of IL-1 $\beta$  was dose-dependently inhibited by 4-CMTB (0.5  $\mu$ M – 50  $\mu$ M;  $n = 4-6$ ;  $p \geq 0.05$ ; Fig. 7). The calculated  $IC_{50}$  value was 8.3  $\mu$ M. After the addition of FFA2 agonist 4-CMTB (1  $\mu$ M) without the addition of BzATP, low amounts of IL-1 $\beta$  (82 pg/ml to 476 pg/ml;  $n = 5$ ; Fig. 7) were detected, which did not significantly differ from those released by cells that were only pulsed with LPS.

The LDH activity measurements are shown in Table S2. The median of the LDH activity measured in cell supernatants, is generally low, under 6.6%. However, a statistically significant increase is seen in some experimental settings. Cells stimulated with LPS +

BzATP and the addition of 4-CMTB (10  $\mu$ M and 50  $\mu$ M) are significantly different compared to data of cells treated with only LPS + BzATP. The number (n) varies between 4-6.

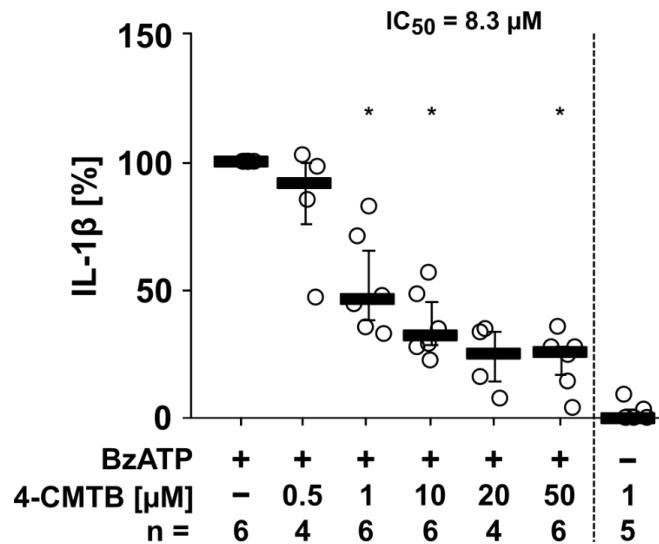


**Figure 7. The FFA2 agonist inhibits the BzATP (3'-O-(4-benzoyl) benzoyl ATP)-induced release of interleukin-1 $\beta$  (IL-1 $\beta$ ) by human peripheral blood mononuclear cells (hPBMCs).** Human blood was freshly drawn from healthy volunteers. HPBMCs were “pulsed” with lipopolysaccharide (LPS; 5 ng/ml for 25 min) during the process of hPBMC isolation. After culturing for 3 h, non-adherent cells were removed. The P2X7 agonist BzATP (100  $\mu$ M) was added in the absence and presence of the FFA2 agonist 4-CMTB (0.5  $\mu$ M, 1  $\mu$ M, 10  $\mu$ M 20  $\mu$ M and 50  $\mu$ M). 4-CMTB inhibits the BzATP-induced IL-1 $\beta$  release in a dose-dependent manner ( $IC_{50} = 8.3 \mu$ M). The IL-1 $\beta$  concentration measured in supernatants of cells treated with LPS alone were deducted accordingly from all other values. The IL-1 $\beta$  concentration in experiments where pulsed hPBMCs were stimulated with BzATP alone was set to 100% and all other values were calculated accordingly. Data are presented as individual data points, bars represent median, whiskers percentiles 25 and 75. Friedmann-test followed by Wilcoxon signed-rank test. \*  $p \leq 0.05$  significantly different from samples where BzATP was given alone to LPS-pulsed hPBMCs.

### 3.1.4 Inhibition of IL-1 $\beta$ release via FFA3 agonist AR420626

Similar experiments compared to the ones performed in 3.1.3 were conducted using the FFA3 agonist AR420626, to test the hypothesis that the stimulation of the FFA3 downregulates the BzATP-induced IL-1 $\beta$  release by hPBMCs. While in supernatants of LPS-pulsed cells low amounts of IL-1 $\beta$  (172 pg/ml to 841 pg/ml; n = 6; not shown) were detected, additional stimulation with BzATP (100  $\mu$ M) resulted in elevated IL-1 $\beta$  levels in the range of 658 to 5771 pg/ml (n = 6; p  $\geq$  0.05; Fig. 8).

The secretion of IL-1 $\beta$  was dose-dependently inhibited by AR420626 (1  $\mu$ M – 50  $\mu$ M; n = 6; p  $\geq$  0.05; Fig. 8). The calculated IC<sub>50</sub> value was 19.7  $\mu$ M. After the addition of FFA3 agonist AR420626 (50  $\mu$ M) without the addition of BzATP, low amounts of IL-1 $\beta$  (128 pg/ml to 958 pg/ml; n = 6; Fig. 8) were detected.

The LDH activity measurements are shown in Table S3. The median of the LDH activity measured in cell supernatants is low, under 3.2%. No significant differences are seen (Friedman-test p = 0.17). The number (n) is 6 for each experimental group.

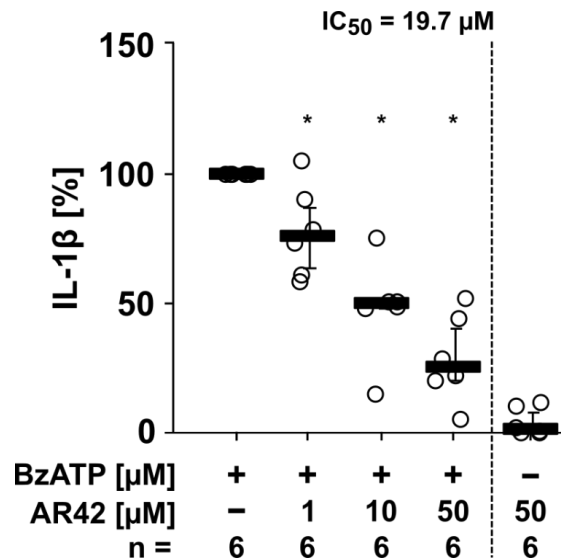


**Figure 8. The FFA3 agonist inhibits the BzATP (3'-O-(4-benzoyl) benzoyl ATP)-induced release of interleukin-1 $\beta$  (IL-1 $\beta$ ) by human peripheral blood mononuclear cells (hPBMCs).** Human blood was freshly drawn from healthy volunteers. HPBMCs were “pulsed” with lipopolysaccharide (LPS; 5 ng/ml for 25 min) during the process of hPBMC isolation. After culturing for 3 h, non-adherent cells were removed. The P2X7

receptor agonist BzATP (100  $\mu$ M) was added in the absence and presence of the FFA3 agonist AR420626 (1  $\mu$ M, 10  $\mu$ M and 50  $\mu$ M). AR420626 inhibits the BzATP-induced IL-1 $\beta$  release in a dose-dependent manner ( $IC_{50} = 19.7 \mu$ M). The IL-1 $\beta$  concentration measured in supernatants of cells treated with LPS alone were deducted accordingly from all other values. The IL-1 $\beta$  concentration in experiments where pulsed hPBMCs were stimulated with BzATP alone was set to 100% and all other values were calculated accordingly. Data are presented as individual data points, bars represent median, whiskers percentiles 25 and 75. Friedmann-test followed by Wilcoxon signed-rank test. \*  $p \leq 0.05$  significantly different from samples where BzATP was given alone to LPS-pulsed hPBMCs.

### **3.1.5 The signaling of the FFA2 involves nAChRs containing subunits $\alpha 7$ and $\alpha 9/\alpha 10$**

Next, the hypothesis was tested that the stimulation of the FFA2 results in an activation of nAChRs, which downregulate the secretion of IL-1 $\beta$  by hPBMCs. First, nAChR antagonists RgIA4 and ArIB [V11L, V16D] were added. After that, the synthetic FFA2 agonist 4-CMTB was added and finally BzATP to induce IL-1 $\beta$  release.

While in supernatants of LPS-pulsed cells low amounts of IL-1 $\beta$  (80 pg/ml to 345 pg/ml;  $n = 6$ ; not shown) were detected, additional stimulation with BzATP (100  $\mu$ M) resulted in elevated IL-1 $\beta$  levels in the range of 422 to 3158 pg/ml ( $n = 6$ ;  $p \geq 0.05$ ; Fig. 9).

The secretion of IL-1 $\beta$  was inhibited by 4-CMTB (1  $\mu$ M – 10  $\mu$ M;  $p \geq 0.05$ ; Fig. 9). When conopeptides RgIA4 (50 nM) and ArIB [V11L, V16D] (500 nM) were combined with 4-CMTB at a concentration of 1  $\mu$ M or 10  $\mu$ M, no significant inhibition was seen anymore ( $n = 6$ ; Fig. 9). However, when comparing the IL-1 $\beta$  concentrations in cell culture supernatants treated with LPS, BzATP and 4-CMTB to those additionally containing RgIA4 or ArIB [V11L, V16D], significant differences were only detected at a 4-CMTB concentration of 10  $\mu$ M. Using RgIA4, the IL-1 $\beta$  concentrations were reversed to levels ranging from 457 pg/ml to 2242 pg/ml ( $n = 6$ ;  $p \geq 0.05$ ; Fig. 9). Furthermore, ArIB [V11L, V16D] reverted the effects of 4-CMTB and resulted in IL-1 $\beta$  levels ranging 512 pg/ml to 2330 pg/ml ( $n = 6$ ;  $p \geq 0.05$ ; Fig. 9). When the FFA2 agonist 4-CMTB (50  $\mu$ M) was given in the absence of BzATP, only low amounts of IL-1 $\beta$  (82 pg/ml to 476 pg/ml;  $n = 6$ ) were detected.

The LDH activity measurements are shown in Table S4. The median of the LDH activity measured, is generally low, under 4.5%. However, a significant increase in the LDH activity is seen for some experiments. Cells stimulated with LPS + BzATP and the addition of 4-CMTB (10  $\mu$ M) as well as LPS + BzATP + 4-CMTB (10  $\mu$ M) + RgIA4 (50 nM) are significantly different compared to data of cells treated with only LPS + BzATP. The number (n) varies between 5-6.

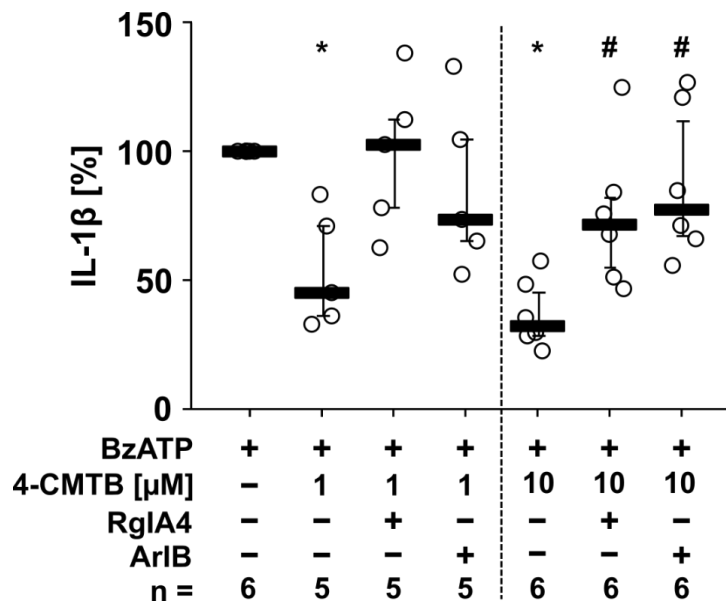


**Figure 9. Involvement of nicotinic acetylcholine receptors (nAChRs) in the FFA2-mediated inhibition of the BzATP (3'-O-(4-benzoyl) benzoyl ATP)-induced release of interleukin-1 $\beta$  (IL-1 $\beta$ ).** Human blood was freshly drawn from healthy volunteers. Peripheral blood mononuclear cells (hPBMCs) were “pulsed” with lipopolysaccharide (LPS; 5 ng/ml for 25 min) during the process of hPBMC isolation. After culturing for 3 h, non-adherent cells were removed. The nAChR antagonists RgIA4 (50 nM) and ArIB [V11L, V16D] (500 nM) were preincubated and added 10 min prior to the addition of the P2X7 receptor agonist BzATP (100  $\mu$ M) in the absence and presence of the FFA2 agonist 4-CMTB (1  $\mu$ M and 10  $\mu$ M). 4-CMTB inhibits the BzATP-induced IL-1 $\beta$  release. This inhibition is partly reversed by the nAChRs antagonists RgIA4 and ArIB [V11L, V16D]. The IL-1 $\beta$  concentration measured in supernatants of cells treated with LPS alone were deducted from all other values. The IL-1 $\beta$  concentration in experiments where pulsed hPBMCs were stimulated with BzATP alone was set to 100% and all other values were calculated accordingly. Data are presented as individual data points, bars represent median, whiskers percentiles 25 and 75. Friedmann-test followed by Wilcoxon signed-

rank test. \*  $p \leq 0.05$  significantly different from samples where BzATP was given alone to LPS-pulsed hPBMCs. #  $p \leq 0.05$  significantly different from samples where BzATP and 4-CMTB were given to LPS-pulsed hPBMCs.

### **3.1.6 The signaling of the FFA3 involves nAChRs containing subunits $\alpha 7$ and $\alpha 9/\alpha 10$**

Comparable experiments to the ones conducted in 3.1.5 were performed here. The hypothesis was tested that the stimulation of the FFA3 results in an activation of nAChRs, which downregulate the secretion of IL-1 $\beta$  by hPBMCs. In a first step the nAChR antagonists RgIA4 and ArIB [V11L, V16D] were added, following the addition of the synthetic FFA3 agonist AR420626. Then, BzATP was added, to induce IL-1 $\beta$  release.

While in supernatants of LPS-pulsed cells low amounts of IL-1 $\beta$  (139 pg/ml to 367 pg/ml;  $n = 5$ ; not shown) were detected, additional stimulation with BzATP (100  $\mu$ M) resulted in elevated IL-1 $\beta$  levels in the range of 468 to 3215 pg/ml ( $n = 5$ ;  $p \geq 0.05$ ; Fig. 10).

The secretion of IL-1 $\beta$  was inhibited by AR420626 (50  $\mu$ M;  $p \geq 0.05$ ; Fig. 10). When conopeptides RgIA4 (50 nM) and ArIB [V11L, V16D] (500 nM) were combined with AR420626 at a concentration of 50  $\mu$ M, significant changes were seen ( $n = 5$ ; Fig. 10). Using RgIA4, the IL-1 $\beta$  concentrations were reversed to a level ranging from 543 pg/ml to 2875 pg/ml ( $n = 5$ ;  $p \geq 0.05$ ; Fig. 10). A similar reverting effect was seen using ArIB [V11L, V16D] with levels of IL-1 $\beta$  ranging from 529 pg/ml to 2693 pg/ml ( $n = 5$ ;  $p \geq 0.05$ ; Fig. 10). When the FFA3 agonist AR420626 (50  $\mu$ M) was given in the absence of BzATP, only low amounts of IL-1 $\beta$  (128 pg/ml to 958 pg/ml;  $n = 5$ ; not shown) were detected.

The LDH activity measurements are shown in Table S5. The median of the LDH activity measured in cell supernatants, is generally low, under 2.0. However, a significant increase is seen in some experiments. Cells stimulated with LPS + BzATP and the addition of AR420626 (50  $\mu$ M) are significantly different compared to data of cells treated with only LPS + BzATP. Furthermore, the addition of both conopeptides ArIB [V11L, V16D] (500 nM) and RgIA4 (50 nM) to AR420626 (50  $\mu$ M) + LPS + BzATP are significantly different compared to data of cells treated with only LPS + BzATP. The number ( $n$ ) varies between 5-6.

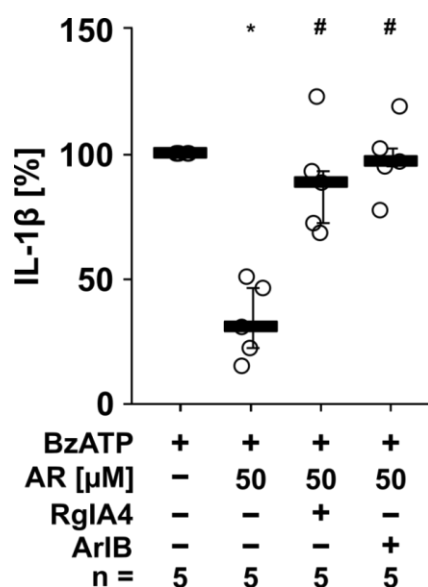


**Figure 10. Involvement of nicotinic acetylcholine receptors (nAChRs) in the FFA3-mediated inhibition of the BzATP (3'-O-(4-benzoyl) benzoyl ATP)-induced release of interleukin-1 $\beta$  (IL-1 $\beta$ ).** Human blood was freshly drawn from healthy volunteers. Peripheral blood mononuclear cells (hPBMCs) were “pulsed” with lipopolysaccharide (LPS; 5 ng/ml for 25 min) during the process of hPBMC isolation. After culturing for 3 h, non-adherent cells were removed. The nAChRs antagonists RgIA4 (50 nM) and ArIB [V11L, V16D] (500 nM) were added 10 min prior to the addition of the P2X7 receptor agonist BzATP (100  $\mu$ M) in the absence and presence of the FFA3 agonist AR420626 (50  $\mu$ M). AR420626 inhibits the BzATP-induced IL-1 $\beta$  release. This inhibition is partly reversed by the nAChRs antagonists RgIA4 and ArIB [V11L, V16D]. The IL-1 $\beta$  concentration measured in supernatants of cells treated with LPS alone were deducted from all other values. The IL-1 $\beta$  concentration in experiments where pulsed hPBMCs were stimulated with BzATP alone was set to 100% and all other values were calculated accordingly. Data are presented as individual data points, bars represent median, whiskers percentiles 25 and 75. Friedmann-test followed by Wilcoxon signed-rank test. \*  $p \leq 0.05$  significantly different from samples where BzATP was given alone to LPS-pulsed hPBMCs. #  $p \leq 0.05$  significantly different from samples where BzATP and AR420626 were given to LPS-pulsed hPBMCs.

## 3.2 SCFAs and synthetic receptor agonists and the effect on the IL-1 $\beta$ release in mPBMCs from wild-type and FFA2 gene-deficient mice

### 3.2.1 The BzATP- or ATP-induced IL-1 $\beta$ release by wild-type mPBMCs

This set of experiments was performed on mPBMCs. The process of isolation is similar to the one performed on the hPBMCs mentioned in 3.1.1. Blood was drawn from the vena cava of sacrificed mice. Cells were “pulsed” with 10 ng/ml LPS, similar to the hPBMCs, being the first of two stimuli for the IL-1 $\beta$  secretion. The mPBMCs were isolated via Percoll™ density gradient centrifugation. Then cultured for 2 h, after which the mPBMCs were purified by adherence selection. After discarding the non-adherent cells, the second stimulus BzATP or ATP was added to the cells for 30 min to induce IL-1 $\beta$  release.

In supernatants of cells pulsed with LPS alone, low amounts of IL-1 $\beta$  (0 pg/ml to 8 pg/ml; n = 28; Fig. 11) were measured. An additional stimulation with BzATP (100  $\mu$ M) resulted in detected IL-1 $\beta$  levels ranging from 5 pg/ml to 43 pg/ml (n = 9; p  $\geq$  0.05; Fig. 11). The stimulation with ATP (1 mM) resulted in higher IL-1 $\beta$  levels from 24 pg/ml to 376 pg/ml (n = 28; p  $\geq$  0.05; Fig. 11). ATP was used as a second stimulus in most following experiments.

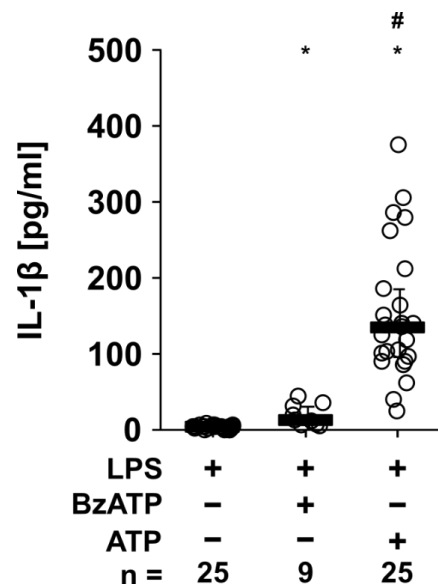


**Figure 11.** The impact of BzATP (3'-O-(4-benzoyl) benzoyl ATP) or ATP on the secretion of interleukin-1 $\beta$  (IL-1 $\beta$ ). Mouse blood was freshly drawn from sacrificed mice. Peripheral blood mononuclear cells (mPBMCs) were “pulsed” with

lipopolysaccharide (LPS; 10 ng/ml for 30 min) during the process of mPBMC isolation. After culturing for 2 h, non-adherent cells were removed. The P2X7 agonists BzATP (100  $\mu$ M) or ATP (1 mM) were added. 30 min later, cell-free cell culture supernatants were harvested and IL-1 $\beta$  was measured by ELISA. The data depicted in this figure are a summary of the respective data shown in figures 8-11. Data are presented as individual data points, bars represent median, whiskers percentiles 25 and 75. Friedmann-test followed by Wilcoxon signed-rank test. \*  $p \leq 0.05$  significantly different from LPS-pulsed mPBMCs. #  $p \leq 0.05$  significantly different from samples where ATP was given to LPS-pulsed mPBMCs.

### **3.2.2 Inhibition of IL-1 $\beta$ release by wild-type mice via SCFAs**

The following pre-experiments were performed on wild-type mPBMCs to test the hypothesis that the SCFAs, being acetate, butyrate and propionate, induce a cholinergic mechanism to inhibit the release of IL-1 $\beta$  in mPBMCs. The cholinergic agonist PC was included as a positive control. In the supernatants of cells “pulsed” with LPS low amounts of IL-1 $\beta$  were measured (0 pg/ml to 7 pg/ml;  $n = 13$ ; Fig. 12). The addition of BzATP showed a slightly higher amount of IL-1 $\beta$  measured in the supernatants (5 pg/ml to 43 pg/ml;  $p \geq 0.05$ ;  $n = 9$ ; Fig. 12). The elevation of IL-1 $\beta$  in the supernatants reached levels of 40 pg/ml to 279 pg/ml ( $n = 13$ ;  $p \geq 0.05$ ; Fig. 12) after addition of ATP.

PC (200  $\mu$ M) was added to the cells, resulting in a significantly reduced amount of IL-1 $\beta$  measured in the supernatants. The values ranging from 6 pg/ml to 55 pg/ml ( $n = 6$ ;  $p \geq 0.05$ ; Fig. 12). The IL-1 $\beta$  secretion was also inhibited significantly by all 3 SCFAs that were added separately. An inhibition was seen with the addition of butyrate (20 mM; 9 pg/ml to 114 pg/ml;  $n = 10$ ;  $p \geq 0.05$ ; Fig. 12). Another reduction of IL-1 $\beta$  was measured in the supernatants after the addition of acetate (20 mM; 7 pg/ml to 87 pg/ml;  $p \geq 0.05$ ;  $n = 7$ ; Fig. 12). Furthermore, reduced IL-1 $\beta$  values were detected in the supernatants of cells after the addition of propionate (9 pg/ml to 131 pg/ml;  $n = 7$ ;  $p \geq 0.05$ ; Fig. 12).

When the SCFAs were added in absence of ATP, only low amounts of IL-1 $\beta$  were detected. For acetate (20 mM) the values started at 2 pg/ml and reached 17 pg/ml ( $n = 6$ ; Fig. 12). Similar low amounts were measured with butyrate (4 pg/ml to 8 pg/ml;  $n = 6$ ; Fig. 12) and propionate (4 pg/ml to 8 pg/ml;  $n = 5$ ; Fig. 12).

The LDH activity measurements are shown in Table S6. The median of the LDH activity measured is under 10.0%. No significant differences are seen among the experimental groups (Friedman-test  $p = 0.08$ ). The number (n) varies between 5-13.

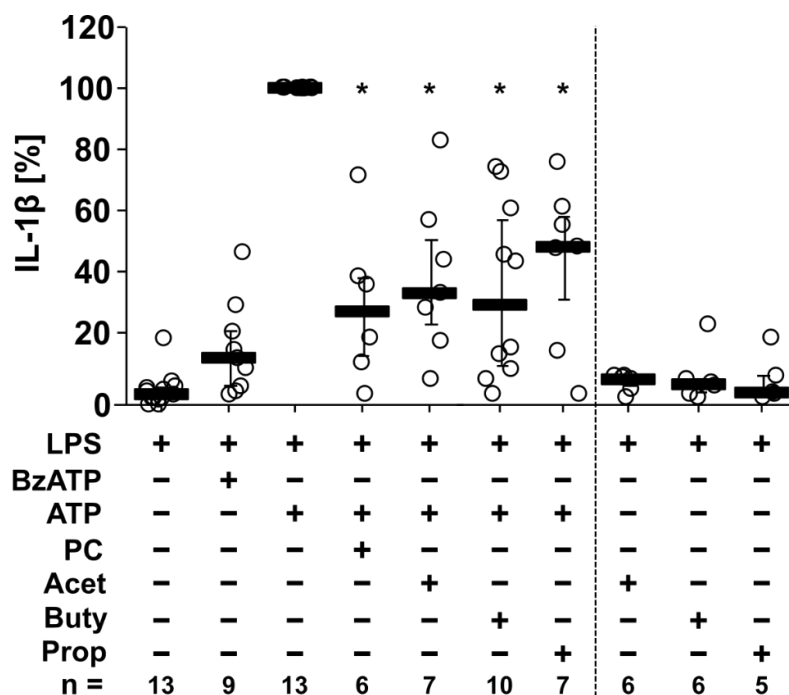


**Figure 12. Inhibition in the ATP-induced release of interleukin-1 $\beta$  (IL-1 $\beta$ ) by phosphocholine (PC), acetate (Acet), butyrate (Buty) and propionate (Prop).** Mouse blood was freshly drawn from sacrificed mice. Mouse peripheral blood mononuclear cells (mPBMCs) were “pulsed” with lipopolysaccharide (LPS; 10 ng/ml for 30 min) during the process of mPBMC isolation. After culturing for 2 h, non-adherent cells were removed. The cholinergic agonist PC (200  $\mu$ M), acetate (20 mM), butyrate (20 mM) and propionate (20 mM) were added 10 min prior to BzATP (100  $\mu$ M) or ATP (1 mM). All compounds inhibited the ATP-induced IL-1 $\beta$  secretion significantly. The IL-1 $\beta$  concentration in experiments where pulsed mPBMCs were stimulated with ATP alone was set to 100% and all other values were calculated accordingly. Data are presented as individual data points, bars represent median, whiskers percentiles 25 and 75. Friedmann-test followed by Wilcoxon signed-rank test. \*  $p \leq 0.05$  significantly different from samples where ATP was given alone to LPS-pulsed mPBMCs.

### 3.2.3 Inhibition of IL-1 $\beta$ release via SCFAs by wild-type and gene-deficient mPBMCs

Next, the hypothesis was tested, that the inhibition of the IL-1 $\beta$  release via SCFAs is dependent on the FFA2. This was done by performing the experiments on FFA2 gene-deficient and corresponding wild-type mPBMCs. The supernatants of cells in both groups of mPBMCs “pulsed” with only LPS showed low amounts of IL-1 $\beta$  from 1 pg/ml to 7 pg/ml (n = 6; Fig. 13) in wild-type mPBMCs and 6 pg/ml to 10 pg/ml (n = 5; Fig. 13) in the gene-deficient group. After the addition of ATP, higher levels of IL-1 $\beta$  were measured in both of the groups. In wild-type mPBMCs the values ranged from 101 pg/ml to 163 pg/ml (n = 6; p  $\geq$  0.05; Fig. 13) and in FFA2 gene-deficient mPBMCs the values showed a higher fluctuation from 43 pg/ml to 348 pg/ml (n = 5; p  $\geq$  0.05; Fig. 13).

PC was added to the cells in both groups of mPBMCs and likewise showed a significant inhibition of the IL-1 $\beta$  measured in the supernatants of the cells. In the wild-type group reduced levels were seen from 17 pg/ml to 64 pg/ml (n = 6; p  $\geq$  0.05; Fig. 13). The gene-deficient group showed values from 29 pg/ml to 129 pg/ml (n = 5; p  $\geq$  0.05; Fig. 13). After the addition of the SCFAs, the group of the wild-type mPBMCs showed a significant inhibition of IL-1 $\beta$  release as seen in the previous experiments performed in 3.2.2. Acetate (20 mM) provoked a reduction of IL-1 $\beta$  values from 53 pg/ml to 133 pg/ml (n = 6; p  $\geq$  0.05; Fig. 13). In propionate (20 mM) similar values were measured (75 pg/ml to 96 pg/ml; n = 6; Fig. 13). Butyrate (20 mM) as seen in 3.2.2 also led to a reduction of the IL-1 $\beta$  release measured in the cell supernatants (41 pg/ml to 71 pg/ml; n = 6; p  $\geq$  0.05; Fig. 13). In direct comparison, no significant reduction in the IL-1 $\beta$  values were measured after the addition of the SCFAs in the corresponding gene-deficient group of mPBMCs. After the addition of acetate (54 pg/ml to 204 pg/ml; n = 5; p  $\geq$  0.05; Fig. 13), propionate (51 pg/ml to 235 pg/ml; n = 5; p  $\geq$  0.05; Fig. 13) or butyrate (66 pg/ml to 204 pg/ml; n = 5; p  $\geq$  0.05; Fig. 13), IL-1 $\beta$  levels did not significantly differ from those treated with LPS and ATP.

When the SCFAs were added in absence of ATP, only low amounts of IL-1 $\beta$  were detected in both groups of mPBMCs. For acetate (20 mM) the values started at 0 pg/ml and reached 8 pg/ml (n = 6; Fig. 13) in the wild-type group and 4 pg/ml to 16 pg/ml (n = 4; Fig. 13) in the gene-deficient group. Similar low amounts were measured with propionate in wild-type mPBMCs (0 pg/ml to 7 pg/ml; n = 6; Fig. 13) and in gene-

deficient mPBMCs (2 pg/ml to 12 pg/ml; n = 3; Fig. 13) as well as with butyrate in the wild-type group (0 pg/ml to 10 pg/ml; n = 6; Fig. 13) and the gene-deficient group (2 pg/ml to 10 pg/ml; n = 3; Fig. 13).

The LDH activity measurements are shown in Table S7. Data from wild-type and the gene-deficient mice were statistically analyzed separately. The median of the LDH activity measured in the cell supernatants of the wild-type group is under 8.5%. A significant increase in the LDH activity is seen in some experiments. Cells stimulated with LPS + ATP + PC (200  $\mu$ M) are significantly different compared to data of cells treated with LPS + ATP. The number (n) is 6 for each experimental group. The median of the LDH activity measured in the cell supernatants of the gene-deficient group is under 9.0%. No significant differences are seen for the values, at a Friedman-test of 0.19. The number (n) varies between 3-5.

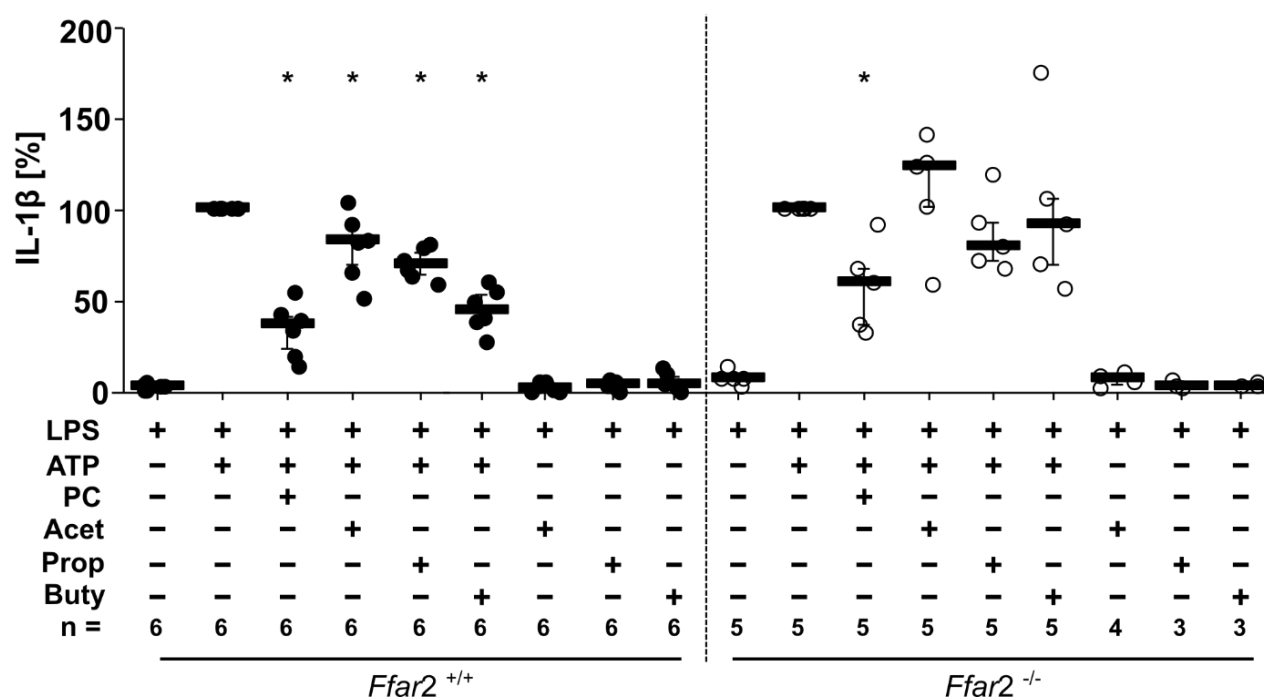


**Figure 13. Effects of short-chain fatty acids (SCFAs) on the release of IL-1 $\beta$  by wild-type and FFA2 gene-deficient mouse peripheral blood mononuclear cells (mPBMCs).** Mouse blood was freshly drawn from sacrificed mice. During the process of isolation, mPBMCs were “pulsed” with lipopolysaccharide (LPS; 10 ng/ml for 30 min). After culturing for 2 h, non-adherent cells were removed. Phosphocholine (PC; 200  $\mu$ M) and the SCFAs acetate (Acet; 20 mM), butyrate (But; 20 mM) or propionate (Prop; 20 mM) were added 10 min prior to the P2X7 agonist ATP (1 mM). PC and the SCFAs

inhibited the ATP-induced IL-1 $\beta$  secretion significantly in wild-type mice. PC also inhibits the ATP-induced IL-1 $\beta$  release in FFA2 gene-deficient mice. The SCFAs do not lead to an IL-1 $\beta$  inhibition in gene-deficient mice. The IL-1 $\beta$  concentration in experiments where pulsed mPBMCs were stimulated with ATP alone was set to 100% and all other values were calculated accordingly. Data are presented as individual data points, bars represent median, whiskers percentiles 25 and 75. Friedmann-test followed by Wilcoxon signed-rank test. \*  $p \leq 0.05$  significantly different from samples where ATP was given alone to LPS-pulsed mPBMCs.

### **3.2.4 Inhibition of IL-1 $\beta$ release via FFA2 and FFA3 agonists**

The following pre-experiments were performed on wild-type mPBMCs to test the hypothesis that the stimulation of the FFA2 and FFA3 via the agonists 4-CMTB and AR420626 downregulates the ATP-induced IL-1 $\beta$  release. While in supernatants of LPS-pulsed cells low amounts of IL-1 $\beta$  were measured (0 pg/ml to 8 pg/ml;  $n = 6$ ; Fig. 14), additional stimulation with ATP resulted in an elevation of the IL-1 $\beta$  concentrations in the supernatants (124 pg/ml to 306 pg/ml;  $n = 6$ ;  $p \geq 0.05$ ; Fig. 14).

The IL-1 $\beta$  secretion was significantly inhibited after the addition of synthetic FFA2 agonist 4-CMTB (10  $\mu$ M; 33 pg/ml to 216 pg/ml;  $n = 5$ ;  $p \geq 0.05$ ; Fig. 14) or FFA3 agonist AR420626 (20  $\mu$ M; 7 pg/ml to 45 pg/ml;  $n = 5$ ;  $p \geq 0.05$ ; Fig. 14). A stronger inhibition was measured after the addition of AR420626 compared to 4-CMTB. When FFA2 agonist 4-CMTB was given without the addition of ATP low amounts of IL-1 $\beta$  were measured (4 pg/ml to 5 pg/ml;  $n = 2$ ; Fig. 14). The same effect was seen with the addition of FFA3 agonist AR420626 without ATP (2 pg/ml to 4 pg/ml;  $n = 2$ ; Fig. 14).

The LDH activity measurements are shown in Table S8. The median of the LDH activity measured is under 22.0%. No significant differences are seen among the experimental groups (Friedman-test  $p = 0.12$ ). The number ( $n$ ) varies between 2-6.

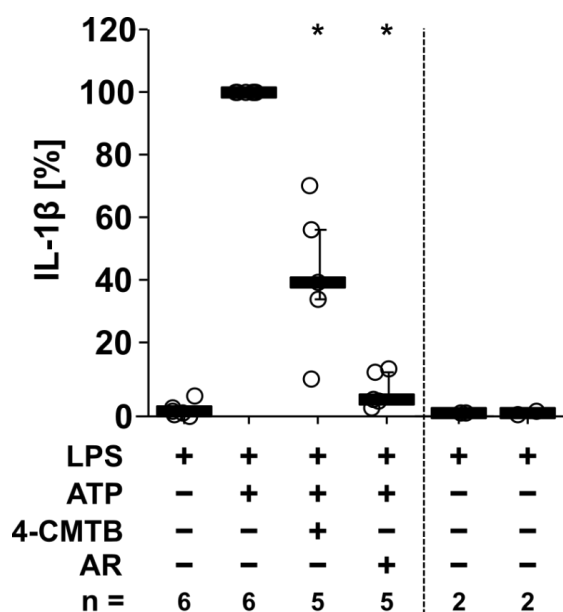


**Figure 14. The FFA2 and FFA3 agonists inhibit the ATP-induced release of interleukin-1 $\beta$  (IL-1 $\beta$ ) by wild-type mouse peripheral blood mononuclear cells (mPBMCs).** Mouse blood was freshly drawn from sacrificed mice. Mouse peripheral blood mononuclear cells (mPBMCs) were “pulsed” with lipopolysaccharide (LPS; 10 ng/ml for 30 min) during the process of mPBMC isolation. After culturing for 2 h, non-adherent cells were removed. The P2X7 agonist ATP (1 mM) was added in the absence and presence of FFA2 agonist 4-CMTB (10  $\mu$ M) or the FFA3 agonist AR420626 (20  $\mu$ M). 4-CMTB and AR420626 inhibited the ATP-induced IL-1 $\beta$  secretion significantly. The IL-1 $\beta$  concentration in experiments where pulsed mPBMCs were stimulated with ATP alone was set to 100% and all other values were calculated accordingly. Data are presented as individual data points, bars represent median, whiskers percentiles 25 and 75. Friedmann-test followed by Wilcoxon signed-rank test. \*  $p \leq 0.05$  significantly different from samples where ATP was given alone to LPS-pulsed mPBMCs.

### 3.2.5 Inhibition of IL-1 $\beta$ release via FFA2 and FFA3 agonists in wild-type and gene-deficient mice

Next, the hypothesis was tested, that AR420626 inhibits the ATP-dependent IL-1 $\beta$  release in FFA2 gene-deficient mPBMCs, while 4-CMTB on the other hand does not. Wild-type

mice of the same genetic background like the gene-deficient mice were included in these experiments. The wild-type and *Ffar2* gene-deficient mPBMCs only stimulated with LPS both showed a low IL-1 $\beta$  release in the supernatants. The wild-type group showed values from 1 pg/ml to 7 pg/ml (n = 6; Fig. 15) and the gene-deficient group values from 6 pg/ml to 10 pg/ml (n = 5; Fig. 15). After the addition of ATP and 0.2% DMSO elevated levels of IL-1 $\beta$  were measured. In wild-type mPBMCs values ranging from 65 pg/ml to 186 pg/ml (n = 6;  $p \geq 0.05$ ; Fig. 15) and in gene-deficient mPBMCs levels from 66 pg/ml to 293 pg/ml (n = 5;  $p \geq 0.05$ ; Fig. 15).

In both groups of mPBMCs a statistically significant reduction of the IL-1 $\beta$  secretion was measured after the addition of FFA3 agonist AR420626 (20  $\mu$ M). A reduction was seen in the wild-type mPBMCs with values from 42 pg/ml to 66 pg/ml (n = 6;  $p \geq 0.05$ ; Fig. 15) as well as in FFA2 gene-deficient mPBMCs (40 pg/ml to 219 pg/ml; n = 5;  $p \geq 0.05$ ; Fig. 15). A significant inhibition of the IL-1 $\beta$  release after the addition of the FFA2 agonist 4-CMTB (20  $\mu$ M) was only measured in wild-type mPBMCs (52 pg/ml to 130 pg/ml; n = 6;  $p \geq 0.05$ ; Fig. 15). In FFA2 gene-deficient mPBMCs values started at 71 pg/ml and reached 205 pg/ml (n = 5; Fig. 15).

When the FFA2 agonist 4-CMTB dissolved in DMSO was given without the addition of ATP, low amounts of IL-1 $\beta$  were measured in both groups. In cell culture supernatants of the wild-type mPBMCs low values of 5 pg/ml to 9 pg/ml (n = 6; Fig. 15) were measured and in supernatants of gene-deficient mPBMCs similar low amounts from 6 pg/ml to 13 pg/ml (n = 5; Fig. 15).

The LDH activity measurements are shown in Table S9. The wild-type and the gene-deficient data were statistically analyzed separately. The median of the LDH activity measured in the supernatants of the wild-type group is under 4.5%. No significant differences are seen among the experimental groups (Friedman-test  $p = 0.06$ ). The number (n) is 6 for each experimental group. The median of the LDH activity measured in the supernatants of the gene-deficient group is under 10.0%. No significant differences are seen for the values, at a Friedman-test of 0.19. The number (n) is 5 for each experimental group.

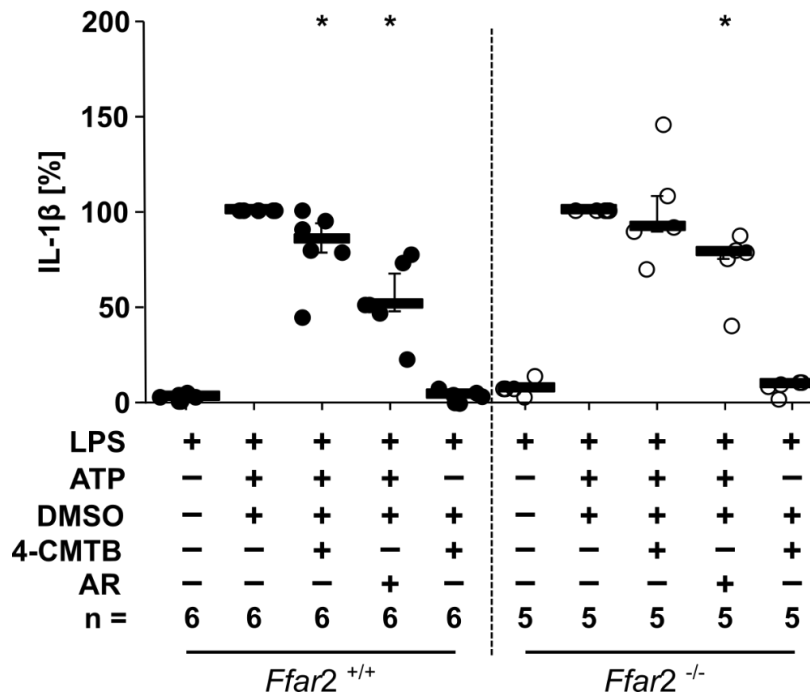
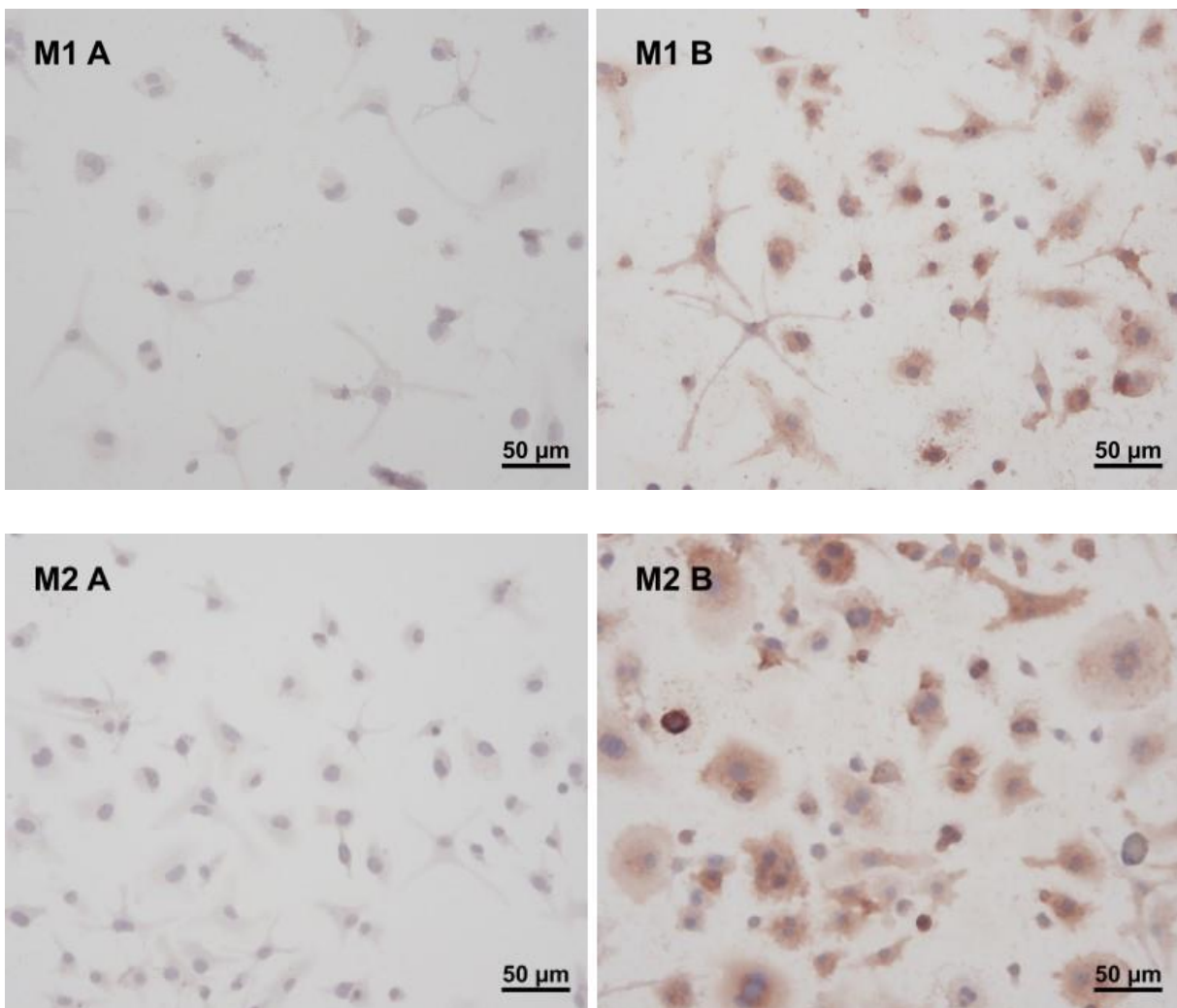


**Figure 15. The FFA2 and FFA3 agonists inhibit the ATP-induced release of interleukin-1 $\beta$  (IL-1 $\beta$ ) in wild-type and FFA2 gene-deficient mouse peripheral blood mononuclear cells (mPBMCs).** Mouse blood was freshly drawn from sacrificed mice. Mouse peripheral blood mononuclear cells (mPBMCs) were “pulsed” with lipopolysaccharide (LPS; 10 ng/ml for 30 min) during the process of mPBMC isolation. After culturing for 2 h, non-adherent cells were removed. ATP (1 mM) as well as DMSO 0.2% were added in the absence and presence of FFA2 agonist 4-CMTB (10  $\mu$ M) or the FFA3 agonist AR420626 (20  $\mu$ M) in both wild-type and gene-deficient mPBMCs. 4-CMTB and AR420626 inhibited the ATP-induced IL-1 $\beta$  secretion significantly in the wild-type group. AR420626 also inhibited the ATP-induced IL-1 $\beta$  secretion in the gene-deficient group, however, 4-CMTB did not inhibit the secretion. The IL-1 $\beta$  concentration in experiments where pulsed mPBMCs were stimulated with ATP alone was set to 100% and all other values were calculated accordingly. Data are presented as individual data points, bars represent median, whiskers percentiles 25 and 75. Friedmann-test followed by Wilcoxon signed-rank test. \*  $p \leq 0.05$  significantly different from samples where ATP was given alone to LPS-pulsed mPBMCs.

### **3.3 SCFA and synthetic FFA agonists induce a cholinergic mechanism to inhibit the ATP-induced release of IL-1 $\beta$ by mouse BMDMs**

#### **3.3.1 Cell characterization via F4/80 staining**

The experiments are performed on mouse BMDMs in this chapter. To verify that the cells are indeed differentiated macrophages, that express the F4/80 glycoprotein, an immunohistochemical staining was performed. Bone marrow cells were treated according to the protocol in 2.2.2.3. Figures 16 M1, M2 and M3 A show the cells with an hemalum coloring. In figures 16 M1, M2 and M3 B F4/80 is stained in brown color in a majority of cells. Furthermore, the typical variable morphological structure of macrophages is detected, classifying them to be macrophages. In technical control experiments, in which the primary antibodies were omitted, virtually no brown staining was visible (data not shown).



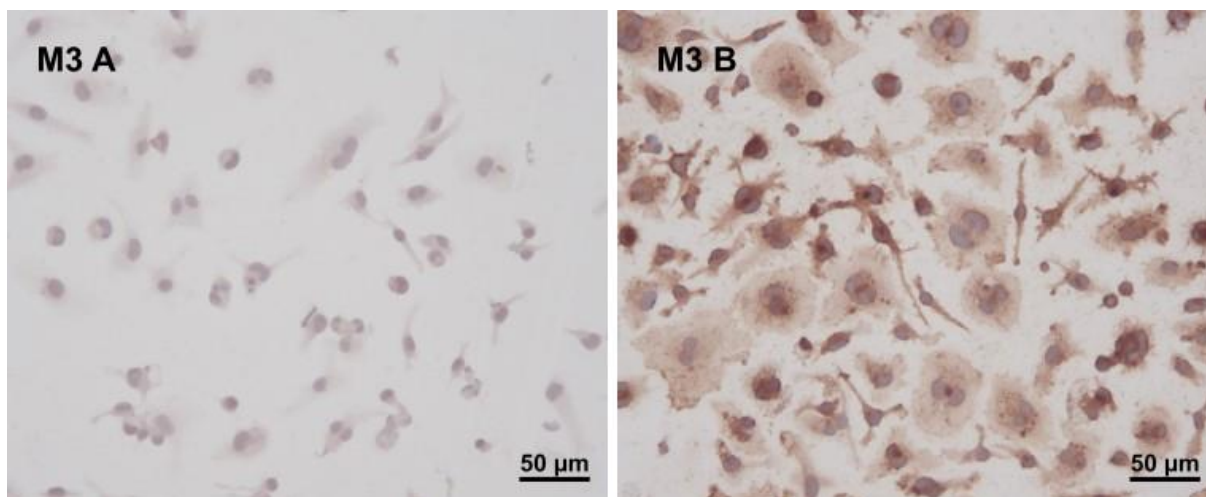


**Figure 16. Immunohistochemical localization of the F4/80 antigen in mouse bone marrow-derived cells.** Mouse bone marrow cells of 3 mice (M1, M2 and M3) were seeded out at a density of  $0.125 \times 10^6$  cells/200  $\mu$ l medium per well and differentiated into bone marrow-derived macrophages via stimulation with M-CSF, LPS and  $\text{INF-}\gamma$  following a certain protocol mentioned in 2.2.2.3. After 6 days of cultivation, the cells were stained using a primary anti-F2/80 antibody and secondary horse-radish peroxidase-labeled rabbit antibodies directed to rat immunoglobulins. **M1 A, M2 A, M3 A:** Bone marrow-derived cells after stimulation for differentiation, with hemalum staining. Light cells with a subtly darker nucleus visible. Cell membrane not clearly delineated. (Bar = 50  $\mu$ M). **M1 B, M2 B, M3 B:** Bone marrow cells after stimulation and with anti-F4/80 staining in brown color (Bar = 50  $\mu$ M).

### 3.3.2 Double-staining of macrophages and the FFA2 within the murine colon

To confirm that the FFA2 is found in the colon and furthermore, that macrophages in the colon also express the FFA2, a double-staining was performed. A mouse strain was used in which monomeric red fluorescent protein (mRFP) was expressed under the control of the FFA2 promoter. The colon was removed from sacrificed mice, fixed and stained according to 2.2.2.6. The brown staining in figure 17 A shows the mRFP present in that area. Figure 17 B shows macrophages within the colon tissue that show a blue color. Figure 17 C shows the double-staining, using antibodies directed to mouse F4/80 and

mRFP. The arrows are pointing to the double-positive macrophages. In negative controls, in which the primary antibodies were omitted, virtually no staining is visible.

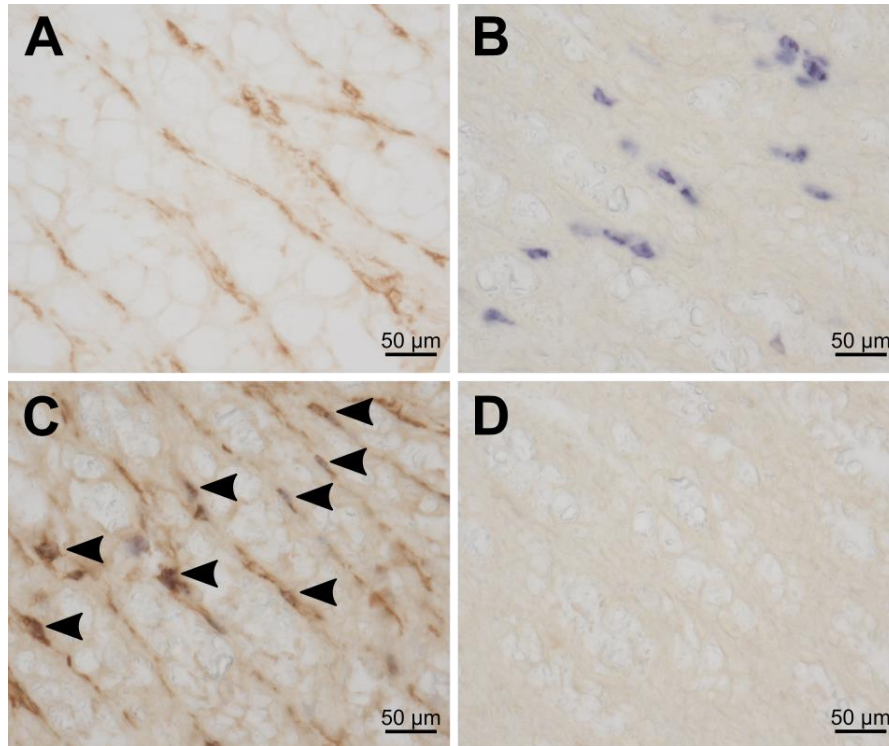


**Figure 17. Double-staining of macrophages and FFA2 within the murine colon.** The expression of FFA2 was studied in the colon of reporter mice expressing monomeric red fluorescent protein (mRFP) under the control of the FFA2 promoter. **A)** Localization of FFA2-mRFP labeled in brown with a peroxidase-coupled detection system in the colon. (Bar = 50 µM) **B)** Immunohistochemical staining of macrophages (F4/80, stained in blue using an AP-coupled detection system) within the colon tissue. (Bar = 50 µM) **C)** Double-staining using antibodies directed to mouse F4/80 and mRFP. The arrows are pointing to double-positive macrophages. (Bar = 50 µM) **D)** Negative control. (Bar = 50 µM)

### 3.3.3 The BzATP or ATP induced release of IL-1 $\beta$ in mouse BMDMs

This set of experiments was performed on mouse BMDMs. Bone marrow cells were isolated from C57BL/6 mice and differentiated by macrophage colony-stimulating factor (M-CSF; 10 ng/ml, 6 days) and interferon- $\gamma$  (IFN- $\gamma$ ; 10 ng/ml, 3 days) to BMDMs. BMDMs were primed for 5 h with LPS (1 µg/ml).

In supernatants of cells that were not primed, low amounts of IL-1 $\beta$  (0 pg/ml to 12 pg/ml; n = 48; Fig. 18) were measured. After the addition of only ATP (1 mM), similar low amounts of IL-1 $\beta$  were measured (4 pg/ml to 223 pg/ml; n = 7; Fig. 18). After the cells were primed with LPS a slight increase of IL-1 $\beta$  was measured, ranging from 9 pg/ml to 595 pg/ml (n = 46; Fig. 18). An additional stimulation with BzATP (100  $\mu$ M) resulted in IL-1 $\beta$  levels ranging from 47 pg/ml to 280 pg/ml (n = 7; p  $\geq$  0.05; Fig. 18). The stimulation with BzATP (300  $\mu$ M) showed elevated IL-1 $\beta$  levels from 109 pg/ml to 295 pg/ml (n = 5; p  $\geq$  0.05; Fig. 18). Compared to cells only primed with LPS, the stimulation with ATP (1 mM) resulted in elevated IL-1 $\beta$  levels from 353 pg/ml to 2029 pg/ml (n = 30; p  $\geq$  0.05; Fig. 18). Furthermore, elevated IL-1 $\beta$  levels were measured after the addition of ATP (2 mM) from 2311 pg/ml to 14738 pg/ml, compared to cells stimulated with LPS alone (n = 22; p  $\geq$  0.05; Fig. 18).

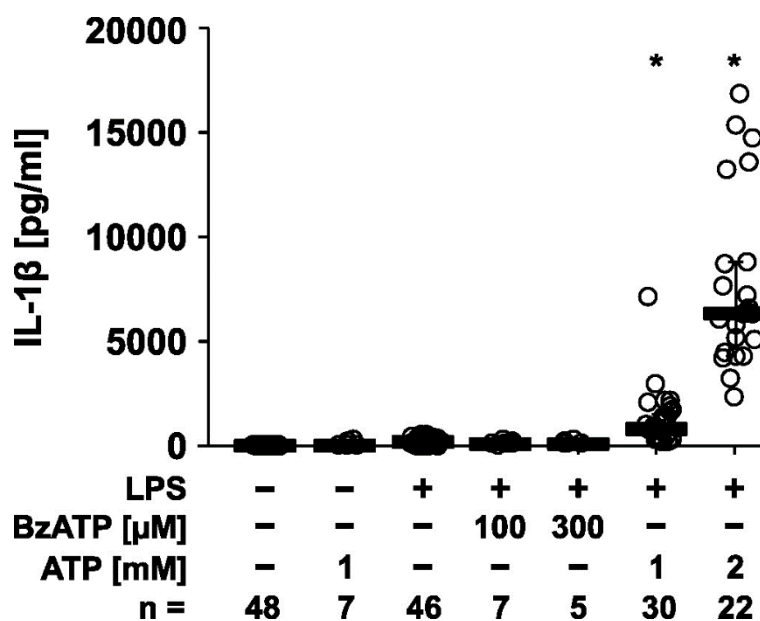


**Figure 18. The impact of BzATP (3'-O-(4-benzoyl) benzoyl ATP) or ATP on the secretion of IL-1 $\beta$ .** Bone marrow cells were isolated from C57BL/6 mice and differentiated by macrophage colony-stimulating factor (M-CSF; 10 ng/ml, 6 days) and interferon- $\gamma$  (IFN- $\gamma$ ; 10 ng/ml, 3 days) to bone marrow-derived macrophages (BMDMs). BMDMs were primed for 5 h with lipopolysaccharide (LPS; 1  $\mu$ g/ml). The P2X7 agonist BzATP (3'-O-(4-benzoyl) benzoyl ATP, 100  $\mu$ M, 300  $\mu$ M) or ATP (1 mM, 2 mM) were added. The IL-1 $\beta$  concentration in experiments where pulsed BMDMs were stimulated with ATP alone was set to 100% and all other values were calculated accordingly. Data

are presented as individual data points, bars represent median, whiskers percentiles 25 and 75. Friedmann-test followed by Wilcoxon signed-rank test. \*  $p \leq 0.05$  significantly different from cells stimulated with LPS alone.

### **3.3.4 The inhibition of ATP-induced IL-1 $\beta$ release in mouse BMDMs via P2X7 receptor antagonist**

To test the hypothesis, that the P2X7 receptor antagonist A438079 leads to an inhibition of the ATP-induced IL-1 $\beta$  secretion in mouse BMDMs the following experiments were performed. In supernatants of cells without the addition of any substance, low amounts of IL-1 $\beta$  were measured (0 pg/ml to 11 pg/ml;  $n = 15$ ; Fig. 19). Furthermore, the stimulation with only ATP (1 mM) also resulted in low IL-1 $\beta$  concentrations in the supernatants (0 pg/ml to 262 pg/ml;  $n = 7$ ; Fig. 19). An elevation in IL-1 $\beta$  concentrations were measured in supernatants of LPS-primed cells (77 pg/ml to 595 pg/ml;  $n = 13$ ;  $p \geq 0.05$ ; Fig. 19).

Low IL-1 $\beta$  levels were measured in the cell supernatants after the addition of 100  $\mu$ M BzATP (97 pg/ml to 280 pg/ml;  $n = 5$ ;  $p \geq 0.05$ ; Fig. 19) or the addition of 300  $\mu$ M BzATP (109 pg/ml to 295 pg/ml;  $n = 5$ ;  $p \geq 0.05$ ; Fig. 19), compared to cells stimulated with LPS + ATP (1 mM). High values of IL-1 $\beta$  were measured after the addition of ATP 1 mM (263 pg/ml to 2029 pg/ml;  $n = 15$ ;  $p \geq 0.05$ ; Fig. 19). Therefore, for the further experiments ATP was used and not BzATP.

After the addition of P2X7 receptor antagonist A438079 10  $\mu$ M together with ATP, a significant reduction of IL-1 $\beta$  was measured, compared to cells stimulated with LPS + ATP (104 pg/ml to 983 pg/ml;  $n = 7$ ;  $p \geq 0.05$ ; Fig. 19). When A439079 was given without ATP, low amounts of IL-1 $\beta$  were measured (622 pg/ml to 678 pg/ml;  $n = 4$ ; Fig. 19).

The LDH activity measurements are shown in Table S10. The median of the LDH activity measured is generally under 15.0%. However, cells stimulated with LPS + ATP + A438079 (10  $\mu$ M) are significantly different compared to data of cells treated with LPS + ATP. The number ( $n$ ) varies between 4-15.

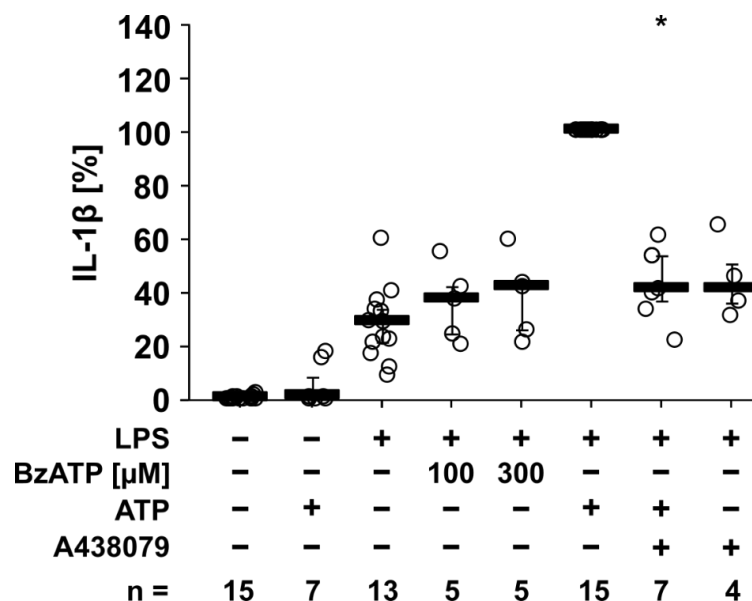


**Figure 19. The impact of P2X7 receptor antagonist A438079 on the ATP-induced release of interleukin-1 $\beta$  (IL-1 $\beta$ ) by mouse bone marrow-derived macrophages (BMDMs).** Bone marrow cells were isolated from C57BL/6 mice and differentiated by macrophage colony-stimulating factor (M-CSF; 10 ng/ml, 6 days) and interferon- $\gamma$  (IFN- $\gamma$ ; 10 ng/ml, 3 days) to BMDMs. BMDMs were primed for 5 h with lipopolysaccharide (LPS; 1  $\mu$ g/ml). The P2X7 agonist BzATP (3'-O-(4-benzoyl) benzoyl ATP) was added in 2 different concentrations (100  $\mu$ M and 300  $\mu$ M). ATP (1 mM) was added in the absence and presence of P2X7 receptor antagonist A439079 (10  $\mu$ M). A439079 inhibits the ATP-induced IL-1 $\beta$  release significantly. The IL-1 $\beta$  concentration in experiments where primed BMDMs were stimulated with ATP alone was set to 100% and all other values were calculated accordingly. Data are presented as individual data points, bars represent median, whiskers percentiles 25 and 75. Friedmann-test followed by Wilcoxon signed-rank test. \*  $p \leq 0.05$  significantly different from cells stimulated with LPS + ATP.

### 3.3.5 The ATP-induced IL-1 $\beta$ release is blunted in the presence of P2X7 and P2X4 receptor antagonists

Next, the hypothesis that the P2X7 and P2X4 receptor antagonists result in a downregulation of the ATP-dependent IL-1 $\beta$  secretion by BMDMs was tested. While in cell culture supernatants of untreated BMDMs (0 pg/ml to 1 pg/ml;  $n = 12$ ; Fig. 20) or BMDMs primed with LPS (37 pg/ml to 403 pg/ml;  $n = 12$ ; Fig. 20) low amounts of IL-

1 $\beta$  were measured, higher levels were measured after the addition of ATP (2 mM; 6041 pg/ml to 16836 pg/ml; n = 12; p  $\geq$  0.05; Fig. 20).

After the addition of P2X4 receptor antagonist 5-BDBD together with ATP, a dose-dependent inhibition of the IL-1 $\beta$  secretion was measured (1  $\mu$ M – 100  $\mu$ M; n = 4-12; p  $\geq$  0.05; Fig. 20). At 1  $\mu$ M a reduction was measured. The IL-1 $\beta$  values ranged from 1400 pg/ml to 15033 pg/ml (n = 8; p  $\geq$  0.05; Fig. 20). The strongest reduction of IL-1 $\beta$  was measured after the addition of 100  $\mu$ M 5-BDBD from 1478 pg/ml and to 4642 pg/ml (n = 6; p  $\geq$  0.05; Fig. 20). The calculated IC<sub>50</sub> value was 34  $\mu$ M.

A similar dose-dependent inhibition of the IL-1 $\beta$  secretion was measured after the addition of P2X7 receptor antagonist A438079 together with ATP (0.5 – 100  $\mu$ M; n = 4-8; p  $\geq$  0.05; Fig. 20). At 0.5  $\mu$ M a slight reduction of the IL-1 $\beta$  concentration was measured (9235 pg/ml to 13407 pg/ml; n = 4; p  $\geq$  0.05; Fig. 20). The strongest reduction of IL-1 $\beta$  was measured after the addition of 100  $\mu$ M of A438079 with values from 77 pg/ml to 479 pg/ml (n = 6; p  $\geq$  0.05; Fig. 20). The calculated IC<sub>50</sub> value was 0.8  $\mu$ M.

When 5-BDBD (10  $\mu$ M) was given without ATP, low amounts of IL-1 $\beta$  were measured (296 pg/ml to 910 pg/ml; n = 8; Fig. 20). Similar low amounts were measured after only A439079 (10  $\mu$ M) was added without ATP (50 pg/ml to 423 pg/ml; n = 6; Fig. 20).

The LDH activity measurements are shown in Table S11. The median of the LDH activity measured in cell supernatants is generally high with values reaching up to 49.9. A significant increase is seen in some experiments. Cells stimulated with LPS + ATP + 5-BDBD (1  $\mu$ M, 10  $\mu$ M, 100  $\mu$ M) are significantly different compared to data of cells treated with LPS + ATP. The same significant difference is seen with LPS + ATP + A438079 (10  $\mu$ M). The number (n) varies between 4-12.

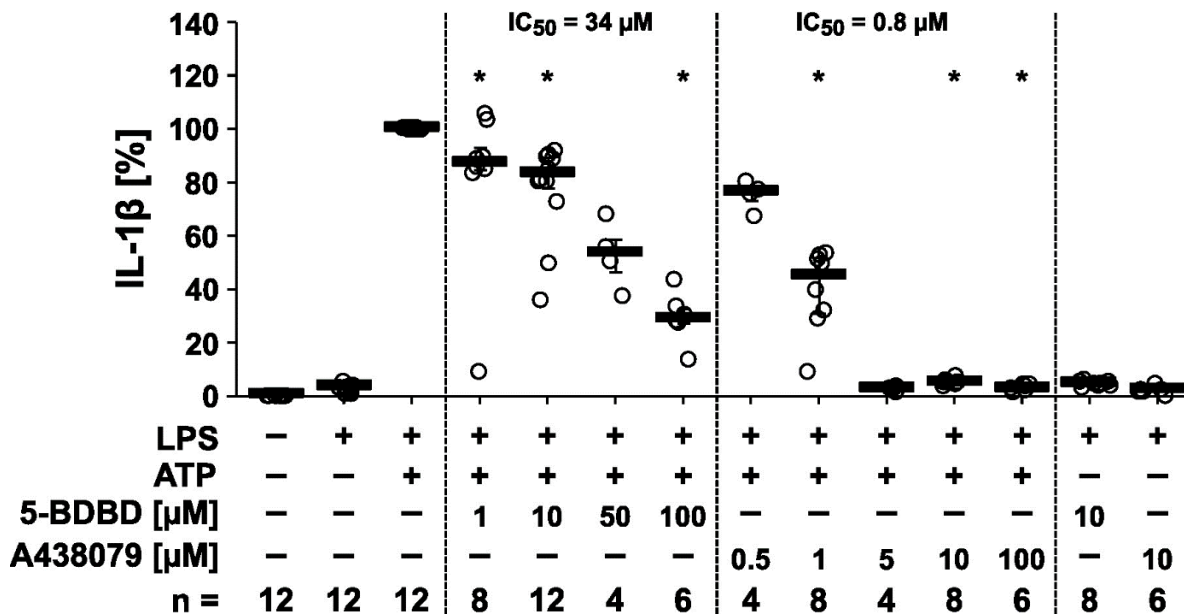


**Figure 20.** The impact of P2X7 receptor antagonist A438079 and P2X4 receptor antagonist 5-BDBD (5-(3-Bromophenyl)-1,3-dihydro-2H-benzofuro[3,2-e]-1,4-diazepin-2-one) on the ATP-induced release of interleukin-1 $\beta$  (IL-1 $\beta$ ) in mouse bone marrow-derived macrophages (BMDMs). Bone marrow cells were isolated from C57BL/6 mice and differentiated by macrophage colony-stimulating factor (M-CSF; 10 ng/ml, 6 days) and interferon- $\gamma$  (IFN- $\gamma$ ; 10 ng/ml, 3 days) to BMDMs. BMDMs were primed for 5 h with lipopolysaccharide (LPS; 1  $\mu$ g/ml). The P2X7 agonist ATP (2 mM) was added in the absence and presence of P2X7 receptor antagonist A439079 (0.5  $\mu$ M, 1  $\mu$ M, 5  $\mu$ M, 10  $\mu$ M, 100  $\mu$ M) and P2X4 receptor antagonist 5-BDBD (1  $\mu$ M, 10  $\mu$ M, 50  $\mu$ M, 100  $\mu$ M). A439079 and 5-BDBD both inhibited the ATP-induced IL-1 $\beta$  release significantly and in a dose-dependent manner ( $IC_{50} = 34 \mu$ M;  $IC_{50} = 0.8 \mu$ M). The IL-1 $\beta$  concentration in experiments where primed BMDMs were stimulated with ATP alone was set to 100% and all other values were calculated accordingly. Data are presented as individual data points, bars represent median, whiskers percentiles 25 and 75. Friedmann-test followed by Wilcoxon signed-rank test. \*  $p \leq 0.05$  significantly different from samples where ATP was given alone to LPS-primed BMDMs.

### **3.3.6 The influence of SCFAs and FFA2 and FFA3 agonists on the ATP-induced IL-1 $\beta$ release**

The hypothesis was tested, that the SCFA butyrate as well as FFA2 and FFA3 agonists inhibit the ATP-induced IL-1 $\beta$  release by murine BMDMs. Cells without any stimulation released only low amounts of IL-1 $\beta$  from 0 pg/ml to 11 pg/ml (n = 8; Fig. 21). The addition of ATP (1 mM) to unprimed BMDMs also resulted in a low amount of IL-1 $\beta$  in the cell culture supernatants (0 pg/ml to 41 pg/ml; n = 6; Fig. 21). Higher values were seen after the cells were primed with LPS (46 pg/ml to 595 pg/ml; n = 8; Fig. 21). After the addition of ATP (1 mM) an increase of IL-1 $\beta$  was measured with values from 263 pg/ml to 2930 pg/ml (n = 8; p  $\geq$  0.05; Fig. 21).

After the addition of nicotinic receptor agonist acetylcholine (10  $\mu$ M) a significant inhibition of the ATP-induced release of IL-1 $\beta$  was measured (105 pg/ml to 530 pg/ml; n = 7; p  $\geq$  0.05; Fig. 21). The addition of butyrate (20 mM) also resulted in a significant inhibition of the IL-1 $\beta$  release (241 pg/ml to 1249 pg/ml; n = 7; p  $\geq$  0.05; Fig. 21). The synthetic FFA2 agonist 4-CMTB (10  $\mu$ M) also resulted in a significant inhibition of the IL-1 $\beta$  secretion (201 pg/ml to 1369 pg/ml; n = 8; p  $\geq$  0.05; Fig. 21) as well as the FFA3 agonist AR420626 (20  $\mu$ M; 125 pg/ml to 734 pg/ml; n = 7; p  $\geq$  0.05; Fig. 21).

The LDH activity measurements are shown in Table S12. The median of the LDH activity measured in cell supernatants is generally low and under 2.0%. However, cells stimulated with LPS + ATP + Butyrate (20 mM) as well as LPS + ATP + 4-CMTB (10  $\mu$ M) and LPS + ATP + AR420626 (20  $\mu$ M) are significantly different compared to data of cells treated with LPS + ATP. The number (n) varies between 6-8.

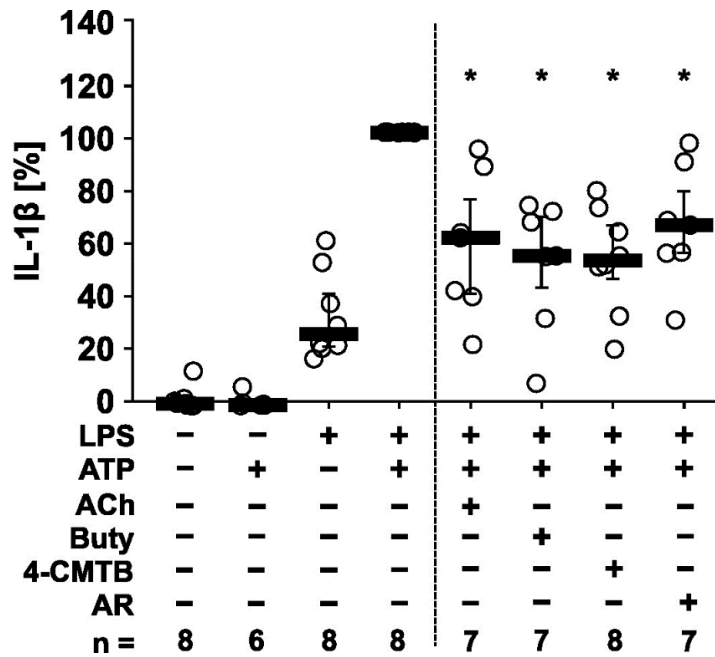


**Figure 21. The influence of short-chain fatty acid (SCFA) butyrate (Buty) on the ATP-induced release of interleukin-1 $\beta$  (IL-1 $\beta$ ) by mouse bone marrow-derived macrophages (BMDMs).** Bone marrow cells were isolated from C57BL/6 mice and differentiated by macrophage colony-stimulating factor (M-CSF; 10 ng/ml, 6 days) and interferon- $\gamma$  (IFN- $\gamma$ ; 10 ng/ml, 3 days) to BMDMs. BMDMs were primed for 5 h with lipopolysaccharide (LPS; 1  $\mu$ g/ml) and ATP (1 mM, 30 min). The induced release of IL-1 $\beta$  was investigated in the cell culture supernatant. ATP (2 mM) was added in the absence and presence of the SCFA, the FFA2 (4-CMTB) and FFA3 (AR420626; AR) agonists. These inhibited the ATP-mediated IL-1 $\beta$  release significantly. The IL-1 $\beta$  concentration in experiments where primed BMDMs were stimulated with ATP alone was set to 100% and all other values were calculated accordingly. Data are presented as individual data points, bars represent median, whiskers percentiles 25 and 75. Friedmann-test followed by Wilcoxon signed-rank test. \*  $p \leq 0.05$  significantly different from samples where ATP was given alone on LPS-primed BMDMs.

### **3.3.7 The signaling of FFA2 and FFA3 involve nAChR containing $\alpha 7$ and $\alpha 9/\alpha 10$**

Finally, the last hypothesis was tested, that the signaling of FFA2 and FFA3 involves the nAChR containing subunits  $\alpha 7$  and  $\alpha 9/\alpha 10$  in murine BMDMs. These experiments were performed on mouse BMDMs not only with the measurement of IL-1 $\beta$ , but also as pilot experiments where IL-1 $\alpha$  was measured (see figure 22 B).

In cell culture supernatants of untreated BMDMs IL-1 $\beta$  concentrations remained below the level of detection (0 pg/ml; n = 5; Fig. 22 A). The cells primed with LPS showed slightly higher values of IL-1 $\beta$  from 123 pg/ml to 148 pg/ml (n = 5; Fig. 22 A). After the addition of ATP (2 mM) to BMDMs, higher IL-1 $\beta$  levels were measured (2311 pg/ml to 6610 pg/ml; n = 5; p  $\geq$  0.05; Fig. 22 A). The addition of FFA2 agonist 4-CMTB (20  $\mu$ M) resulted in a significant inhibition of the ATP-induced IL-1 $\beta$  release (48 pg/ml to 212 pg/ml; n = 5; p  $\geq$  0.05; Fig. 22 A). This inhibition was significantly reversed by the addition of nAChR antagonists RgIA4 (2315 pg/ml to 5646 pg/ml; n = 5; p  $\geq$  0.05; Fig. 22 A) and ArIB [V11L, V16D] (1605 pg/ml to 6716 pg/ml; n = 5; p  $\geq$  0.05; Fig. 22 A).

A significant reduction of the ATP-induced release of IL-1 $\beta$  similar to that provoked by 4-CMTB was seen after the addition of the FFA3 agonist AR420626 (50  $\mu$ M; 32 pg/ml to 166 pg/ml; n = 5; p  $\geq$  0.05; Fig. 22 A). This inhibition was also significantly reversed by the addition of nAChR antagonists RgIA4 (1315 pg/ml to 7082 pg/ml; n = 5; p  $\geq$  0.05; Fig. 22 A) and also by ArIB [V11L, V16D] (1240 pg/ml to 7304 pg/ml; n = 5; p  $\geq$  0.05; Fig. 22 A).

When RgIA4 or ArIB [V11L, V16D] were added to primed BMDMs, which were stimulated with ATP in the absence of the FFA2 or FFA3 agonists, the IL-1 $\beta$  release was not significantly inhibited. Without the addition of 4-CMTB or AR420626, but with the addition of ATP and LPS, RgIA4 showed measured levels from 3043 pg/ml to 8362 pg/ml (n = 5; p  $\geq$  0.05; Fig. 22 A) and ArIB [V11L, V16D] levels from 4054 pg/ml to 7035 pg/ml (n = 5; p  $\geq$  0.05; Fig. 22 A).

The LDH activity measurements are shown in Table S13. The IL-1 $\beta$  and the IL-1 $\alpha$  data were statistically analyzed separately. The median of the LDH activity measured in cell supernatants of the IL-1 $\beta$  group is high with values under 24.0%. Cells stimulated with LPS are significantly different compared to data of untreated cells. Additionally, cells

stimulated with LPS + ATP are significantly different compared to data of cells treated with LPS. Furthermore, cells stimulated with LPS + ATP + AR420626 (50  $\mu$ M) + ArIB [V11L, V16D] (500 nM) are significantly different compared to data of cells treated with LPS + ATP. The number (n) is 5 for each experimental group.

The same experiments were performed on mouse BMDMs with the measurement of IL-1 $\alpha$  in cell supernatants. These pilot experiments showed similar results to the ones measured above (see figure 22 A).

Untreated cells secreted low levels of IL-1 $\alpha$  in the supernatant (1.5 pg/ml to 3 pg/ml; n = 5; Fig. 22 B). The cells primed with LPS showed similar low values of IL-1 $\alpha$  from 15 pg/ml to 23 pg/ml (n = 5; Fig. 22 B). After the addition of ATP (2 mM) higher IL-1 $\alpha$  levels were measured (208 pg/ml to 623 pg/ml; n = 5;  $p \geq 0.05$ ; Fig. 22 B). The addition of FFA2 agonist 4-CMTB (20  $\mu$ M) resulted in a significant inhibition of the ATP-induced IL-1 $\alpha$  release by primed BMDMs (48 pg/ml to 100 pg/ml; n = 5;  $p \geq 0.05$ ; Fig. 22 B). This inhibition was significantly reversed by the addition of nAChR antagonists RgIA4 (92 pg/ml to 493 pg/ml; n = 5;  $p \geq 0.05$ ; Fig. 22 B) and ArIB [V11L, V16D] (106 pg/ml to 588 pg/ml; n = 5;  $p \geq 0.05$ ; Fig. 22 B).

A similar significant reduction of the ATP-induced IL-1 $\alpha$  release by primed BMDMs was seen after the addition of the FFA3 agonist AR420626 (50  $\mu$ M; 33 pg/ml to 95 pg/ml; n = 5;  $p \geq 0.05$ ; Fig. 22 B). This inhibition was also significantly reversed by the addition of nAChR antagonists RgIA4 (176 pg/ml to 689 pg/ml; n = 5;  $p \geq 0.05$ ; Fig. 22 B) and ArIB [V11L, V16D] (93 pg/ml to 683 pg/ml; n = 5;  $p \geq 0.05$ ; Fig. 22 B).

When RgIA4 and ArIB [V11L, V16D] were added to primed BMDMs, which were stimulated with ATP in the absence of the FFA2 or FFA3 agonists, the IL-1 $\alpha$  release was not significantly inhibited (Fig. 22 B).

The LDH activity measurements are shown in Table S13. The median of the LDH activity measured in cell supernatants of the IL-1 $\beta$  group is under 23.0%. Cells stimulated with LPS are significantly different compared to data of untreated cells. Additionally, cells stimulated with LPS + ATP are significantly different compared to data of cells treated with LPS. Furthermore, cells stimulated with LPS + ATP + AR420626 (50  $\mu$ M) + ArIB [V11L, V16D] (500 nM) are significantly different compared to data of cells treated with LPS + ATP. The number (n) is 5 for each experimental group.

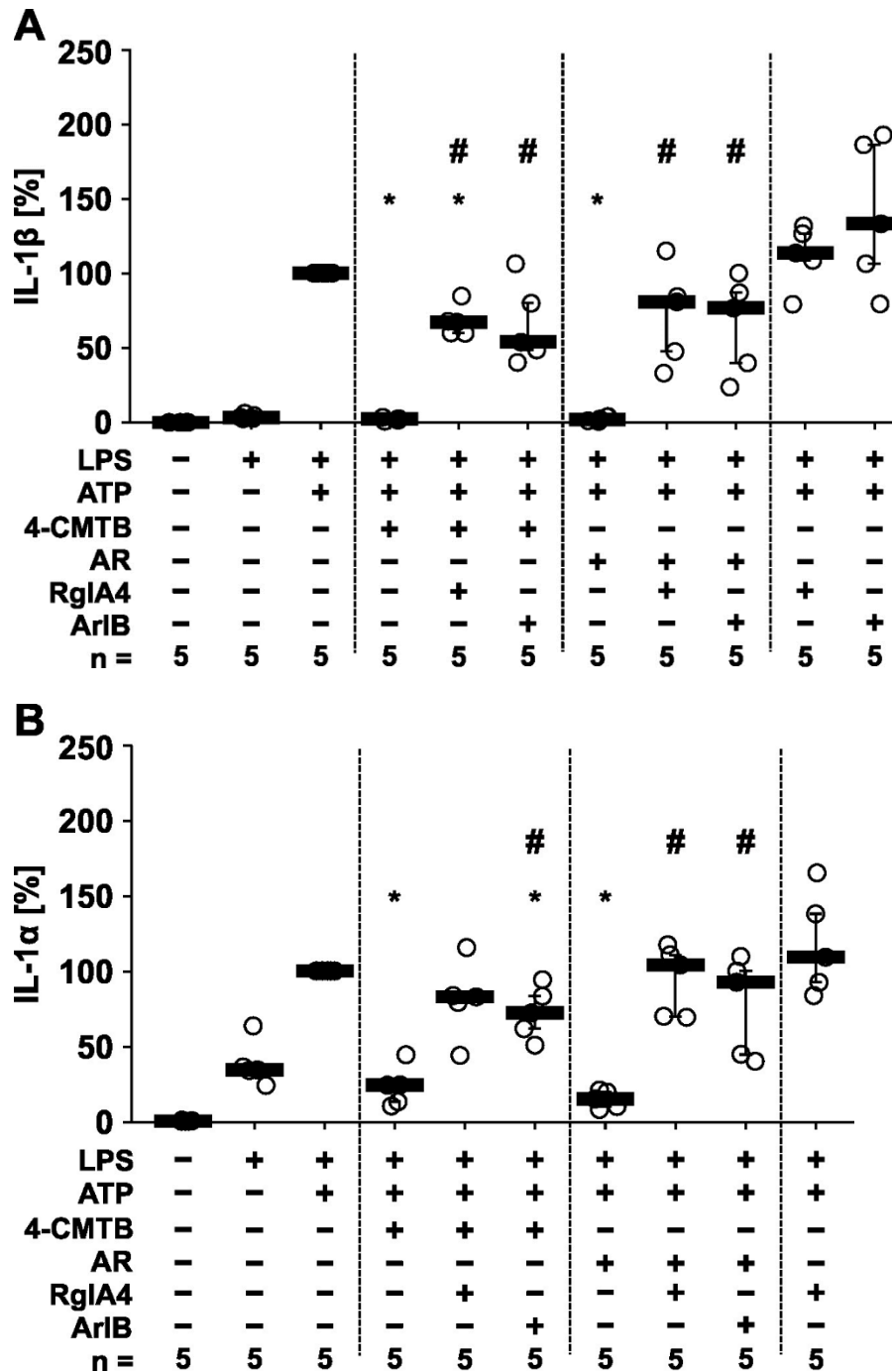


**Figure 22.** The signaling of FFA2 and FFA3 involve nAChR containing  $\alpha 7$  and  $\alpha 9/\alpha 10$ . Bone marrow cells were isolated from C57BL/6 mice and differentiated by macrophage colony-stimulating factor (M-CSF; 10 ng/ml, 6 days) and interferon- $\gamma$  (IFN- $\gamma$ ; 10 ng/ml, 3 days) to BMDMs. BMDMs were primed for 5 h with lipopolysaccharide (LPS; 1  $\mu$ g/ml) and ATP (2 mM, 30 min). **A)** The induced release of IL-1 $\beta$  was investigated in the cell culture supernatant. **B)** The induced release of IL-1 $\alpha$  was investigated in the cell culture supernatant. **A and B)** The nAChRs antagonists RglA4

(50 nM) and ArIB [V11L, V16D] (500 nM) were added 10 min prior to the addition of the P2X7 receptor agonist ATP (2 mM) in the absence and presence of the FFA2 (4-CMTB, 20  $\mu$ M) and FFA3 agonist (AR420626, 50  $\mu$ M). AR420626 and 4-CMTB inhibited the ATP-induced IL-1 $\beta$  release. This inhibition was significantly reversed by the nAChRs antagonists RgIA4 and ArIB [V11L, V16D]. The IL-1 $\beta$  and IL-1 $\alpha$  concentration in experiments where primed BMDMs were stimulated with ATP alone was set to 100% and all other values were calculated accordingly. Data are presented as individual data points, bars represent median, whiskers percentiles 25 and 75. Friedmann-test followed by Wilcoxon signed-rank test. \*  $p \leq 0.05$  significantly different from samples where ATP was given alone on LPS-primed BMDMs.

## 4. Discussion

### 4.1 Summary of the results

The experiments for this thesis were performed on 3 different cell types, hPBMCs, mPBMCs and murine BMDMs. The important focus is the ATP- or BzATP-dependent IL-1 $\beta$  secretion and its inhibition via SCFAs or synthetic FFA2 and FFA3 agonists. Furthermore, it investigates a cholinergic mechanism that is induced by FFA agonists to inhibit the ATP- or BzATP-dependent IL-1 $\beta$  secretion.

The results in the first group of cells, the hPBMCs, indicate that the BzATP-mediated IL-1 $\beta$  secretion is dependent on the P2X7 and partly on the P2X4 receptor. Both synthetic FFA2 and FFA3 agonists show a clear dose-dependent inhibition of the IL-1 $\beta$  secretion, which is significantly reversed by the addition of nAChR antagonists. These results indicate that the inhibition of the BzATP-induced IL-1 $\beta$  secretion via synthetic FFA2 and FFA3 agonists is dependent on a cholinergic mechanism. Similar experiments were then performed on mPBMCs to contrast the results to FFA2 gene-deficient mice.

In mPBMCs an efficient secretion of IL-1 $\beta$  can be induced by ATP but not by BzATP. Further, the data suggest that SCFAs as well as the synthetic FFA2 and FFA3 agonists lead to an inhibition of the ATP-dependent IL-1 $\beta$  secretion as seen in hPBMCs. This inhibition via SCFAs and the FFA2 agonist is not seen in FFA2 gene-deficient mice, while, the inhibition via FFA3 agonist is still detected.

Moreover, in mouse BMDMs, ATP induced a more efficient release of IL-1 $\beta$  compared to BzATP. This ATP-mediated release is dependent on the P2X7 as well as on the P2X4 receptor. The further analysis supports the theory that the FFA2 and FFA3 agonists including the SCFAs inhibit the ATP-mediated IL-1 $\beta$  release dependent on nAChRs. Finally, the pilot experiments performed on mouse BMDMs measuring the IL-1 $\alpha$  secretion, showed an ATP-dependent secretion resembling that of IL-1 $\beta$  that is inhibited via SCFAs, FFA2 and FFA3 agonists depending on nAChRs.

## **4.2 FFA-mediated regulation of ATP-dependent IL-1 $\beta$ secretion by hPBMCs**

### **4.2.1 ATP receptor-dependent secretion of IL-1 $\beta$**

The first group of experiments was performed on hPBMCs. HPBMCs, as mentioned in section 1.1, are human blood cells with a single non-fragmented nucleus, which include lymphocytes, monocytes and natural killer cells (Delves et al. 2006). Activated monocytes show pro-inflammatory features and have the ability to produce and secrete IL-1 $\beta$  as well as other pro-inflammatory mediators (Canè et al. 2019; Oppenheim et al. 1986; Dinarello 2009) (see 1.1). They are also among the prominent cells in this activity (Canè et al. 2019; Dinarello 2009). Furthermore, monocytes are known to express FFA2 and FFA3 (Ang et al. 2016). Initially, experiments had already been performed on monocytes along with other cell types such as neutrophils, to investigate the ATP-dependent IL-1 $\beta$  secretion (Karmakar et al. 2016; Ferrari et al. 1997). The provided information, make the monocyte a suitable choice of cell to specifically investigate the BzATP- or ATP-mediated IL-1 $\beta$  secretion and its inhibition via synthetic FFA2 and FFA3 agonists and SCFAs. This topic remains unexplored in this form in literature.

In the methods of this thesis, monocytes were enriched using two steps. First, PBMCs were isolated by gradient centrifugation. Thereafter, monocytes were enriched from PBMCs by adherence selection. According to the manufacturer of the monocyte attachment medium, this method allows a purity of 80-90% of obtained monocytes (see 2.2.1.1). Hence, there still exists a certain number of other cells among the monocytes, that might influence the measured IL-1 $\beta$  concentrations to a certain point. Further options for the monocyte isolation are known some of which show higher or lower monocyte purity levels (Nielsen et al. 2020). The positive selection method of monocytes showed the highest purity (98.7%) and is therefore a possible option to avoid impurities caused by other cells and therefore specifically only measure the monocyte IL-1 $\beta$  secretion (Nielsen et al. 2020). However, the positive selection method does come with drawbacks. Since antibodies are used targeting specific cell surface markers, these surface markers can be blocked by the antibodies (Bhattacharjee et al. 2017). Furthermore, studies show that the monocyte can be activated by the antibodies, disrupting any further experiments performed on the cell (Nielsen et al. 2020; Bhattacharjee et al. 2017).

According to literature, IL-1 $\beta$  secretion by monocytes is typically achieved by 2 independent stimuli (Martinon et al. 2009). As mentioned in section 1.2, the first signal, a danger signal such as LPS being a PAMP, can be recognized by TLR4 and results in an elevated expression of the constituents of the NLRP3 inflammasome and also to an increased production of the precursor protein pro-IL-1 $\beta$  (Kawasaki & Kawai 2014; Iwasaki and Medzhitov 2015). A second stimulus, such as ATP, leads to the formation of the NLRP3-inflammasome and the maturation of pro-IL-1 $\beta$  to IL-1 $\beta$  which is subsequently released (see 1.3) (Adinolfi et al. 2018; Cekic and Linden 2016).

Here, hPBMCs were stimulated with LPS from *E.coli* and both, BzATP or ATP. An alignment with literature was seen in the results, since BzATP is said to have a higher affinity to the P2X7 receptor in humans and also a higher potency, compared to ATP, which is important for the signaling leading to the formation of the NLRP3-inflammasome (Adinolfi et al. 2018; Young et al. 2007). Moreover, BzATP is known to be a more stable alternative compared to ATP and is therefore used for experiments in contemporary and historical literature (Gicquel et al. 2014; Williams and Coleman 1982). Additionally, ATP is also known to be unstable in vitro (Chen and Xia 2021). Furthermore, a higher ATP concentration is needed to achieve the same effect seen with BzATP as an agonist of the P2X7 receptor, which might account for the lower efficacy of ATP observed in figure 5 (Young et al. 2007). Therefore, the significantly higher secretion of IL-1 $\beta$  using BzATP resulted in the further utilization of BzATP for all the experiments on hPBMCs. Moreover, LPS alone shows no significant raise in IL-1 $\beta$ , confirming that 2 stimuli are needed for IL-1 $\beta$  to be secreted by monocytes.

In addition to measuring the IL-1 $\beta$  in cellular supernatants, the LDH activity was also measured parallel to each experiment performed and compared to the maximum LDH activity of lysed cells, corresponding to the respective experiments.

The measurement of the LDH activity is a commonly used method to determine cell death in a cell culture (Legrand et al. 1992). LDH is an enzyme found in the cytoplasm of most cells (Legrand et al. 1992). Its function is to catalyze the reduction of pyruvate to lactate, which is reversible (Legrand et al. 1992; Markert 1984). In the early stages of research and medicine, the LDH activity was measured and an increase associated with disease (Hsieh and Blumenthal 1956). Then, in 1992, the LDH activity was associated with cell death and became the preferred method used (Legrand et al. 1992).

The measurement of the LDH activity is of importance, since it represents cell vitality. In all performed experiments the IL-1 $\beta$  levels were measured in cell supernatants. Not only the LDH is released by dying cells and therefore found in a higher concentration in supernatants, but additionally cytosolic IL-1 $\beta$  is also released. The IL-1 $\beta$  levels can therefore be unreliably high if the cells are dying or are dead. A certain level of LDH is tolerable, however if the LDH activity is too high, the credibility of the measured IL-1 $\beta$  is not given. In most experiments on hPBMCs, however, the addition of LPS, BzATP or ATP did not result in a relevant increase in LDH activity (supplementary tables S1-S4), suggesting that increased IL-1 $\beta$  levels are not caused by cell death.

#### **4.2.2 Involvement of the ATP receptors P2X4 and P2X7**

A further question that arises is whether BzATP or ATP do indeed act as agonists specifically for the P2X7 receptor, or if further P2X receptors are also involved in the IL-1 $\beta$  secretion and therefore activated by BzATP or ATP.

The P2X receptor superfamily consists of 7 subforms of which the P2X7 receptor is the most extensively researched (Adinolfi et al. 2018; Jarvis and Khakh 2009) (see 1.3). Since all 7 receptors are ATP-gated, an involvement of other receptors apart from the P2X7 receptor in the BzATP-dependent IL-1 $\beta$  secretion is possible and requires further investigation. Recent studies on human embryonic kidney (HEK) 293 cells show that there is a potential interaction between the P2X4 and P2X7 receptor, which leads to an increase of the IL-1 $\beta$  and IL-18 secretion (Kanellopoulos et al. 2021; Sakaki et al. 2013). However, the exact interaction as well as the heterotrimeric or homotrimeric formation of the 2 receptors has not yet been fully understood (Kanellopoulos et al. 2021). Other studies show that there is no heteromerization of the P2X4 and P2X7 receptor in microglia and that they are activated independently (Trang et al. 2020). In dendritic cells a decrease in the expression of the P2X4 receptor leads to a decrease of IL-1 $\beta$  and IL-18 release, indicating a dependency of the 2 mentioned receptors and the involvement of the P2X4 receptor in the IL-1 $\beta$  secretion (Sakaki et al. 2013). Another study shows, that the co-expression of the P2X4 and the P2X7 receptor enhances the P2X7-mediated inflammation (Kawano et al. 2012). Furthermore, BzATP has also shown to be a partial agonist of the P2X4 receptor, allowing the possibility of a potential significant impact of the P2X4 receptor in the BzATP-dependent IL-1 $\beta$  secretion (Bowler et al. 2003).

To assess the extent of the involvement of the P2X4 and P2X7 receptors in human monocytes, the ATP- or BzATP-dependent IL-1 $\beta$  secretion was measured after the addition of P2X7 receptor antagonist A438079 or P2X4 receptor antagonist 5-BDBD in different concentrations (see figure 6). A significant reduction of the IL-1 $\beta$  release is measured in the supernatants of cells stimulated with ATP or BzATP with the addition of A438079. This indicates that the IL-1 $\beta$  secretion is P2X7 dependent, as evident from the existing literature (Ferrari et al. 2006). After the addition of 5-BDBD in combination with BzATP, a slight but statistically significant inhibition of the IL-1 $\beta$  secretion was measured. This result suggests that the P2X4 receptor is also involved in the BzATP-dependent IL-1 $\beta$  secretion in monocytes, however, not to the extent of the P2X7 receptor (see figure 6 A). In past studies, the involvement of the P2X4 receptor and the NLRP3-inflammasome activation has already been confirmed, which could explain the results seen in figure 6 A (Chen et al. 2013). Additionally, some studies have already shown, that P2X7-deficient mouse macrophages have led to the release of mature IL-1 $\beta$  after the stimulation with ATP (Kanellopoulos et al. 2021). This concept could potentially be extrapolated to human monocytes. This needs to be further investigated. The effect depicted in figure 6 A is not seen after the addition of 5-BDBD in combination with ATP. An explanation of these results would be based on speculation. However, this could be due to the higher potency and affinity of BzATP to the P2X7 receptor compared to ATP (figure 5) (Young et al. 2007).

The specificity of both antagonists is of importance to confirm the credibility of the results. In literature, A438079 is known as a selective P2X7 receptor antagonist (Nelson et al. 2006). Furthermore, it does not inhibit other P2 receptors (Manaka et al. 2015). The IC<sub>50</sub> value is 300 nM, making the antagonist potent (Potula et al. 2023).

5-BDBD has been tested and has been described as a selective and potent antagonist in studies with an IC<sub>50</sub> of 0.75  $\mu$ M (Coddou et al. 2019). Furthermore, 5-BDBD has not been seen to affect the ATP-induced P2X7 receptor's current amplitude and therefore it may be deduced that the P2X7 receptor remains unaffected by 5-BDBD (Coddou et al. 2019). For more specific results, the experiments could be repeated on P2X7 or P2X4 gene-deficient mice. Further research on the other P2X receptors, such as the P2X3 receptor and the potential interactions can be performed in future studies.

Apart from some exceptions that will be mentioned next, the cell death median in figure 6 A and B ranged between 2.0 – 6.0%. Due to centrifugation or generally the isolation of the hPBMCs, a small percentage of cells are damaged and die which is common (Chien et al. 2006). After the addition of BzATP or ATP a significant increase in cell death was seen. In literature, similar experiments were performed, adding BzATP to cell lines such as RAW264.7 and THP-1 that also resulted in a rising LDH activity (Kawano et al. 2012; Humphreys and Dubyak 1996). A possible explanation could be that the binding of BzATP to the P2X7 receptor also leads to pyroptosis and therefore to the formation of pores in the cell membrane, allowing LDH to pass through (Sborgi et al. 2016).

Furthermore, after the addition of 5-BDBD (10  $\mu$ M, 20  $\mu$ M, 50  $\mu$ M) to the cells, a significant raise in cell death, compared to only LPS + BzATP was seen. However, the addition of 5-BDBD (10  $\mu$ M) to only LPS did not lead to a significant raise in cell death. There is no data on the substance 5-BDBD and cell death in literature. In combination with BzATP or ATP (see figure 6 B and figure 20) 5-BDBD might disrupt the membrane structure of the cell and lead to a formation of pores and the release of LDH. However, a contradiction becomes apparent as the IL-1 $\beta$  levels measured still show a significant reduction after the addition of 5-BDBD, despite rising LDH activity levels. The results with 5-BDBD can be viewed with more caution. A concentration-response curve can be conducted in future experiments and might demonstrate more insight. However, an explanation is based on pure speculation.

### **4.2.3 Control of IL-1 $\beta$ secretion by synthetic FFA2 and FFA3 agonists**

The next step, was to investigate whether synthetic ligands of FFA2 and FFA3 reduce the BzATP-induced secretion of IL-1 $\beta$  by LPS-primed hPBMCs.

FFA2 and FFA3 are found on immune cells and have a high expression on monocytes (Maslowski et al. 2009) (see 1.8). The ligands for both receptors are SCFAs (Brown et al. 2003). It is thought that FFA2 is activated more efficiently by acetate and propionate, and FFA3, on the other hand, is activated most efficiently by butyrate and propionate (Brown et al. 2003). First, to test the anti-inflammatory effect that the activation of the FFA2 and FFA3 results in, synthetic agonists were added to hPBMCs in rising concentrations (see figure 7 and 8).

The addition of the synthetic FFA2 agonist 4-CMTB resulted in an inhibition of the BzATP-mediated IL-1 $\beta$  release. With a rising concentration of 4-CMTB from 0.5 to 50  $\mu$ M a dose-dependent inhibition was seen (see figure 7). The IC<sub>50</sub> value was calculated being 8.3  $\mu$ M. This value is higher than the ones mentioned in literature which are said to be around 1.62  $\mu$ M (Grundmann et al. 2016). This difference shows that in the experiments conducted for this thesis, the FFA2 agonist 4-CMTB has a slightly lower potency as seen in other studies (Grundmann et al. 2016). 4-CMTB is, however, the most studied agonist (Bolognini et al. 2016). Moreover, 4-CMTB shows no effect at the FFA3 and is described as moderately potent and FFA2 selective (Bolognini et al. 2016). An additional optimization effort to achieve a ligand with an even better potency and specificity to only FFA2 has failed so far (Grundmann et al. 2016). Furthermore, the binding site has not been successfully mapped (Grundmann et al. 2016). Therefore, it is not known whether 4-CMTB does indeed activate the exact signaling pathway as do the SCFA and furthermore, whether there is “functional selectivity” at the FFA2 (Bolognini et al. 2016). This devaluates the direct transferability of the synthetic agonist to the SCFAs, as being the natural agonists. To solve this problem, experiments were performed on FFA2 gene-deficient mice, to evaluate the role of the FFA2.

Similar to the addition of 4-CMTB the synthetic FFA3 agonist AR420626 was added in increasing concentrations (1 – 50  $\mu$ M) resulting in a dose-dependent inhibition of the BzATP-dependent IL-1 $\beta$  secretion, showing an anti-inflammatory effect (see figure 8). AR420626 is used and mentioned in multiple studies as being a selective FFA3 agonist (Mikami et al. 2020; Christiansen et al. 2018). The IC<sub>50</sub> value in the experiments conducted for this thesis was calculated being 19.7  $\mu$ M. In other papers, a value of 117 nM has been mentioned (Engelstoft et al. 2013). Here, a more reduced potency of the FFA3 agonist is seen, as with 4-CMTB, compared to other literature. AR420626 has been seen not to activate the FFA2 up to a concentration of 100  $\mu$ M, making it a good agonist in the concentrations used for the experiments conducted here (Engelstoft et al. 2013). In order to have a clearer understanding of the role of the FFA3 in the inhibition of the BzATP-induced IL-1 $\beta$  secretion, further experiments can be performed on FFA3 gene-deficient mice.

In figure 7, cell death was generally low under 6.6%, however after the addition of 4-CMTB (10  $\mu$ M and 50  $\mu$ M), a significant raise in cell death was seen compared to data of cells treated with LPS + BzATP. Additionally, in figure 9, the addition of 4-CMTB

(10  $\mu\text{M}$ ) also led to a significantly higher cell death, compared to LPS + BzATP at a general median cell death of under 4.5%. In figure 21, there was also a significant increase in cell death after the addition of 4-CMTB (10  $\mu\text{M}$ ) to mouse BMDMs. Interestingly, not all 4-CMTB concentrations had the effect of a cell death increase. It is primarily seen in the concentration of 10  $\mu\text{M}$ . No explanation for this increase in cell death is found in literature. However, the possibility exists that this could be coincidental, therefore, further investigation is needed.

In the experiments performed for figure 8, no significant increase in cell death was measured.

#### **4.2.4 Signaling of FFA2 and FFA3 via nAChRs**

After having observed that the activation of both FFA2 and FFA3 leads to an inhibition of the BzATP-dependent IL-1 $\beta$  secretion by hPBMCs, the inhibitory mechanism needs to be studied further.

Since unpublished pilot experiments already suggested that nAChRs might be involved in the signaling of the synthetic FFA2 agonist 4-CMTB, the conopeptides RgIA4 and ArIB [V11L, V16D], which are specific for nAChR subunits  $\alpha 7$  and  $\alpha 9/\alpha 10$ , respectively, were used (Grau et al. 2018). Indeed, both conopeptides blunted the inhibitory effect of 4-CMTB on the BzATP-mediated release of IL-1 $\beta$  (Fig. 9). In the same set of experiments, the BzATP-induced release of IL-1 $\beta$  by LPS-pulsed hPBMCs in the presence or absence of 4-CMTB was included as controls. The results of these experiments confirmed well the results shown in figure 5 and 7.

According to 1.6, nAChRs are found in the immune system (Fujii et al. 2017). In immune cells the receptor can be made up of the subunits  $\alpha 7$  and  $\alpha 9/10$  (Hecker et al. 2015; Zoli et al. 2018). Studies show, that the nAChR and the P2X7 receptor can interact (Di et al. 2018; Richter et al. 2016). The metabotropic activation of the nAChR can lead to an inhibition of the P2X7 receptor that cannot react with ATP/BzATP in an ionotropic manner (Hecker et al. 2015; Richter et al. 2016). Recent studies show, that the inhibitory signaling of the ATP-mediated IL-1 $\beta$  secretion via the nAChRs involved an activation of the endothelial NO synthase as well as a modification of the P2X7 receptor (Richter et al. 2023). ACh is known to be an agonist for the nAChR, as well as other substances with a

choline group (Hecker et al. 2015; Richter et al. 2016). These agonists bind to the nAChR and lead to an inhibition of the BzATP-dependent NLRP3-inflammasome activation and therefore lead to an inhibition of the IL-1 $\beta$  release (Hecker et al. 2015; Richter et al. 2016; Backhaus et al. 2017). ACh of neuronal origin and non-neuronal origin can regulate immune cell functions (Mashimo et al. 2021; Borovikova et al. 2000). ACh and PC both unfold their effect via nAChR subunits  $\alpha 7$ ,  $\alpha 9$  and  $\alpha 10$ . The conopeptide ArIB [V11L, V16D], acts as an antagonist for the subunit  $\alpha 7$  and the conopeptide RgIA4 as an antagonist for the subunits  $\alpha 9/\alpha 10$  (Grau et al. 2018).

If the FFA2 and FFA3 are dependent on nAChRs to lead to an inhibition of the BzATP-induced IL-1 $\beta$  secretion by hPBMCs, the expected result, after the addition of an antagonistic conopeptide, would be that the inhibitory effect is reversed, leading to a higher secretion of IL-1 $\beta$ . The 2 different conopeptides were added in order to differentiate which subunit may be responsible for the inhibition. With an addition of 4-CMTB at a concentration of 1  $\mu$ M, none of the conopeptides showed a significant effect. This might be explained by the observation that the variance of these data was high. However, the conopeptides showed a significant effect when combined with a higher concentration of 4-CMTB (10  $\mu$ M). This indicates that the anti-inflammatory effect conducted via FFA2 is indeed in some unknown way connected to all nAChR subunits  $\alpha 7$  and  $\alpha 9/\alpha 10$  and in need for further investigation.

Similar results, compared to 4-CMTB, were seen after the addition of the synthetic FFA3 agonist AR420626 (Fig. 10). As seen in figure 8, AR420626 leads to a significant inhibition of the BzATP-induced IL-1 $\beta$  release, while conopeptides RgIA4 and ArIB [V11L, V16D] significantly reversed this effect. The reversed effect points to the FFA3 being dependent on nAChR subunits  $\alpha 7$  and  $\alpha 9/\alpha 10$ .

RgIA4 is a second-generation antagonist, derived from the natural RgIA antagonist isolated from *Conus regius* (Huynh et al. 2022). Its selectivity and potency was altered for human  $\alpha 9/\alpha 10$  nAChR (Huynh et al. 2022). Studies on knockout mice have shown, that the  $\alpha 9$  subunit is essential for RgIA4 (Huynh et al. 2022). Further studies have also shown a low IC<sub>50</sub> value and a high selectivity, indicating that RgIA4 is a potent antagonist (Christensen et al. 2017; Romero et al. 2017). However, the exact mechanism of action remains unknown (Huynh et al. 2022).

Moreover, ArIB is an antagonist isolated from the hepatopancreas of the *Conus arenatus* (Whiteaker et al. 2007). ArIB was altered and amino acids were added making ArIB [V11L, V16D] thereby increasing the activity for the  $\alpha 7$  subunit (Grau et al. 2018). The IC<sub>50</sub> value was measured to be 1.1 nM, making ArIB [V11L, V16D] a highly potent antagonist and the most selective one reported in literature (Grau et al. 2018).

Reviewing the efficacy and potency of both FFA2 and FFA3 agonists as well as the nAChR antagonists, there is a possibility that the synthetic substances do indeed not act in a way that most studies suggest. It might be possible, however, that 4-CMTB or AR420626 act directly at the nAChR and for that reason reverse the inhibition or the nAChR antagonists are not as potent and specific as claimed to be. In order to clarify any potential questions, further experiments need to be performed on gene-deficient mice. Therefore, mouse data is collected, since the human data cannot be directly extrapolated to mice (Bolognini et al. 2016).

Figure 9 shows that not only the addition of 4-CMTB (10  $\mu$ M) led to a significant increase of cell death, as already mentioned in 4.2.3, but also the addition of RgIA4. The same increase in cell death was seen after the addition of RgIA4 to AR420626 in figure 10. In some cases, though, RgIA4 does not lead to a higher cell death. This is seen in figure 9 and figure 22 A, B. In these figures there are also controls where RgIA4 is added only to LPS without BzATP or ATP. Here, no increase in cell death is observed. A combination of RgIA4 with FFA2 and FFA3 agonists might disrupt the cell membrane in some unknown way. This also warrants further research as no answers have been found in the existing literature.

Similar to the LDH activity results seen in figure 9, figure 10 also shows a significant raise in cell death after the addition of AR420626 compared to LPS + BzATP alone, at a general cell death median of under 2.0%. Considering the general low cell death, the data need to be put in perspective. In figure 21, in mouse BMDMs, the addition of AR420626 also showed a significant increase in the LDH activity compared to LPS + ATP alone. Here, the cell death is higher as seen in figure 10. The level is at 24.9%, making the IL-1 $\beta$  results questionable. Generally speaking, the higher the LDH activity, the less reliable are the measured IL-1 $\beta$  results, since dying cells have no intact cell membrane releasing cytosolic pro-IL-1 $\beta$  or IL-1 $\beta$  besides LDH. This can result in a falsely high IL-1 $\beta$  measured. However, the IL-1 $\beta$  levels are significantly reduced by the addition of

AR420626, which is difficult to be explained. No comparative data were found in the literature. In figure 10, after the further addition of ArIB [V11L, V16D] a significantly higher cell death was measured, however also ranging below 2.0%. These data also need to be put in perspective, considering the very low general cell death. In figure 22 A and B, AR420626 and ArIB [V11L, V16D] were added to mouse BMDMs. Both showed a significant increase in cell death, the LDH activity being high, at 19.0%. No data was found on ArIB [V11L, V16D] and cell death in literature. A concentration-response curve might clarify the phenomena.

### **4.3 FFA-mediated regulation of ATP-dependent IL-1 $\beta$ secretion by mPBMCs**

#### **4.3.1 ATP receptor-dependent secretion of IL-1 $\beta$**

The next set of experiments was performed on mPBMCs. This step was taken to gather data and establish a foundational basis for subsequent work involving FFA2 gene-deficient mice. Human data is shown not to be transferrable to murine cells, since differences in the selectivity for ligands are seen for example with the synthetic FFA2 and FFA3 agonists (Bolognini et al. 2016). Furthermore, another difference in species is seen in the human P2X7 receptor compared to the murine receptor (Moore and Mackenzie 2008). The human P2X7 receptor has a higher affinity to BzATP and ATP as well as a higher deactivation speed (Urbina-Treviño et al. 2022; Moore and Mackenzie 2008). Therefore, separate data were collected. The monocyte, as mentioned in 4.2.1, is a good choice of cell to specifically investigate the ATP-mediated IL-1 $\beta$  secretion and its inhibition via synthetic FFA2 and FFA3 agonists and SCFAs.

The isolation method used for the mPBMCs is a density gradient. The manufacturer, as well as other studies, mention different purity levels of monocytes after the usage of the gradient and the adherence selection with the usage of RPMI. A high range is seen between 75% purity and 95% (Repnik et al. 2003; Nielsen et al. 2020). The same problem occurs as discussed with the hPBMCs. Impurities from other cells are possible and can act as a disruptive factor (Nelson et al. 2006). According to literature, a positive isolation mechanism shows the highest purity levels. This can also be used here, the aim being to have less impurities and then only to investigate the monocyte and the IL-1 $\beta$  secretion (see 4.2.1) (Nelson et al. 2006). However, as mentioned in 4.2.1 the antibodies used can

either lead to a blockade or activation of cell surface receptors (Bhattacharjee et al. 2017; Nielsen et al. 2020).

As mentioned in 4.2.1, a secretion of IL-1 $\beta$  in mouse monocytes is typically achieved by 2 independent stimuli (Martinon et al. 2009). Contrasting results, as suggested in literature and seen in hPBMCs, were measured in mPBMCs after the addition of LPS and BzATP or ATP acting as a second signal. BzATP, as mentioned in 4.2.1, is said to have a higher affinity and potency to the P2X7 receptor in humans as well as being more stable, compared to ATP (Young et al. 2007; Gicquel et al. 2014). However, in the experiments performed with mPBMCs, ATP (1 mM) has shown to lead to a significantly higher release of IL-1 $\beta$  compared to BzATP. A possible explanation for this phenomenon, might be the fact that the P2X7 receptor needs higher ATP concentration to be activated, compared to other P2X receptors, making other receptors more involved in the IL-1 $\beta$  secretion (Urbina-Treviño et al. 2022). Since BzATP is seen to be a partial agonist to the P2X4 receptor and ATP on the other hand shows a higher potency, there is a possibility that ATP demonstrates this strong effect due to its efficiency to the P2X4 and not the P2X7 receptor (Bowler et al. 2003). The P2X4 receptor has shown to contribute to the induction of the IL-1 $\beta$  secretion in hPBMCs (see figure 6 A, B). Additionally, studies have shown, that there is a reduced amount of the P2X7 receptor on the cell surface of T- cells of C57BL/6 mice (Sluyter et al. 2023). This might also be the case in monocytes, it is however, in need of further investigation.

Reviewing the results, a possible lower expression of the P2X7 receptor and a higher potency of ATP to the P2X4 receptor might be a cause for the stronger IL-1 $\beta$  secretion using ATP as a second stimulus. This theory needs to be investigated more. A possibility would be to perform a polymerase chain reaction (PCR) and demonstrate the presence of the mRNA of the P2X7 receptor on the murine cells. Additionally, the experiments could be repeated using cells isolated from P2X7 receptor knockout mice and mice that over express the receptor. Due to the time limit, the experiments as seen in figure 6, were not repeated for mPBMCs. This could be a further point of investigation, demonstrating the impact of the P2X4 receptor. ATP was used for all experiments performed in mPBMCs.

### **4.3.2 Control of IL-1 $\beta$ secretion by endogenous and synthetic FFA agonists**

Similar to the experiments performed in 4.2.3, synthetic or endogenous FFA2 and FFA3 ligands were added to LPS-pulsed mPBMCs to investigate whether they reduce the ATP-induced secretion of IL-1 $\beta$ .

It is thought that FFA2 is activated more efficiently by acetate and propionate, and FFA3, on the other hand, is activated most efficiently by butyrate and propionate in humans (Brown et al. 2003). However, in mice differences have been seen (Bolognini et al. 2016). Here, FFA2 is activated most efficiently by acetate and butyrate and FFA3 by butyrate and propionate (Bolognini et al. 2016). This has to be taken into consideration when comparing human to murine data as well as the efficiency of each SCFAs.

Animal models are often used for research. However, a difference that also needs to be kept in mind, when researching on animals, is the difference in microbiome found in mice and in humans. The production and ratio of SCFAs is dependent on the bacteria present in the gut (Savage 1986). The mice used for these experiments are known to have a more simplified microbiome compared to wild mice or humans (Zhang et al. 2021). Therefore, the collected data is not entirely transferrable (Zhang et al. 2021). The experiments performed on mononuclear phagocytes isolated from gene-deficient mice do however allow insight into the role of FFA2 and FFA3 in the ATP-dependent IL-1 $\beta$  secretion and its inhibition.

Since the SCFAs are the natural endogenous agonists for the FFA2 and FFA3 and are found physiologically in the mouse or human body, they are the best representation of how the ligands lead to a potential inhibition of the ATP-induced IL-1 $\beta$  (Brown et al. 2003).

In the experiments performed on mPBMCs, all SCFAs led to a significant inhibition of the ATP-dependent IL-1 $\beta$  secretion. This underlines the statements mentioned above, that the SCFAs display an anti-inflammatory effect. The synthetic FFA2 agonist 4-CMTB and the synthetic FFA3 agonist AR420626 were also added to mPBMCs and a similar inhibition of the ATP-dependent IL-1 $\beta$  release was seen compared to hPBMCs. In literature, no difference in selectivity of 4-CMTB and AR420626 in humans and mice

has been mentioned and might be an interesting point for further research (Bolognini et al. 2016).

PC as well as further substances having a choline group are known to be non-canonical cholinergic agonists and therefore have an anti-inflammatory effect, leading to inhibition of the ATP-induced IL-1 $\beta$  secretion (Hecker et al. 2015; Richter et al. 2016; Backhaus et al. 2017). This inhibitory effect was also seen in the experiments performed. In this experimental setting, PC was added as a positive control, to confirm indirectly the presence of the nAChR. Since time was too short to run a PCR and check for the definite presence of the nAChR, PC and in further experiments also ACh act as a positive control that confirm the nAChR being present and active in mPBMCs.

In the experiments performed for figure 12 and 14, no significant increase in cell death was measured.

#### **4.3.3 Role of FFA2 in the control of IL-1 $\beta$ secretion**

The initially performed experiments mentioned in previous chapters resulted in the experiments being conducted on FFA2 gene-deficient mPBMCs. Here, the synthetic FFA2 and FFA3 agonists as well as SCFAs were added to LPS-pulsed wild-type and FFA2 gene-deficient mPBMCs, which were both from the same genetic background to determine the role of the FFA2.

In wild-type mPBMCs, the synthetic FFA2 agonist 4-CMTB leads to an expected significant reduction of ATP-induced IL-1 $\beta$ , measured in the cellular supernatants, as seen in previous experiments. However, in FFA2 gene-deficient mPBMCs, 4-CMTB does not lead to a reduction of IL-1 $\beta$ . This allows the assumption that 4-CMTB is indeed a specific agonist for the FFA2 that does not lead to a reduction of the ATP-dependent IL-1 $\beta$  release. Since the FFA3 is still present in the gene-deficient mPBMCs and 4-CMTB does not lead to a reduction of the ATP-dependent IL-1 $\beta$  release. Therefore, the specificity of 4-CMTB is assumed to be as specific to FFA2 as mentioned in 4.3.2. Furthermore, the blunted ATP-dependent IL-1 $\beta$  secretion by FFA2 gene-deficient mPBMCs through 4-CMTB, also brings up the question of the FFA2 signal transduction. In previous experiments performed, the FFA2 or FFA3 and the nAChR have been observed to be linked (see 4.2.4). This is specifically seen by the fact that the ATP-

dependent IL-1 $\beta$  secretion is blunted through the blockade of the nAChRs or the absence of FFA2 in the gene-deficient mice. The exact mechanism is in need of further research.

After the addition of AR420626 in wild-type mPBMCs, a reduction of the ATP-induced IL-1 $\beta$  was measured in the cell supernatants. Additionally, a reduction of the ATP-induced IL-1 $\beta$  in the supernatants of the FFA2 gene-deficient mPBMCs was also measured. This allows the assumption that the FFA3 is present and functioning, if the specificity of AR420626 is thought to be as mentioned in 4.3.2. Furthermore, AR420626 is not seen to be dependent on FFA2. The role of the FFA3 and the specificity of AR420626 can be tested in future experiments performed on FFA3 gene-deficient mPBMCs.

However, the data on FFA2 gene-deficient mice should be interpreted with care. Although there were statistically significant differences among gene-deficient and wild-type mice, these differences were small.

The addition of all 3 SCFAs to the wild-type mPBMCs, showed a significant reduction of the ATP-induced IL-1 $\beta$  release, measured in the cell supernatants. In the FFA2 gene-deficient mPBMCs supernatants no significant reduction of the ATP-induced IL-1 $\beta$  value was measured. This shows that all 3 SCFAs are dependent on the FFA2 to activate the signal transduction and lead to a reduction of the measured IL-1 $\beta$ . This experiment needs to be repeated in FFA3 gene-deficient mPBMCs. Since studies show, that the FFA2 and FFA3 are able to interact and form a heteromeric structure, there is a possibility that the SCFAs need both receptors to lead to a reduction of the ATP-dependent IL-1 $\beta$  secretion (Ang et al. 2018).

As seen in the previous chapter (see 4.3.2) PC was added as a positive control for the nAChR, in order to make sure the nAChR is still functioning in the cells. PC led to a significant inhibition in the wild-type mPBMCs, as seen in previous experiments. In the FFA2 gene-deficient mPBMCs, a significant reduction of the ATP-dependent IL-1 $\beta$  was also measured in cell supernatants. This does not only show the functioning of the nAChR, but also that 4-CMTB does not directly bind to the nAChRs, which could have been possible. Furthermore, this shows that the nAChR acts independently of the FFA2.

The addition of PC to mPBMCs showed a significant increase in the LDH activity. Additionally, it was the highest value in the set of experiments, being 8.5%. This, put in

perspective, is significantly higher, however still under 10%. Furthermore, in literature, no similar phenomenon was documented. Interestingly, the addition of ACh did not lead to the same increase in cell death (see Fig. 21). Perhaps this is coincidental.

In the experiments performed for figure 15, no significant increase in cell death was measured.

#### **4.4 FFA-mediated regulation of ATP-dependent IL-1 $\beta$ secretion by murine macrophages**

##### **4.4.1 Localization of FFA2-expressing macrophages in the murine colon**

In this thesis, experiments were not only conducted on monocytes, due to their capability of a high IL-1 $\beta$  secretion, but also bone marrow-derived macrophages were used.

To ensure that the cells used for the following experiments, are indeed bone marrow-derived macrophages, a staining with F4/80 antibodies was performed. This monoclonal antibody called F4/80, was developed in 1981 and targets the F4/80 glycoprotein thought to be specific to macrophages (Austyn and Gordon 1981). Therefore, this immunohistochemical staining method was used to identify macrophages. The stains were performed on 3 different mice to rule out coincidence. All slides clearly show the brown staining of the cells. This underlines the fact that the cells are indeed macrophages. Additionally, the variable morphological structure with filopodia seen is typical for macrophages (Kress et al. 2007). The F4/80 antibody turns out not to be specific to the macrophage. There are a few cells like the eosinophils and Langerhans cells that also express the F4/80 antigen (McGarry and Stewart 1991). The morphological structure seen in these cells would, however, be different compared to the typical macrophage structure.

A double-staining was performed on macrophages within the murine colon. Macrophages, as mentioned above, are cells that secrete a higher amount of IL-1 $\beta$  compared to other cells and are also known to highly express the FFA2 (Bolognini et al. 2021; Milligan et al. 2009). Additionally, the colon is the organ in which the production of the SCFAs takes place (Wong et al. 2006; Brody 1999). Therefore, the macrophages in the colon are exposed to high concentrations of SCFAs. To further confirm the presence of the FFA2 in the murine colon the double-staining was performed. In literature, the FFA2 is known to be present in the murine colon (Milligan et al. 2009).

As mentioned in 3.3.2 a mouse strain was used in which mRFP was expressed under the control of the FFA2 promoter. It is clearly seen that the FFA2 gene is expressed in the colon, hence the brown staining (Fig. 17 A). Furthermore, the blue staining in figure 17 B shows the presence of macrophages. Figure 17 C represents the double-staining. Here, it is clear to see that both macrophages are present in the colon as well as the mRFP under the control of the FFA2 promoter. This double-staining emphasizes the macrophages as being an optimal cell to further pursue the experiments on bone marrow-derived macrophages.

#### **4.4.2 ATP receptor-dependent secretion of IL-1 $\beta$**

As mentioned previously, the last set of experiments was performed on mouse BMDMs. The experiments previously conducted on hPBMCs and mPBMCs were partly repeated in mouse BMDMs in order to compare the effect of specific substances on the IL-1 $\beta$  secretion by macrophages. Since macrophages are, as mentioned earlier, one of the main cells to produce IL-1 $\beta$ , besides monocytes, these cells were also of experimental interest.

The isolation mechanism used for mouse BMDMs differs to the one performed on hPBMCs or mPBMCs. After isolating the bone marrow cells from C57BL/6 mice, the cells were differentiated into macrophages following a certain stimulation protocol (see 2.2.2.3). To ensure the success of the stimulation and that the cells had indeed differentiated into macrophages the staining mentioned above (see 4.4.1) was performed. However, since not every single BMDM culture was stained, it is important to know that the contamination risk in the whole isolation protocol is high (Troupin et al. 2013). This would lead to impurified cells and falsified results. Additionally, a slight difference to keep in mind when comparing PBMCs to BMDMs is the stimulation with LPS. In PBMCs the cells were “pulsed” meaning the addition of LPS took place early, before the monocytes were isolated. In BMDMs the cells were primed with LPS for 5 h on day 6 of cultivation.

A secretion of IL-1 $\beta$  in mouse macrophages, as mentioned in 4.2.1, is typically achieved by 2 independent stimuli (Martinon et al. 2009). Contrasting results were observed in mPBMCs, compared to hPBMCs and compared to literature, when stimulated with BzATP and ATP as a second stimulus (see 4.3.1). ATP resulted in a significant IL-1 $\beta$  secretion in mPBMCs.

Therefore, mouse BMDMs were stimulated with BzATP or ATP in 2 different concentrations, in order to understand what effect a raise in concentration would have on the IL-1 $\beta$  secretion. The addition of BzATP (100  $\mu$ M) led to no significant IL-1 $\beta$  secretion measured in cell supernatants compared to LPS alone. The same was seen after the addition of BzATP (300  $\mu$ M). On the other hand, the stimulation with ATP (1 mM) shows a significant IL-1 $\beta$  secretion compared to LPS alone. This is also seen after the addition of ATP (2 mM). These results show, that mouse BMDMs react to ATP as seen in mPBMCs. The exact reason can be assumed to be similar to the ones mentioned in 4.3.1. 2 mM of ATP is on the margin of being an unphysiologically high concentration. It will however be used in further experiments performed on the mouse BMDMs.

In literature, BzATP is said to have a higher affinity to the P2X7 receptor compared to ATP (Young et al. 2007; Gicquel et al. 2014). It is interesting to observe that an even higher concentration of BzATP still does not result in a significant IL-1 $\beta$  secretion. This observation cannot be explained. ATP however, as seen in 4.3.1 results in a higher IL-1 $\beta$  secretion when the concentration is doubled. The explanation may be similar to the one mentioned in 4.3.1. The P2X7 receptor in macrophages may be expressed less and the ATP may have a higher affinity to other P2X receptors (Sluyter et al. 2023; Urbina-Treviño et al. 2022). Further research on P2X7 knockout mice could allow further insight.

After the addition of the P2X7 receptor antagonist A438079 the ATP-dependent IL-1 $\beta$  secretion was significantly blunted. The selectivity of A438079 is mentioned in literature to be high to the P2X7 receptor (see. 4.2.2) (Nelson et al. 2006). Furthermore, it is seen as a potent antagonist (Potula et al. 2023). Considering all the information, the P2X7 receptor must be present, if the potency of the antagonist is indeed as described in literature.

Figure 19 shows a definite significant increase in the LDH activity in mouse BMDMs, after the addition of A438079 compared to LPS + ATP. The cell death median is 57%, stating that very few viable cells are left. A similar significant increase in the LDH activity was seen in figure 20 after the addition of A438079 in mouse BMDMs compared to LPS + ATP. The cell death median is lower, at 16.0%. No comparable data were found in literature.

Generally, a higher LDH activity was seen in mouse BMDMs compared to the other cell groups. There is a possibility that the cells might be more susceptible after the 6 days of

cultivation. This needs further research and perhaps an improvement can be found to allow the IL-1 $\beta$  levels measured to be more credible.

#### **4.4.3 Involvement of the ATP receptors P2X4 and P2X7**

To test the involvement of other P2X receptors in mouse BMDMs, such as the P2X4 receptor in the ATP-dependent IL-1 $\beta$  secretion, both P2X4 and P2X7 receptor antagonists were added in rising concentrations and the IL-1 $\beta$  concentration was measured in the cell supernatants. 5-BDBD was added as an antagonist for the P2X4 receptor and A438079 as an antagonist for the P2X7 receptor. A similar experiment was performed in 4.2.2 on hPBMCs.

After the addition of 5-BDBD a significant reduction in the ATP-dependent IL-1 $\beta$  concentration in cell supernatants was measured. This fact suggests, that the P2X4 receptor is involved in the ATP-dependent IL-1 $\beta$  secretion to a certain degree. Literature has already confirmed the involvement of the P2X4 receptor and the NLRP3-inflammasome activation which could be a possible explanation (Chen et al. 2013). Furthermore, experiments performed on P2X7 gene-deficient mouse macrophages have led to a secretion of mature IL-1 $\beta$  after the stimulation with ATP (Kanellopoulos et al. 2021). This underlines the fact that further receptors, such as the P2X4 receptor seen in these experiments performed, must be involved in the ATP-dependent IL-1 $\beta$  release in mouse macrophages.

The addition of P2X7 receptor antagonist A438079, a significant reduction of the IL-1 $\beta$  release was also measured in the cell supernatants. This was already seen in the previous experiments discussed in 4.4.2. Literature states that the P2X7 receptor is involved in the ATP-dependent IL-1 $\beta$  secretion, which can be confirmed by the experiments performed in this thesis (Ferrari et al. 2006).

Both antagonists were added in rising concentrations and the IC<sub>50</sub> value was calculated, being 34  $\mu$ M with 5-BDBD and 0.8  $\mu$ M with A438079. In literature, both antagonists are stated to be potent (Coddou et al. 2019; Nelson et al. 2006). The IC<sub>50</sub> values given in different studies are however smaller and therefore slightly more potent than the values calculated for this thesis (see 4.2.2). P2X7 or even P2X4 receptor knockout mice could help and give more specific insight into the involvement of both receptors.

A significant increase of the LDH activity has been seen after the addition of 5-BDBD (1  $\mu$ M, 10  $\mu$ M, 100  $\mu$ M) and after the addition of A438079. The LDH activity was high ranging between 15.8% and 49.5%. An explanation cannot be found in the literature. The results have also been discussed in 4.2.2 and 4.4.2.

#### **4.4.4 Control of IL-1 $\beta$ secretion by synthetic FFA agonists**

Similar to the experiments performed on mPBMCs, endogenous and synthetic FFA2 and FFA3 agonists as well as ACh were added to mouse BMDMs. This was done in order to see what effect the substances have on the IL-1 $\beta$  secretion of macrophages. Furthermore, in order to generally compare the results of the macrophages with the ones of monocytes. The experiments performed on mouse BMDMs should ultimately lead up to FFA2 gene-deficient mouse BMDM experiments, which are not part of this thesis.

As seen in 4.3.2, the FFA2 agonist 4-CMTB and FFA3 agonist A420626 were added to mouse BMDMs and led to a significant inhibition of the ATP-dependent IL-1 $\beta$  secretion measured in cell supernatants. This indicates, that macrophages do indeed express the FFA2 and FFA3 as suggested in literature (Bolognini et al. 2021). This can only be assumed if the potency and specificity of the agonists is as mentioned in 4.2.3. Additionally, this inhibitory effect is seen in both monocytes and macrophages. In further experiments performed on FFA2 and FFA3 gene-deficient mouse BMDMs, the role of both receptors can be analyzed further.

The SCFA butyrate was added to mouse BMDMs and acts as a representative for the other SCFAs that were not added. The results show that butyrate also led to a significant inhibition of the ATP-dependent IL-1 $\beta$  secretion measured in the cell supernatants of macrophages. This inhibitory effect is also similar to the significant inhibition seen in mPBMCs, allowing the conclusion that SCFAs have an anti-inflammatory effect on mouse BMDMs.

A further similarity between the mouse BMDMs and the mPBMCs is the significant inhibition of the ATP-induced IL-1 $\beta$  secretion when ACh is added to the cells. ACh is the control for the nAChRs, indicating that they are present and working. This was tested as a pilot experiment on mouse BMDMs at this stage for the nAChRs antagonization experiments viewed in the next chapter.

A significant increase in cell death was seen after the addition of 4-CMTB, AR420626 and butyrate. The results considering 4-CMTB and AR420626 have been previously discussed (see 4.2.3 and 4.2.4). The only significant increase in the LDH activity has been seen in mouse BMDMs after the addition of SCFA butyrate. This has also not been addressed in literature and might be considered as being a coincidence.

#### **4.4.5 Signaling of FFAs via nAChRs**

The final experiments for this thesis were performed to ascertain the involvement of nAChRs containing subunits  $\alpha 7$  and  $\alpha 9/\alpha 10$  in the inhibition of the ATP-induced IL-1 $\beta$  secretion. As seen in prior experiments (see 4.4.4), after the addition of endogenous or synthetic FFA2 and FFA3 agonists to mouse BMDMs, a significant inhibition of the IL-1 $\beta$  secretion was measured in cell supernatants. This inhibition was also seen in mPBMCs as well as hPBMCs. Additionally, in hPBMCs the IL-1 $\beta$  secretion was blunted by nAChRs antagonists (see 4.2.4). This antagonization was repeated in mouse BMDMs.

After the addition of FFA2 agonist 4-CMTB, an expected inhibition of the ATP-induced IL-1 $\beta$  secretion was measured in cell supernatants. As nAChRs antagonists, the conopeptides RgIA4 and ArIB [V11L, V16D] were used (Grau et al. 2018). The conopeptide ArIB [V11L, V16D], acts as an antagonist for the subunit  $\alpha 7$  and the conopeptide RgIA4 as an antagonist for the subunits  $\alpha 9/\alpha 10$  (Grau et al. 2018). Both significantly blunted the inhibitory effect of 4-CMTB on the ATP-mediated release of IL-1 $\beta$  (see Fig. 22 A).

Similar to 4-CMTB, the addition of FFA3 agonist AR420626 also led to an expected significant inhibition of the ATP-mediated IL-1 $\beta$  secretion that was measured in cellular supernatants. The addition of the conopeptides also significantly blunted the inhibitory effect of AR420626 on the ATP-mediated IL-1 $\beta$  release (see Fig. 22 A).

The precise correlation between the P2X7 receptor and the nAChR are still partly unknown. However, it is known that the nAChR and the P2X7 receptor can interact (Di et al. 2018; Richter et al. 2016). The fact that the FFA2 and FFA3 are dependent on the nAChRs subunits  $\alpha 7$  and  $\alpha 9/\alpha 10$  has not only been confirmed by experiments performed on hPBMCs in this thesis, but also seen in mouse BMDMs.

The final experiment for this thesis has the same experimental method as performed for figure 22 A. The synthetic FFA2 and FFA3 agonists were added to mouse BMDMs as well as the conopeptides RgIA4 and ArIB [V11L, V16D]. At this point, as a pilot experiment, the IL-1 $\alpha$  was measured in cellular supernatants instead of IL-1 $\beta$ . Surprisingly, similar results to the ones where IL-1 $\beta$  was measured were seen (Fig. 22 B).

IL-1 $\alpha$ , like IL-1 $\beta$ , belongs to the IL-1 family and are both pro-inflammatory cytokines (Malik and Kanneganti 2018; Cavalli et al. 2021). IL-1 $\alpha$  and IL-1 $\beta$  bind to the IL-1 receptor 1 (IL-1R1), which induces pro-inflammatory effects (Cavalli et al. 2021). IL-1 $\alpha$  is found in hematopoietic and nonhematopoietic cells (Cavalli et al. 2021). IL-1 $\alpha$  is found as a precursor in a variety of cells (Cavalli et al. 2021). In literature, opposing facts are given on the synthesis, processing and cleavage of pro-IL-1 $\alpha$ . Some state that as with pro-IL-1 $\beta$ , pro-IL-1 $\alpha$  is also cleaved by caspase-1 to its mature form IL-1 $\alpha$  (Malik and Kanneganti 2018). On the other hand, other studies state that caspase-1 and the inflammasome have no role in the cleavage of pro-IL-1 $\alpha$  (Cavalli et al. 2021). Nevertheless, both sources agree on the fact that pro-IL-1 $\alpha$  is already biologically active, unlike pro-IL-1 $\beta$  (Cavalli et al. 2021).

After examining the IL-1 $\alpha$  results of the experiments in this thesis, it might be possible to say, that the synthesis and release of IL-1 $\alpha$  may be similar to the one of IL-1 $\beta$ . This may be said because the cells were treated with a first and second stimulus just as performed when IL-1 $\beta$  was measured in the cell supernatants. What is surely observed, is that both synthetic FFA2 and FFA3 agonists lead to a significant inhibition of the IL-1 $\alpha$  release, which is partly but significantly blunted by both conopeptides RgIA4 and ArIB [V11L, V16D]. This indicates that there might be a similar connection between the FFA2 and FFA3 as well as the nAChRs. However, all this is based on speculation and therefore in need of further more intensive experimental research.

Finally, in figure 22 A and B, the addition of LPS to mouse BMDMs led to a significantly higher LDH activity, compared with cells without any stimulus. Furthermore, the addition of ATP to mouse BMDMs, also led to a significantly higher measured LDH activity. This might be due to pyroptosis being activated and has been recorded in literature (Humphreys and Dubyak 1996; Kawano et al. 2012) (see 4.2.2). Furthermore, the addition of AR420626 and ArIB [V11L, V16D] also led to a significant increase in cell death compared to cells stimulated with LPS + ATP alone. No concluding explanation

has been found, since the inhibition of IL-1 $\beta$  was still measured and also blunted by the addition of ArIB [V11L, V16D]. This was also seen in 4.2.4.

All in all, the LDH activity was significantly increased by specific substances, generally lowering the credibility for the IL-1 $\beta$  measurements. However, most cell death increases were kept in range and the substances still led to a significant inhibition of the IL-1 $\beta$  level measured. Therefore, more research needs to be done for each substance, such as concentration-responsive curves.

## 5. Conclusion

In this thesis, the emphasis lies on the anti-inflammatory regulation of the ATP-induced IL-1 $\beta$  release by SCFAs acetate, propionate and butyrate. Some main points mentioned in the following, can be concluded from the experiments performed.

It has been observed, that both the P2X4 and P2X7 receptors play a role in the IL-1 $\beta$  secretion by activated “pulsed” monocytes. This enables the possibility of further P2X receptors to be involved in the ATP-dependent IL-1 $\beta$  secretion and therefore acts as a foundation for further research.

Furthermore, the stimulation of the FFA2 and FFA3 with SCFAs and synthetic agonists clearly results in an inhibition of the IL-1 $\beta$  secretion. Additionally, the FFA2 has shown to play a definite role in this process. Moreover, the data indicates that the downstream signaling of the FFA2 and FFA3 runs via the nAChRs. The exact mechanism remains unknown and should be further researched.

In multiple research papers, SCFAs have been shown to have significant health benefits (Maslowski et al. 2009; Filippo et al. 2010) (see 1.7). The exact mechanism of action remains unclear. These experiments in this thesis, shed some light on the signal transduction. It is however, still in need of more research.

Chronic inflammatory diseases, including those which affect the intestine, play a major socio-economic role. The results collected in this thesis demonstrate that the ATP-dependent IL-1 $\beta$  secretion can be reduced by submitting SCFAs. The exact way of application or use of the SCFAs is yet to be shown. Future research may demonstrate that, the increase of SCFAs might reduce inflammation and prevent or even cure diseases.

## 6. Summary

### 6.1 German

Interleukin-1 $\beta$  (IL-1 $\beta$ ) ist ein proinflammatorisches Zytokin, das hauptsächlich von aktivierten Monozyten und Makrophagen ausgeschüttet wird. Wenn IL-1 $\beta$  freigesetzt wird, sind zahlreiche Wirkungen zu beobachten, wie die Freisetzung von Zytokinen und Chemokinen, die zusätzlich das Knochenmark stimulieren. Eine Dysregulation der IL-1 $\beta$ -Sekretion kann zu systemischen Erkrankungen führen. Daher muss die Freisetzung von IL-1 $\beta$  streng reguliert werden.

Der erste Stimulus durch ein pathogen-assoziiertes molekulares Muster (PAMP) wie Lipopolysaccharid (LPS), führt zur Produktion des Vorläuferproteins pro-Interleukin-1 $\beta$  (pro-IL-1 $\beta$ ) und der Proteine, die das NLRP3-Inflammasom bilden. Der P2X7-Rezeptor wird durch den zweiten Stimulus, zum Beispiel ATP aus geschädigten Zellen, aktiviert, was zur Bildung des NLRP3-Inflammasoms und der anschließenden Freisetzung von reifem IL-1 $\beta$  führt.

In dieser Arbeit wurden Experimente mit mononukleären Zellen des menschlichen peripheren Blutes (hPBMCs), mononukleären Zellen des peripheren Blutes der Maus (mPBMCs) und Makrophagen aus dem Knochenmark der Maus (Maus-BMDMs) durchgeführt. BzATP in hPBMCs wirkte als starkes zweites Signal, es zeigte sich ein Widerspruch zur Literatur, da ATP sich jedoch in mPBMCs und Maus-BMDMs als stärkerer P2X7-Agonist erwies. Außerdem hat sich gezeigt, dass nicht nur der P2X7-Rezeptor, sondern auch der P2X4-Rezeptor eine Rolle bei der BzATP- oder ATP-abhängigen Freisetzung von IL-1 $\beta$  in hPBMCs und Maus-BMDMs spielt.

Neuere Studien zeigen, dass die Freisetzung von ATP-induziertem IL-1 $\beta$  über einen cholinergen Mechanismus gehemmt werden kann. In der vorliegenden Arbeit wurde festgestellt, dass der cholinerge Mechanismus durch synthetische FFA-Agonisten und die natürlichen FFA-Agonisten, bei denen es sich um kurzkettige Fettsäuren (SCFAs) handelt, in allen getesteten Zellen induziert wird. Insbesondere hat sich gezeigt, dass FFA2 für die Hemmung der Sekretion von ATP-abhängigem IL-1 $\beta$  notwendig ist. Dies wurde bei Experimenten mit mPBMCs festgestellt, denen das FFA2-Gen fehlt.

Die genaue Signaltransduktion der entzündungshemmenden Wirkung von SCFAs muss weiter erforscht werden. Darüber hinaus wird in den SCFAs ein großes Potenzial als

therapeutischer Ansatz gegen Entzündungskrankheiten gesehen. Daher sind weitere Forschungen auf diesem Gebiet von großer Bedeutung.

## 6.2 English

Interleukin-1 $\beta$  (IL-1 $\beta$ ) is a pro-inflammatory cytokine, that is mainly secreted by activated monocytes and macrophages. When IL-1 $\beta$  is released, numerous effects are seen, such as the release of cytokines and chemokines which additionally stimulate the bone marrow. A dysregulation of the IL-1 $\beta$  secretion can lead to systemic diseases. Therefore, the release of IL-1 $\beta$  needs to be strictly regulated.

The first stimulus by a pathogen-associated molecular pattern (PAMP) such as lipopolysaccharide (LPS), results in the production of the precursor protein pro-interleukin-1 $\beta$  (pro-IL-1 $\beta$ ) and the proteins that form the NLRP3-inflammasome. The P2X7 receptor is activated via the second stimulus being for example ATP from damaged cells, which leads to the assembly of the NLRP3-inflammasome and consecutive release of mature IL-1 $\beta$ .

In this thesis, experiments were performed on human peripheral blood mononuclear cells (hPBMCs), mouse peripheral blood mononuclear cells (mPBMCs) and mouse bone marrow-derived macrophages (mouse BMDMs). BzATP acted as a potent second signal in hPBMCs, however, contrary to published literature, ATP has seen to be a more potent P2X7 agonist in mPBMCs and mouse BMDMs. Furthermore, not only the P2X7 receptor but also the P2X4 receptor was shown to play a role in the BzATP- or ATP-dependent release of IL-1 $\beta$  in hPBMCs and mouse BMDMs.

Recent studies show, that the release of ATP-induced IL-1 $\beta$  can be inhibited via a cholinergic mechanism. In this present work, the cholinergic mechanism is seen to be induced by synthetic FFA agonists and the natural FFA agonists being short-chain fatty acids (SCFAs), in all cells tested. Specifically, the FFA2 has shown to be necessary for the inhibition of the secretion of ATP-dependent IL-1 $\beta$ . This was seen by performing experiments on FFA2 gene-deficient mPBMCs.

The exact signal transduction of the anti-inflammatory role shown by SCFAs is in need of further research. Additionally, there is a high potential seen in SCFAs as a therapeutic approach against inflammatory diseases. Therefore, further research in this field is of importance.

## 7. List of abbreviations

Abbreviation	Meaning
4-CMTB	4-chloro- $\alpha$ -(1-methylethyl)-N-2-thiazolylbenzeneacetamide
5-BDBD	5-(3-Bromophenyl)-1,3-dihydro-2H-benzofuro[3,2-e]-1,4-diazepin-2-on
Acet	Acetate
ACh	Acetylcholine
AP	Alkaline phosphatase
AP-1	Activator protein 1
Aqua dest.	Aqua destillata
ASC	Apoptosis-associated speck like protein
ATP	Adenosine triphosphate
BDNF	Brain-derived neurotrophic factor
BMDMs	Bone marrow-derived macrophages
BSA	Bovine serum albumin
Buty	Butyrate
BzATP	3'-O-(4-benzoyl) benzoyl ATP
CAMP	Cyclic AMP
CARD	Caspase-recruitment domain
CD14	Cluster of differentiation 14
CDNA	Complementary DNA
COX-2	Cyclooxygenase-2
CRP	C-reactive protein
DAB	3,3'-Diaminobenzidine
DAMPs	Damage-associated molecular patterns
DMSO	Dimethyl sulfoxide

DNA	Deoxyribonucleic acid
DPPC	Dipalmitoylphosphatidylcholine
EDTA	Ethylenediamine tetraacetic acid
ELISA	Enzyme-linked Immunosorbent Assay
ERK1/2	Extracellular-signal regulated kinases
FCS	Fetal calf serum
FFA2	Free fatty acid receptor 2
FFA3	Free fatty acid receptor 3
G-CSF	Granulocyte-colony stimulating factor
GDNA	Genomic DNA
GLP-1	Glucagon-like peptide-1
GPC	Glycerophosphocholine
G-proteins	Guanine nucleotide binding proteins
HEK	human embryonic kidney
HPBMCs	Human peripheral blood mononuclear cells
HPLC	High performance liquid chromatography
HRP	Horseradish peroxidase
IBD	Inflammatory bowel disease
IBM	International Business Machines
IL-1	Interleukin-1
IL-18	Interleukin-18
IL-18R	Interleukin-18 receptor
IL-1R1	Interleukin-1 receptor
IL-1Ra	Interleukin-receptor antagonist
IL-1 $\alpha$	Interleukin-1 $\alpha$

IL-1 $\beta$	Interleukin-1 $\beta$
IL-1R2	Interleukin-2 receptor
IL-1R3	Interleukin-3 receptor
INF- $\gamma$	Interferon- $\gamma$
IRF3	Interferon regulatory factor 3
JLU	Justus-Liebig University
LDH	Lactate dehydrogenase
LPS	Lipopolysaccharide
LRRs	Leucine rich copies
MAM	Monocyte Attachment Medium
M-CSF	Macrophage colony-stimulating factor
Mouse BMDMs	Mouse bone marrow-derived macrophages
MPBMCs	Mouse peripheral blood mononuclear cells
MRFP	Red fluorescent protein
MRNA	Messenger RNA
MyD88	Myeloid differentiation primary response 88
NACHRs	Nicotinic ACh receptors
NAD <sup>+</sup>	Nicotine-adenine-dinucleotide
NCBI	National Center for Biotechnology Information
NF- $\kappa$ B	Nuclear factor $\kappa$ B
NIH	National Institutes of Health
NLR	Nod-like receptor
NMS	Normal mouse serum
PAMPs	Pathogen-associated molecular patterns
PBMCs	Peripheral blood mononuclear cells

PBS	Dulbecco's phosphate buffered saline
PC	Phosphocholine
PCR	Polymerase chain reaction
PenStrep	Penicillin streptomycin
Pro-IL-18	Pro-interleukin-18
Pro-IL-1 $\beta$	Pro-interleukin-1 $\beta$
Prop	Propionate
PRRs	Pattern recognition receptors
PYY	Peptide YY
RCB	Red blood cell lysis buffer
RFP	Red fluorescent protein
RNA	Ribonucleic acid
RPMI	Roswell Park Memorial Institute
RT-PCR	Real-time PCR
SCFA	Short-chain fatty acid
SCFAs	Short-chain fatty acids
SPSS	Statistical Package for the Social Sciences
TBS	Tris buffered saline
TIR	Toll-IL receptor
TLR4	Toll-like receptor 4
TLRs	Toll-like receptors
TNF $\alpha$	Tumor necrosis factor $\alpha$
Treg	Regulatory T-cells
TRIF	TIR-domain-containing adapter-inducing interferon- $\beta$

## 8. List of figures

<b>Figure 1.</b> Schematic overview of the first danger signal pathway.....	4
<b>Figure 2.</b> Schematic overview of the first and second signal pathway.....	7
<b>Figure 3.</b> Schematic overview of the cholinergic inhibition mechanism of the adenosine triphosphate (ATP)-mediated interleukin-1 $\beta$ (IL-1 $\beta$ ) and interleukin-18 (IL-18) release.....	14
<b>Figure 4.</b> Schematic overview of the short-chain fatty acid (SCFA)-induced inhibition mechanism of the adenosine triphosphate (ATP)-mediated interleukin-1 $\beta$ (IL-1 $\beta$ ) and interleukin-18 (IL-18) release.....	25
<b>Figure 5.</b> The impact of BzATP (3'-O-(4-benzoyl) benzoyl ATP) or ATP on the secretion of IL-1 $\beta$ .....	50
<b>Figure 6 A, B.</b> The impact of P2X7 and P2X4 receptors on the BzATP (3'-O-(4-benzoyl) benzoyl ATP) and ATP-induced release of interleukin-1 $\beta$ (IL-1 $\beta$ ) by human peripheral blood mononuclear cells (hPBMCs).....	52
<b>Figure 7.</b> The FFA2 agonist inhibits the BzATP (3'-O-(4-benzoyl) benzoyl ATP)-induced release of interleukin-1 $\beta$ (IL-1 $\beta$ ) by human peripheral blood mononuclear cells (hPBMCs).....	54
<b>Figure 8.</b> The FFA3 agonist inhibits the BzATP (3'-O-(4-benzoyl) benzoyl ATP)-induced release of interleukin-1 $\beta$ (IL-1 $\beta$ ) by human peripheral blood mononuclear cells (hPBMCs).....	55
<b>Figure 9.</b> Involvement of nicotinic acetylcholine receptors (nAChRs) in the FFA2-mediated inhibition of the BzATP (3'-O-(4-benzoyl) benzoyl ATP)-induced release of interleukin-1 $\beta$ (IL-1 $\beta$ ).....	57
<b>Figure 10.</b> Involvement of nicotinic acetylcholine receptors (nAChRs) in the FFA3-mediated inhibition of the BzATP (3'-O-(4-benzoyl) benzoyl ATP)-induced release of interleukin-1 $\beta$ (IL-1 $\beta$ ).....	59
<b>Figure 11.</b> The impact of BzATP (3'-O-(4-benzoyl) benzoyl ATP) or ATP on the secretion of interleukin-1 $\beta$ (IL-1 $\beta$ ).....	60
<b>Figure 12.</b> Inhibition in the ATP-induced release of interleukin-1 $\beta$ (IL-1 $\beta$ ) by phosphocholine (PC), acetate (Acet), butyrate (Buty) and propionate (Prop).....	62
<b>Figure 13.</b> Effects of short-chain fatty acids (SCFAs) on the release of IL-1 $\beta$ by wild-type and FFA2 gene-deficient mouse peripheral blood mononuclear cells (mPBMCs)..	64
<b>Figure 14.</b> The FFA2 and FFA3 agonists inhibit the ATP-induced release of interleukin-1 $\beta$ (IL-1 $\beta$ ) by wild-type mouse peripheral blood mononuclear cells (mPBMCs).....	66
<b>Figure 15.</b> The FFA2 and FFA3 agonists inhibit the ATP-induced release of interleukin-1 $\beta$ (IL-1 $\beta$ ) in wild-type and FFA2 gene-deficient mouse peripheral blood mononuclear cells (mPBMCs).....	68
<b>Figure 16.</b> Immunohistochemical localization of the F4/80 antigen in mouse bone marrow-derived cells.....	69
<b>Figure 17.</b> Double-staining of macrophages and FFA2 within the murine colon.....	71

<b>Figure 18.</b> The impact of BzATP (3'-O-(4-benzoyl) benzoyl ATP) or ATP on the secretion of IL-1 $\beta$ .....	72
<b>Figure 19.</b> The impact of P2X7 receptor antagonist A438079 on the ATP-induced release of interleukin-1 $\beta$ (IL-1 $\beta$ ) by mouse bone marrow-derived macrophages (BMDMs).....	74
<b>Figure 20.</b> The impact of P2X7 receptor antagonist A438079 and P2X4 receptor antagonist 5-BDBD (5-(3-Bromophenyl)-1,3-dihydro-2H-benzofuro[3,2-e]-1,4-diazepin-2-one) on the ATP-induced release of interleukin-1 $\beta$ (IL-1 $\beta$ ) in mouse bone marrow-derived macrophages (BMDMs).....	76
<b>Figure 21.</b> The influence of short-chain fatty acid (SCFA) butyrate (Buty) on the ATP-induced release of interleukin-1 $\beta$ (IL-1 $\beta$ ) by mouse bone marrow-derived macrophages (BMDMs).....	78
<b>Figure 22 A, B.</b> The signaling of FFA2 and FFA3 involve nAChR containing $\alpha$ 7 and $\alpha$ 9/ $\alpha$ 10.....	81

## 9. List of tables

<b>Table 1.</b> Embedding in paraffin.....	46
--	----

## 10. List of references

- Adinolfi, E.; Giuliani, A. L.; Marchi, E. d.; Pegoraro, A.; Orioli, E.; Di Virgilio, F. (2018): The P2X7 receptor: A main player in inflammation. *Biochemical pharmacology* 151: 234–244. DOI: 10.1016/j.bcp.2017.12.021.
- Agrenzio, R. A.; Southworth, M. (1975): Sites of organic acid production and absorption in gastrointestinal tract of the pig. *American Journal of Physiology* 228: 454–460. DOI: 10.1152/ajplegacy.1975.228.2.454.
- Albuquerque, E. X.; Pereira, E. F. R.; Alkondon, M.; Rogers, S. W. (2009): Mammalian nicotinic acetylcholine receptors: from structure to function. *Physiological reviews* 89: 73–120. DOI: 10.1152/physrev.00015.2008.
- Amadio, S.; Parisi, C.; Piras, E.; Fabbriozio, P.; Apolloni, S.; Montilli, C. et al. (2017): Modulation of P2X7 receptor during inflammation in multiple sclerosis. *Frontiers in immunology* 8: 1529. DOI: 10.3389/fimmu.2017.01529.
- Ang, Z.; Ding, J. L. (2016): GPR41 and GPR43 in obesity and inflammation - protective or causative? *Frontiers in immunology* 7: 28. DOI: 10.3389/fimmu.2016.00028.
- Ang, Z.; Er, J. Z.; Ding, J. L. (2015): The short-chain fatty acid receptor GPR43 is transcriptionally regulated by XBP1 in human monocytes. *Scientific reports* 5: 8134. DOI: 10.1038/srep08134.
- Ang, Z.; Er, J. Z.; Tan, N. S.; Lu, J.; Liou, Y.-C.; Grosse, J.; Ding, J. L. (2016): Human and mouse monocytes display distinct signalling and cytokine profiles upon stimulation with FFAR2/FFAR3 short-chain fatty acid receptor agonists. *Scientific reports* 6: 341–345. DOI: 10.1038/srep34145.
- Ang, Z.; Xiong, D.; Wu, M.; Ding, J. L. (2018): FFAR2-FFAR3 receptor heteromerization modulates short-chain fatty acid sensing. *FASEB journal* 32: 289–303. DOI: 10.1096/fj.201700252RR.
- Archer, S. Y.; Meng, S.; Shei, A.; Hodin, R. A. (1998): p21WAF1 is required for butyrate-mediated growth inhibition of human colon cancer cells. *Proceedings of the National Academy of Sciences* 95: 6791–6796.
- Armant, M. A. and Fenton, M. J. (2002): Toll-like receptors: A family of pattern- recognition receptors in mammals. *Genome Biology* 3: 1–6. DOI: 10.1186/gb-2002-3-8-reviews3011.
- Arpaia, N.; Campbell, C.; Fan, X.; Dikiy, S.; van der Veeken, J.; Roos, P. et al. (2013): Metabolites produced by commensal bacteria promote peripheral regulatory T-cell generation. *Nature* 504: 451–455. DOI: 10.1038/nature12726.
- Austyn, J. M.; Gordon, S. (1981): F4/80, a monoclonal antibody directed specifically against the mouse macrophage. *European journal of immunology* 11: 805–815. DOI: 10.1002/eji.1830111013.
- Bach, K.; Knud, E.; Lærke, H. N.; Hedemann, M. S.; Nielsen, T. S.; Ingerslev, A. K. et al. (2018): Impact of diet-modulated butyrate production on intestinal barrier function and inflammation. *Nutrients* 10: 13-16. DOI: 10.3390/nu10101499.
- Backhaus, S.; Zakrzewicz, A.; Richter, K.; Damm, J.; Wilker, S.; Fuchs-Moll, G. et al. (2017): Surfactant inhibits ATP-induced release of interleukin-1 $\beta$ ; via nicotinic acetylcholine receptors. *Journal of lipid research* 58: 1055–1066. DOI: 10.1194/jlr.M071506.
- Bailón, E.; Cueto-Sola, M.; Utrilla, P.; Rodríguez-Cabezas, M. E.; Garrido-Mesa, N.; Zarzuelo, A. et al. (2010): Butyrate in vitro immune-modulatory effects might be mediated through a

- proliferation-related induction of apoptosis. *Immunobiology* 215: 863–873. DOI: 10.1016/j.imbio.2010.01.001.
- Baker, K. J.; Houston, A.; Brint, E. (2019): IL-1 family members in cancer; two sides to every story. *Frontiers in immunology* 10: 1197. DOI: 10.3389/fimmu.2019.01197.
- Bank, S.; Julsgaard, M.; Abed, O. K.; Burisch, J.; Broder-Brodersen, J.; Pedersen, N. K. et al. (2019): Polymorphisms in the NF $\kappa$ B, TNF-alpha, IL-1beta, and IL-18 pathways are associated with response to anti-TNF therapy in Danish patients with inflammatory bowel disease. *Alimentary pharmacology & therapeutics* 49: 890–903. DOI: 10.1111/apt.15187.
- Barberà-Cremades, M.; Baroja-Mazo, A.; Gomez, A. I.; Machado, F.; Di Virgilio, F.; Pelegrín, P. (2012): P2X7 receptor-stimulation causes fever via PGE2 and IL-1 $\beta$  release. *FASEB journal* 26: 2951–2962. DOI: 10.1096/fj.12-205765.
- Baroja-Mazo, A.; Barberà-Cremades, M.; Pelegrín, P. (2013): The participation of plasma membrane hemichannels to purinergic signaling. *Biochimica et biophysica acta* 1828: 79–93. DOI: 10.1016/j.bbamem.2012.01.002.
- Barrett, J. P.; Costello, D. A.; O'Sullivan, J.; Cowley, T. R.; Lynch, M. A. (2015): Bone marrow-derived macrophages from aged rats are more responsive to inflammatory stimuli. *Journal of neuroinflammation* 12: 67. DOI: 10.1186/s12974-015-0287-7.
- Bauernfeind, F. G.; Horvath, G.; Stutz, A.; Alnemri, E. S.; MacDonald, K.; Speert, D. et al. (2009): Cutting edge: NF-kappaB activating pattern recognition and cytokine receptors license NLRP3 inflammasome activation by regulating NLRP3 expression. *Journal of immunology* 183: 787–791. DOI: 10.4049/jimmunol.0901363.
- Bernier, L.-P.; Ase, A. R.; Séguéla, P. (2018): P2X receptor channels in chronic pain pathways. *British journal of pharmacology* 175: 2219–2230. DOI: 10.1111/bph.13957.
- Besten, G. D.; van Eunen, K.; Groen, A. K.; Venema, K.; Reijngoud, D.-J.; Bakker, B. M. (2013): The role of short-chain fatty acids in the interplay between diet, gut microbiota, and host energy metabolism. *Journal of lipid research* 54: 2325–2340. DOI: 10.1194/jlr.R036012.
- Bhattacharjee, J.; Das, B.; Mishra, A.; Sahay, P.; Upadhyay, P. (2017): Monocytes isolated by positive and negative magnetic sorting techniques show different molecular characteristics and immunophenotypic behaviour. *F1000Res* 6: 25–40. DOI: 10.12688/f1000research.12802.1.
- Bianchi, M. E. (2007): DAMPs, PAMPs and alarmins: all we need to know about danger. *Journal of leukocyte biology* 81: 1–5. DOI: 10.1189/jlb.0306164.
- Birt, D. F.; Boylston, T.; Hendrich, S.; Jane, J.-L.; Hollis, J.; Li, L. et al. (2013): Resistant starch: promise for improving human health. *Advances in nutrition* 4: 587–601. DOI: 10.3945/an.113.004325.
- Bobanovic, L. K.; Royle, S. J.; Murrell-Lagnado, R. D. (2002): P2X receptor trafficking in neurons is subunit specific. *The Journal of Neuroscience* 22: 4814–4824. DOI: 10.1523/JNEUROSCI.22-12-04814.2002.
- Bolognini, D.; Dedeo, D.; Milligan, G. (2021): Metabolic and inflammatory functions of short-chain fatty acid receptors. *Current opinion in endocrine and metabolic research* 16: 1–9. DOI: 10.1016/j.coemr.2020.06.005.
- Bolognini, D.; Tobin, A. B.; Milligan, G.; Moss, C. E. (2016): The pharmacology and function of receptors for short-chain fatty acids. *Molecular pharmacology* 89: 388–398. DOI: 10.1124/mol.115.102301.

- Boraschi, D.; Italiani, P.; Weil, S.; Martin, M. U. (2018): The family of the interleukin-1 receptors. *Immunological reviews* 281: 197–232. DOI: 10.1111/imr.12606.
- Bornet, F. R. J.; Brouns, F.; Tashiro, Y.; Duvillier, V. (2002): Nutritional aspects of short-chain dructooligosaccharides: natural occurrence, chemistry, physiology and health implications. *Digestive and Liver Disease* 34: 111–120. DOI: 10.1016/s1590-8658(02)80177-3.
- Borovikova, L. V.; Ivanova, S.; Zhang, M.; Yang, H.; Botchkina, G. I.; Watkins, L. R.; Wang, H. (2000): Vagus nerve stimulation attenuates the systemic inflammatory response to endotoxin. *Nature* 405: 458–462. DOI: 10.1038/35013070.
- Botos, I.; Segal, D. M.; Davies, D. R. (2011): The structural biology of Toll-like receptors. *Structure* 19: 447–459. DOI: 10.1016/j.str.2011.02.004.
- Boumechache, M.; Masin, M.; Edwardson, J. M.; Górecki, D. C.; Murrell-Lagnado, R. (2009): Analysis of assembly and trafficking of native P2X4 and P2X7 receptor complexes in rodent immune cells. *The Journal of biological chemistry* 284: 13446–13454. DOI: 10.1074/jbc.M901255200.
- Bowler, J. W.; Bailey, R. J.; North, R. A.; Surprenant, A. (2003): P2X4, P2Y1 and P2Y2 receptors on rat alveolar macrophages. *British journal of pharmacology* 140: 567–575. DOI: 10.1038/sj.bjp.0705459.
- Bragança, B.; Correia-de-Sá, P. (2020): Resolving the ionotropic P2X4 receptor mystery points towards a new therapeutic target for cardiovascular diseases. *International journal of molecular sciences* 21: 1230-1234. DOI: 10.3390/ijms21145005.
- Brody, Tom (1999): *Nutritional Biochemistry*. 2<sup>nd</sup> ed.: Academic Press.
- Brown, A. J.; Goldsworthy, S. M.; Barnes, A. A.; Eilert, M. M.; Tcheang, L.; Daniels, D. et al. (2003): The Orphan G protein-coupled receptors GPR41 and GPR43 are activated by propionate and other short chain carboxylic acids. *The Journal of biological chemistry* 278: 11312–11319. DOI: 10.1074/jbc.M211609200.
- Broz, P.; Dixit, V. M. (2016): Inflammasomes: mechanism of assembly, regulation and signalling. *Nature reviews. Immunology* 16: 407–420. DOI: 10.1038/nri.2016.58.
- Busse, R.; Mülsch, A. (1990): Induction of nitric oxide synthase by cytokines in vascular smooth muscle cells. *FEBS letters* 275: 87–90. DOI: 10.1016/0014-5793(90)81445-T.
- Byrne, C. S.; Chambers, E. S.; Morrison, D. J.; Frost, G. (2015): The role of short chain fatty acids in appetite regulation and energy homeostasis. *International journal of obesity* 39: 1331–1338. DOI: 10.1038/ijo.2015.84.
- Canè, S.; Ugel, S.; Trovato, R.; Marigo, I.; Sanctis, F.; Sartoris, S.; Bronte, V. (2019): The endless saga of monocyte diversity. *Frontiers in immunology* 10: 1786. DOI: 10.3389/fimmu.2019.01786.
- Canfora, E. E.; Jocken, J. W.; Blaak, E. E. (2015): Short-chain fatty acids in control of body weight and insulin sensitivity. *Nature reviews. Endocrinology* 11: 577–591. DOI: 10.1038/nrendo.2015.128.
- Carrick, J. B.; Begg, A. P. (2008): Peripheral blood leukocytes. *The Veterinary clinics of North America* 24: 239-259. DOI: 10.1016/j.cveq.2008.05.003.
- Casas-Pruneda, G.; Reyes, J. P.; Pérez-Flores, G.; Pérez-Cornejo, P.; Arreola, J. (2009): Functional interactions between P2X4 and P2X7 receptors from mouse salivary epithelia. *The Journal of physiology* 587: 2887–2901. DOI: 10.1113/jphysiol.2008.167395.

- Cascio, M. (2004): Structure and function of the glycine receptor and related nicotinic receptors. *The Journal of biological chemistry* 279: 19383–19386. DOI: 10.1074/jbc.R300035200.
- Cavalli, G.; Colafrancesco, S.; Emmi, G.; Imazio, M.; Lopalco, G.; Maggio, M. C. et al. (2021): Interleukin 1 $\alpha$ : a comprehensive review on the role of IL-1 $\alpha$  in the pathogenesis and treatment of autoimmune and inflammatory diseases. *Autoimmunity reviews* 20: 102–123. DOI: 10.1016/j.autrev.2021.102763.
- Cekic, C.; Linden, J. (2016): Purinergic regulation of the immune system. *Nature reviews. Immunology* 16: 177–192. DOI: 10.1038/nri.2016.4.
- Chambers, E. S.; Viardot, A.; Psichas, A.; Morrison, D. J.; Murphy, K. G.; Zac-Varghese, S. E. K. et al. (2015): Effects of targeted delivery of propionate to the human colon on appetite regulation, body weight maintenance and adiposity in overweight adults. *Gut* 64: 1744–1754. DOI: 10.1136/gutjnl-2014-307913.
- Chen, K.; Zhang, J.; Zhang, W.; Yang, J.; Li, K.; He, Y. (2013): ATP-P2X4 signaling mediates NLRP3 inflammasome activation: a novel pathway of diabetic nephropathy. *The international journal of biochemistry & cell biology* 45: 932–943. DOI: 10.1016/j.biocel.2013.02.009.
- Chen, Y.; Xia, S. (2021): Determination of the stability of plasma ATP in vitro. *American journal of blood research* 11: 96–99.
- Chevreul, M. E. (1813): Sur plusieurs corps gras, et particulièrement sur leurs combinaisons avec les alcalis. *Annales de Chimie*: 225–261.
- Chien, C. H.; Shahead A. C.; Hiroshi S.; Haruhide K. (2006): Enhancement of sodium fluoride-induced cell death by centrifugal force. *In Vivo* 20: 103–105.
- Christensen, S. B.; Hone, A. J.; Roux, I.; Kniazeff, J.; Pin, J.-P.; Upert, G. et al. (2017): RgIA4 potently blocks mouse  $\alpha 9\alpha 10$  nAChRs and provides long lasting protection against oxaliplatin-induced cold allodynia. *Frontiers in cellular neuroscience* 11: 219–222. DOI: 10.3389/fncel.2017.00219.
- Christiansen, C. B.; Gabe, M. B. N.; Svendsen, B.; Dragsted, L. O.; Rosenkilde, M. M.; Holst, J. J. (2018): The impact of short-chain fatty acids on GLP-1 and PYY secretion from the isolated perfused rat colon. *American journal of physiology. Gastrointestinal and liver physiology* 315: 53–65. DOI: 10.1152/ajpgi.00346.2017.
- Cifuentes, A. (2013): Foodomics: advanced mass spectrometry in modern food science and nutrition: John Wiley & Sons.
- Coddou, C.; Sandoval, R.; Hevia, M. J.; Stojilkovic, S. S. (2019): Characterization of the antagonist actions of 5-BDBD at the rat P2X4 receptor. *Neuroscience letters* 690: 219–224. DOI: 10.1016/j.neulet.2018.10.047.
- Cook, S. (1998): Review article: short chain fatty acids in health and disease. *Alimentary pharmacology & therapeutics* 12: 499–507.
- Corrêa-Oliveira, R.; Fachi, J. L.; Vieira, A.; Sato, F. T.; Vinolo, M. A. R. (2016): Regulation of immune cell function by short-chain fatty acids. *Clinical & translational immunology* 5: 73–77. DOI: 10.1038/cti.2016.17.
- Cox, M. A.; Bassi, C.; Saunders, M. E.; Nechanitzky, R.; Morgado-Palacin, I.; Zheng, C.; Mak, T. W. (2020): Beyond neurotransmission: acetylcholine in immunity and inflammation. *Journal of internal medicine* 287: 120–133. DOI: 10.1111/joim.13006.

- Crown, J.; Jakubowski, A.; Gabrilove, J. (1993): Interleukin-1: biological effects in human hematopoiesis. *Leukemia & lymphoma* 9: 433–440. DOI: 10.3109/10428199309145750.
- Cummings, J. H. (1981): Short chain fatty acids in the human colon. *Gut* 22: 763–779. DOI: 10.1136/gut.22.9.763.
- Dawson, A. M.; Holdsworth, C. D.; Webb, J. (1964): Absorption of short chain fatty acids in man. *Proceedings of the society for experimental biology and medicine* 117: 97–100. DOI: 10.3181/00379727-117-29505.
- Deleu, S.; Arnauts, K.; Deprez, L.; Machiels, K.; Ferrante, M.; Huys, G.R.B. et al. (2023): High acetate concentration protects intestinal barrier and exerts anti-inflammatory effects in organoid-derived epithelial monolayer cultures from Patients with Ulcerative Colitis. *International journal of molecular sciences* 24: 768–772. DOI: 10.3390/ijms24010768.
- Delves, P. J.; Martin, S.; Burton, D.; Roitt, I. M. (2006): Roitt's Essential Immunology. 11<sup>th</sup> ed.: Blackwell Publishing Ltd.
- Di Virgilio, F.; Dal Ben, D.; Sarti, A. C.; Giuliani, A. L.; Falzoni, S. (2017): The P2X7 receptor in infection and inflammation. *Immunity* 47: 15–31. DOI: 10.1016/j.immuni.2017.06.020.
- Di, A.; Xiong, S.; Ye, Z.; Malireddi, R. K. S.; Kometani, S.; Zhong, M. et al. (2018): The TWIK2 potassium efflux channel in macrophages mediates NLRP3 inflammasome-induced inflammation. *Immunity* 49: 56–65. DOI: 10.1016/j.immuni.2018.04.032.
- Dinarello, C. A. (2009): Immunological and inflammatory functions of the interleukin-1 family. *Annual review of immunology* 27: 519–550. DOI: 10.1146/annurev.immunol.021908.132612.
- Dinarello, C. A. (2018a): Introduction to the interleukin-1 family of cytokines and receptors: Drivers of innate inflammation and acquired immunity. *Immunological reviews* 281: 5–7. DOI: 10.1111/imr.12624.
- Dinarello, C. A.; Simon, A.; van der Meer, J. W. M. (2012): Treating inflammation by blocking interleukin-1 in a broad spectrum of diseases. *Nature reviews. Drug discovery* 11: 633–652. DOI: 10.1038/nrd3800.
- Engelstoft, M. S.; Park, W.-M.; Sakata, I.; Kristensen, L. V.; Husted, A. S.; Osborne-Lawrence, S. et al. (2013): Seven transmembrane G protein-coupled receptor repertoire of gastric ghrelin cells. *Molecular metabolism* 2: 376–392. DOI: 10.1016/j.molmet.2013.08.006.
- Ennion, S. J.; Evans, R. J. (2001): Conserved cysteine residues in the extracellular loop of the human P2X1 receptor form disulfide bonds and are involved in receptor trafficking to the cell surface. *Molecular pharmacology* 61: 303–311. DOI: 10.1124/mol.61.2.303.
- Feldman, N.; Rotter-Maskowitz, A.; Okun, E. (2015): DAMPs as mediators of sterile inflammation in aging-related pathologies. *Ageing research reviews* 24: 29–39. DOI: 10.1016/j.arr.2015.01.003.
- Ferrari, D.; Chiozzi, P.; Falzoni, S.; Dal Susino, M.; Melchiorri, L.; Baricordi, O. R.; Di Virgilio, F. (1997): Extracellular ATP triggers IL-1 beta release by activating the purinergic P2Z receptor of human macrophages. *The Journal of Immunology* 159: 1451–1458. DOI: 10.4049/jimmunol.159.3.1451.
- Ferrari, D.; Pizzirani, C.; Adinolfi, E.; Lemoli, R. M.; Curti, A.; Idzko, M. et al. (2006): The P2X7 receptor: a key player in IL-1 processing and release. *The Journal of Immunology* 176: 3877–3883. DOI: 10.4049/jimmunol.176.7.3877.
- Filippo, C.; Cavalieri, D.; Di Paola, M.; Ramazzotti, M.; Poullet, J. B.; Massart, S. et al. (2010): Impact of diet in shaping gut microbiota revealed by a comparative study in children from Europe

- and rural Africa. *Proceedings of the National Academy of Sciences of the United States of America* 107: 14691–14696. DOI: 10.1073/pnas.1005963107.
- Filippone, A.; Lanza, M.; Campolo, M.; Casili, G.; Paterniti, I.; Cuzzocrea, S.; Esposito, E. (2020): The anti-inflammatory and antioxidant effects of sodium propionate. *International journal of molecular sciences* 21: 1459–1463. DOI: 10.3390/ijms21083026.
- Fitzgerald, K. A.; Kagan, J. C. (2020): Toll-like receptors and the control of immunity. *Cell* 180: 1044–1066. DOI: 10.1016/j.cell.2020.02.041.
- Fleming, L. L.; Floch, M. H. (1986): Digestion and absorption of fiber carbohydrate in the colon. *The American journal of gastroenterology* 81: 507–511.
- Francistiová, L.; Bianchi, C.; Di Lauro, C.; Sebastián-Serrano, Á.; Diego-García, L.; Kobolák, J. et al. (2020): The role of P2X7 receptor in Alzheimer's disease. *Frontiers in molecular neuroscience* 13: 94. DOI: 10.3389/fnmol.2020.00094.
- Franklin, K. M.; Asatryan, L.; Jakowec, M. W.; Trudell, J. R.; Bell, R. L.; Davies, D. L. (2014): P2X4 receptors (P2X4Rs) represent a novel target for the development of drugs to prevent and/or treat alcohol use disorders. *Frontiers in neuroscience* 8: 176. DOI: 10.3389/fnins.2014.00176.
- Fujii, T.; Mashimo, M.; Moriwaki, Y.; Misawa, H.; Ono, S.; Horiguchi, K.; Kawashima, K. (2017): Expression and function of the cholinergic system in immune cells. *Frontiers in immunology* 8: 1085. DOI: 10.3389/fimmu.2017.01085.
- Galozzi, P.; Bindoli, S.; Doria, A.; Sfriso, P. (2021): The revisited role of interleukin-1 alpha and beta in autoimmune and inflammatory disorders and in comorbidities. *Autoimmunity reviews* 20: 102785. DOI: 10.1016/j.autrev.2021.102785.
- Garlanda, C.; Dinarello, C. A.; Mantovani, A. (2013): The interleukin-1 family: back to the future. *Immunity* 39: 1003–1018. DOI: 10.1016/j.immuni.2013.11.010.
- Geyer, M.; Müller-Ladner, U. (2010): Actual status of antiinterleukin-1 therapies in rheumatic diseases. *Current opinion in rheumatology* 22: 246–251. DOI: 10.1097/BOR.0b013e3283373fa0.
- Gicquel, T.; Victoni, T.; Fautrel, A.; Robert, S.; Gleonnec, F.; Guezingar, M. et al. (2014): Involvement of purinergic receptors and NOD-like receptor-family protein 3-inflammasome pathway in the adenosine triphosphate-induced cytokine release from macrophages. *Clinical and experimental pharmacology & physiology* 41: 279–286. DOI: 10.1111/1440-1681.12214.
- Gonçalves, P.; Araújo, J. R.; Di Santo, J. P. (2018): A cross-talk between microbiota-derived short-chain fatty acids and the host mucosal immune system regulates intestinal homeostasis and inflammatory bowel disease. *Inflammatory bowel diseases* 24: 558–572. DOI: 10.1093/ibd/izx029.
- Gong, T.; Liu, L.; Jiang, W.; Zhou, R. (2020): DAMP-sensing receptors in sterile inflammation and inflammatory diseases. *Nature reviews. Immunology* 20: 95–112. DOI: 10.1038/s41577-019-0215-7.
- Grabitzki, J.; Ahrend, M.; Schachter, H.; Geyer, R.; Lochnit, G. (2008): The PCome of *Caenorhabditis elegans* as a prototypic model system for parasitic nematodes: identification of phosphorylcholine-substituted proteins. *Molecular and biochemical parasitology* 161: 101–111. DOI: 10.1016/j.molbiopara.2008.06.014.
- Grabitzki, J.; Lochnit, G. (2009): Immunomodulation by phosphocholine--biosynthesis, structures and immunological implications of parasitic PC-epitopes. *Molecular immunology* 47: 149–163. DOI: 10.1016/j.molimm.2009.09.035.

- Gracie, J. A.; Forsey, R. J.; Chan, W. L.; Gilmour, A.; Leung, B. P.; Greer, M. R. et al. (1999): A proinflammatory role for IL-18 in rheumatoid arthritis. *The Journal of clinical investigation* 104: 1393–1401. DOI: 10.1172/JCI7317.
- Grau, V.; Richter, K.; Hone, A. J.; McIntosh, J. M. (2018): Conopeptides V11L;V16D Ar1B and RgIA4: Powerful tools for the identification of novel nicotinic acetylcholine receptors in monocytes. *Frontiers in pharmacology* 9: 1499. DOI: 10.3389/fphar.2018.01499.
- Greaney, A. J.; Leppla, S. H.; Moayeri, M. (2015): Bacterial exotoxins and the inflammasome. *Frontiers in immunology* 6: 570. DOI: 10.3389/fimmu.2015.00570.
- Grierson, J. P.; Meldolesi, J. S. (1995): Stress-induced  $[Ca^{2+}]_i$  transients and oscillations in mouse fibroblasts are mediated by endogenously released ATP. *Journal of Biological Chemistry* 270: 4451–4456.
- Grundmann, M.; Tikhonova, I. G.; Hudson, B. D.; Smith, N. J.; Mohr, K.; Ulven, T. et al. (2016): A molecular mechanism for sequential activation of a G protein-coupled receptor. *Cell chemical biology* 23: 392–403. DOI: 10.1016/j.chembiol.2016.02.014.
- Grunstein, M. (1997): Histone acetylation in chromatin structure and transcription. *Nature* 389: 349–352.
- Gu, Y.; Kuida, K.; Tsutsui, H.; Ku, G.; Hsiao, K.; Fleming, M. A. et al. (1997): Activation of interferon-gamma inducing factor mediated by interleukin-1beta converting enzyme. *Science* 275: 206–209. DOI: 10.1126/science.275.5297.206.
- Guerriero, J. L. (2019): Macrophages: Their untold story in T cell activation and function. *International review of cell and molecular biology* 342: 73–93. DOI: 10.1016/bs.ircmb.2018.07.001.
- Guilliams, M.; Mildner, A.; Yona, S. (2018): Developmental and functional heterogeneity of monocytes. *Immunity* 49: 595–613. DOI: 10.1016/j.immuni.2018.10.005.
- Guo, C.; Masin, M.; Qureshi, O. S.; Murrell-Lagnado, R. D. (2007): Evidence for functional P2X4/P2X7 heteromeric receptors. *Molecular pharmacology* 72: 1447–1456. DOI: 10.1124/mol.107.035980.
- Gwilt, C. R.; Donnelly, L. E.; Rogers, D. F. (2007): The non-neuronal cholinergic system in the airways: an unappreciated regulatory role in pulmonary inflammation? *Pharmacology & therapeutics* 115: 208–222. DOI: 10.1016/j.pharmthera.2007.05.007.
- Hague, A.; Elder, D. J.; Hicks, D. J.; Paraskeva, C. (1995): Apoptosis in colorectal tumour cells: induction by the short chain fatty acids butyrate, propionate and acetate and by the bile salt deoxycholate. *International journal of cancer* 60: 400–406. DOI: 10.1002/ijc.2910600322.
- Hanriot, M. (1911): Contribution a l'étude des acides gras et des lipochromes contenus dans les matières fécales des chevaux. *Bulletin de la Société Chimique de France* 9: 88–97.
- Hecker, A.; Küllmar, M.; Wilker, S.; Richter, K.; Zakrzewicz, A.; Atanasova, S. et al. (2015): Phosphocholine-modified macromolecules and canonical nicotinic agonists inhibit ATP-induced IL-1 $\beta$  release. *Journal of immunology* 195: 2325–2334. DOI: 10.4049/jimmunol.1400974.
- Hernández, M. A. G.; Canfora, E. E.; Jocken, J. W. E.; Blaak, E. E. (2019): The short-chain fatty acid acetate in body weight control and insulin sensitivity. *Nutrients* 11: 144–156. DOI: 10.3390/nu11081943.
- Hosseini, E.; Grootaert, C.; Verstraete, W.; van de Wiele, T. (2011): Propionate as a health-promoting microbial metabolite in the human gut. *Nutrition reviews* 69: 245–258. DOI: 10.1111/j.1753-4887.2011.00388.x.

- Hsieh K. M.; Blumenthal, H. T. (1956): Serum lactic dehydrogenase levels in various disease states. *Proceedings of the Society for Experimental Biology and Medicine. Society for Experimental Biology and Medicine* 91: 626–630. DOI: 10.3181/00379727-91-22353.
- Hume, D. A.; Robinson, A. P.; MacPherson, G. G.; Gordon, S. (1983): The mononuclear phagocyte system of the mouse defined by immunohistochemical localization of antigen F4/80. Relationship between macrophages, Langerhans cells, reticular cells, and dendritic cells in lymphoid and hematopoietic organs. *The Journal of experimental medicine* 158: 1522–1536. DOI: 10.1084/jem.158.5.1522.
- Humphreys, B. D.; Dubyak, G. R. (1996): Induction of the P2z/P2X7 nucleotide receptor and associated phospholipase D activity by lipopolysaccharide and IFN-gamma in the human THP-1 monocytic cell line. *The Journal of Immunology* 157: 5627–5637.
- Huynh, P. N.; Christensen, S. B.; McIntosh, J. M. (2022): RgIA4 prevention of acute oxaliplatin-induced cold allodynia Requires  $\alpha 9$ -containing nicotinic acetylcholine receptors and CD3+ T-cells. *Cells* 11: 235-241. DOI: 10.3390/cells11223561.
- Issekutz, A. C.; Issekutz, T. B. (1993): Quantitation and kinetics of blood monocyte migration to acute inflammatory reactions, and IL-1 alpha, tumor necrosis factor-alpha, and IFN-gamma. *The Journal of Immunology* 151: 2105–2115.
- Iwasaki, A.; Medzhitov, R. (2004): Toll-like receptor control of the adaptive immune responses. *Nature immunology* 5: 987–995. DOI: 10.1038/ni1112.
- Iwasaki, A.; Medzhitov, R. (2015): Control of adaptive immunity by the innate immune system. *Nature immunology* 16: 343–353. DOI: 10.1038/ni.3123.
- Jakubzick, C. V.; Randolph, G. J.; Henson, P. M. (2017): Monocyte differentiation and antigen-presenting functions. *Nature reviews. Immunology* 17: 349–362. DOI: 10.1038/nri.2017.28.
- Janeway, C. A. (1989): Approaching the asymptote? Evolution and revolution in immunology. *Cold Spring Harbor symposia on quantitative biology* 54: 1–13. DOI: 10.1101/sqb.1989.054.01.003.
- Janeway, C. A.; Medzhitov, R. (2002): Innate immune recognition. *Annual review of immunology* 20: 197–216. DOI: 10.1146/annurev.immunol.20.083001.084359.
- Janeway, C. A.; Travers, P.; Walport, M.; Shlomchik, M. J. (2001): Immunobiology. The immune system in health and disease. 5<sup>th</sup> ed.: Garland Science.
- Jarvis, M. F.; Khakh, B. S. (2009): ATP-gated P2X cation-channels. *Neuropharmacology* 56: 208–215. DOI: 10.1016/j.neuropharm.2008.06.067.
- Jenkins, D. J.; Wolever, T. M.; Collier, G. R.; Ocana, A.; Rao, A. V.; Buckley, G. et al. (1987): Metabolic effects of a low-glycemic-index diet. *The American journal of clinical nutrition* 46: 968–975. DOI: 10.1093/ajcn/46.6.968.
- Kahlenberg, J. M.; Dubyak, G. R. (2004): Mechanisms of caspase-1 activation by P2X7 receptor-mediated K<sup>+</sup> release. *American journal of physiology. Cell physiology* 286: 1100-1108. DOI: 10.1152/ajpcell.00494.2003.
- Kanellopoulos, J. M.; Almeida-da-Silva, C. L. C.; Rüttel Boudinot, S.; Ojcius, D. M. (2021): Structural and functional features of the P2X4 receptor: An immunological perspective. *Frontiers in immunology* 12: 645-654. DOI: 10.3389/fimmu.2021.645834.
- Karmakar, M.; Katsnelson, M. A.; Dubyak, G. R.; Pearlman, E. (2016): Neutrophil P2X7 receptors mediate NLRP3 inflammasome-dependent IL-1 $\beta$  secretion in response to ATP. *Nature communications* 7: 55-59. DOI: 10.1038/ncomms10555.

- Katritch, V.; Cherezov, V.; Stevens, R. C. (2013): Structure-function of the G protein-coupled receptor superfamily. *Annual review of pharmacology and toxicology* 53: 531–556. DOI: 10.1146/annurev-pharmtox-032112-135923.
- Kawai, T.; Akira, S. (2010): The role of pattern-recognition receptors in innate immunity: update on Toll-like receptors. *Nature immunology* 11: 373–384. DOI: 10.1038/ni.1863.
- Kawano, A.; Tsukimoto, M.; Mori, D.; Noguchi, T.; Harada, H.; Takenouchi, T. et al. (2012a): Regulation of P2X7-dependent inflammatory functions by P2X4 receptor in mouse macrophages. *Biochemical and biophysical research communications* 420: 102–107. DOI: 10.1016/j.bbrc.2012.02.122.
- Kawano, A.; Tsukimoto, M.; Noguchi, T.; Hotta, N.; Harada, H.; Takenouchi, T. et al. (2012b): Involvement of P2X4 receptor in P2X7 receptor-dependent cell death of mouse macrophages. *Biochemical and biophysical research communications* 419: 374–380. DOI: 10.1016/j.bbrc.2012.01.156.
- Kawasaki, T.; Kawai, T. (2014): Toll-like receptor signaling pathways. *Frontiers in immunology* 5: 461. DOI: 10.3389/fimmu.2014.00461.
- Kawashima, K.; Fujii, T. (2000): Extraneuronal cholinergic system in lymphocytes. *Pharmacology and therapeutics* 86: 29–48.
- Kawashima, K.; Fujii, T.; Moriwaki, Y.; Misawa, H.; Horiguchi, K. (2015): Non-neuronal cholinergic system in regulation of immune function with a focus on  $\alpha 7$  nAChRs. *International immunopharmacology* 29: 127–134. DOI: 10.1016/j.intimp.2015.04.015.
- Kawate, T.; Michel, J. C.; Birdsong, W. T.; Gouaux, E. (2009): Crystal structure of the ATP-gated P2X(4) ion channel in the closed state. *Nature* 460: 592–598. DOI: 10.1038/nature08198.
- Kawate, T.; Robertson, J. L.; Li, M.; Silberberg, S. D.; Swartz, K. J. (2011): Ion access pathway to the transmembrane pore in P2X receptor channels. *The Journal of general physiology* 137: 579–590. DOI: 10.1085/jgp.201010593.
- Khakh, B. S.; North, R. A. (2012): Neuromodulation by extracellular ATP and P2X receptors in the CNS. *Neuron* 76: 51–69. DOI: 10.1016/j.neuron.2012.09.024.
- Kim, S.; Kim, J.-H.; Park, B. O.; Kwak, Y. S. (2014): Perspectives on the therapeutic potential of short-chain fatty acid receptors. *BMB reports* 47: 173–178. DOI: 10.5483/bmbrep.2014.47.3.272.
- Kimura, I.; Ozawa, K.; Inoue, D.; Imamura, T.; Kimura, K.; Maeda, T. et al. (2013): The gut microbiota suppresses insulin-mediated fat accumulation via the short-chain fatty acid receptor GPR43. *Nature communications* 4: 1829. DOI: 10.1038/ncomms2852.
- Kostura, M. J.; Tocci, M. J.; Limjuco, G.; Chin, J.; Cameron, P.; Hillman, A. G. (1989): Identification of a monocyte specific pre-interleukin 1 beta convertase activity. *Proceedings of the National Academy of Sciences of the United States of America* 86: pp. 5227–5231.
- Kress, H.; Stelzer, E. H. K.; Holzer, D.; Buss, F.; Griffiths, G.; Rohrbach, A. (2007): Filopodia act as phagocytic tentacles and pull with discrete steps and a load-dependent velocity. *Proceedings of the National Academy of Sciences of the United States of America* 104: 11633–11638. DOI: 10.1073/pnas.0702449104.
- Lamkanfi, M.; Dixit, V. M. (2014): Mechanisms and functions of inflammasomes. *Cell* 157: 1013–1022. DOI: 10.1016/j.cell.2014.04.007.
- Lang, T.; Lee, J. P. W.; Elgass, K.; Pinar, A. A.; Tate, M. D.; Aitken, E. H. et al. (2018): Macrophage migration inhibitory factor is required for NLRP3 inflammasome activation. *Nature communications* 9: 2223. DOI: 10.1038/s41467-018-04581-2.

- Layden, B. T.; Angueira, A. R.; Brodsky, M.; Durai, V.; Lowe, W. L. (2013): Short chain fatty acids and their receptors: new metabolic targets. *The journal of laboratory and clinical medicine* 161: 131–140. DOI: 10.1016/j.trsl.2012.10.007.
- Le Poul, E.; Loison, C.; Struyf, S.; Springael, J.-Y.; Lannoy, V.; Decobecq, M.-E. et al. (2003): Functional characterization of human receptors for short chain fatty acids and their role in polymorphonuclear cell activation. *The Journal of biological chemistry* 278: 25481–25489. DOI: 10.1074/jbc.M301403200.
- Lee, S. U.; In, H. J.; Kwon, M. S.; Park, B. O.; Jo, M.; Kim, M.-O. et al. (2013):  $\beta$ -Arrestin 2 mediates G protein-coupled receptor 43 signals to nuclear factor- $\kappa$ B. *Biological and Pharmaceutical Bulletin* 36: 1754–1759. DOI: 10.1248/bpb.b13-00312.
- Lee, S.; Suh, G.-Y.; Ryter, S. W.; Choi, A. M. K. (2016): Regulation and function of the nucleotide binding domain leucine-rich repeat-containing receptor, pyrin domain-containing-3 inflammasome in lung disease. *American journal of respiratory cell and molecular biology* 54: 151–160. DOI: 10.1165/rcmb.2015-0231TR.
- Lee, T.; Schwandner, R.; Swaminath, G.; Weiszmann, J.; Cardozo, M.; Greenberg, J. et al. (2008): Identification and functional characterization of allosteric agonists for the G protein-coupled receptor FFA2. *Molecular pharmacology* 74: 1599–1609. DOI: 10.1124/mol.108.049536.
- Legrand, C.; Bour, J. M.; Jacob, C.; Capiamont, J.; Martial, A.; Marc, A. et al. (1992): Lactate dehydrogenase (LDH) activity of the cultured eukaryotic cells as marker of the number of dead cells in the medium corrected. *Journal of biotechnology* 25: 231–243. DOI: 10.1016/0168-1656(92)90158-6.
- Li, Y.; Li, N.; Yan, Z.; Li, H.; Chen, L.; Zhang, Z. et al. (2016): Dysregulation of the NLRP3 inflammasome complex and related cytokines in patients with multiple myeloma. *Hematology* 21: 144–151. DOI: 10.1179/1607845415Y.0000000029.
- Li, Z.; Guo, J.; Bi, L. (2020): Role of the NLRP3 inflammasome in autoimmune diseases. *Biomedicine & pharmacotherapy* 130: 1105-1142. DOI: 10.1016/j.biopha.2020.110542.
- Liu, J.; Li, H.; Gong, T.; Chen, W.; Mao, S.; Kong, Y. et al. (2020): Anti-neuroinflammatory effect of short-chain fatty acid acetate against Alzheimer's disease via upregulating GPR41 and inhibiting ERK/JNK/NF- $\kappa$ B. *Journal of agricultural and food chemistry* 68: 7152–7161. DOI: 10.1021/acs.jafc.0c02807.
- Lopez-Castejon, G.; Brough, D. (2011): Understanding the mechanism of IL-1 $\beta$  secretion. *Cytokine & growth factor reviews* 22: 189–195. DOI: 10.1016/j.cytogfr.2011.10.001.
- Lupton, J. R. (2004): Microbial degradation products influence colon cancer risk: the butyrate controversy. *The Journal of nutrition* 134: 479–482. DOI: 10.1093/jn/134.2.479.
- Ma, W.; Korngreen, A.; Weil, S.; Cohen, E. B.-T.; Priel, A.; Kuzin, L.; Silberberg, S. D. (2006): Pore properties and pharmacological features of the P2X receptor channel in airway ciliated cells. *The Journal of physiology* 571: 503–517. DOI: 10.1113/jphysiol.2005.103408.
- Ma, W.-T.; Gao, F.; Gu, K.; Chen, D.-K. (2019): The role of monocytes and macrophages in autoimmune diseases: A comprehensive review. *Frontiers in immunology* 10: 1140. DOI: 10.3389/fimmu.2019.01140.
- Mahla, R. S.; Kumar, A.; Tutill, H. J.; Krishnaji, S. T.; Sathyamoorthy, B.; Noursadeghi, M. et al. (2021): NIX-mediated mitophagy regulate metabolic reprogramming in phagocytic cells during mycobacterial infection. *Tuberculosis* 126: 102–112. DOI: 10.1016/j.tube.2020.102046.
- Malik, A.; Kanneganti, T.-D. (2018): Function and regulation of IL-1 $\alpha$  in inflammatory diseases and cancer. *Immunological reviews* 281: 124–137. DOI: 10.1111/imr.12615.

- Manaka, S.; Tanabe, N.; Kariya, T.; Naito, M.; Takayama, T.; Nagao, M. et al. (2015): Low-intensity pulsed ultrasound-induced ATP increases bone formation via the P2X7 receptor in osteoblast-like MC3T3-E1 cells. *FEBS letters* 589: 310–318. DOI: 10.1016/j.febslet.2014.12.013.
- March, C. J.; Mosley, B.; Larsen, A.; Cerretti, D. P.; Braedt, G.; Price, V. (1985): Cloning, sequence and expression of two distinct human interleukin-1 complementary DNAs. *Nature* 315: 641–647. DOI: 10.1038/315641a0.
- Mariathasan, S.; Newton, K.; Monack, D. M.; Vucic, D.; French, D. M.; Lee, W. P. et al. (2004): Differential activation of the inflammasome by caspase-1 adaptors ASC and Ipaf. *Nature* 430: 213–218. DOI: 10.1038/nature02664.
- Mariathasan, S.; Weiss, D. S.; Newton, K.; McBride, J.; O'Rourke, K.; Roose-Girma, M. et al. (2006): Cryopyrin activates the inflammasome in response to toxins and ATP. *Nature* 440: 228–232. DOI: 10.1038/nature04515.
- Marim, F. M.; Silveira, T. N.; Lima, D. S. [JR]; Zamboni, D. S. (2010): A method for generation of bone marrow-derived macrophages from cryopreserved mouse bone marrow cells. *The public library of science one* 5: 152-163. DOI: 10.1371/journal.pone.0015263.
- Markert, C. L. (1984): Lactate dehydrogenase. Biochemistry and function of lactate dehydrogenase. *Cell biochemistry and function* 2: 131–134. DOI: 10.1002/cbf.290020302.
- Marques, F. Z.; Nelson, E.; Chu, P.-Y.; Horlock, D.; Fiedler, A.; Ziemann, M. et al. (2017): High-fiber diet and acetate supplementation change the gut microbiota and prevent the development of hypertension and heart failure in hypertensive mice. *Circulation* 135: 964–977. DOI: 10.1161/CIRCULATIONAHA.116.024545.
- Martin-Gallausiaux, C.; Marinelli, L.; Blottière, H. M.; Larraufie, P.; Lapaque, N. (2021): SCFA: mechanisms and functional importance in the gut. *The Proceedings of the Nutrition Society* 80: 37–49. DOI: 10.1017/S0029665120006916.
- Martinon, F.; Burns, K.; Tschopp, J. (2002): The inflammasome: A molecular platform triggering activation of inflammatory caspases and processing of proIL- $\beta$ . *Molecular cell* 10: 417-126. DOI: 10.1016/S1097-2765(02)00599-3.
- Martinon, F.; Mayor, A.; Tschopp, J. (2009): The inflammasomes: guardians of the body. *Annual review of immunology* 27: 229–265. DOI: 10.1146/annurev.immunol.021908.132715.
- Mashimo, M.; Moriwaki, Y.; Misawa, H.; Kawashima, K.; Fujii, T. (2021): Regulation of immune functions by non-neuronal acetylcholine (ACh) via muscarinic and nicotinic ACh receptors. *International journal of molecular sciences* 22: 438–452. DOI: 10.3390/ijms22136818.
- Maslin, C.; Kedzierska, K.; Webster, N.; Muller, W.; Crowe, S. (2005): Transendothelial migration of monocytes: The underlying molecular mechanisms and consequences of HIV-1 infection. *Current HIV research* 3: 303–317. DOI: 10.2174/157016205774370401.
- Maslowski, K. M.; Vieira, A. T.; Ng, A.; Kranich, J.; Sierro, F.; Di Y. et al. (2009): Regulation of inflammatory responses by gut microbiota and chemoattractant receptor GPR43. *Nature* 461: 1282–1286. DOI: 10.1038/nature08530.
- Matzinger, P. (1994): Tolerance, Danger, and the Extended Family. *Annual review of immunology* 12: 991–1045. DOI: 10.1146/annurev.iy.12.040194.005015.
- McGarry, M. P.; Stewart, C. C. (1991): Murine eosinophil granulocytes bind the murine macrophage-monocyte specific monoclonal antibody F4/80. *Journal of leukocyte biology* 50: 471–478. DOI: 10.1002/jlb.50.5.471.

- McNeil, N. I.; Cummings, J. H.; James, W. P. (1978): Short chain fatty acid absorption by the human large intestine. *Gut* 19: 819–822. DOI: 10.1136/gut.19.9.819.
- Medzhitov, R. (2001): Toll-like receptors and innate immunity. *Nature reviews. Immunology* 1: 135–145. DOI: 10.1038/35100529.
- Merchak, A.; Gaultier, A. (2020): Microbial metabolites and immune regulation: New targets for major depressive disorder. *Brain, behavior, & immunity - health* 9: 1001-1069. DOI: 10.1016/j.bbih.2020.100169.
- Mikami, D.; Kobayashi, M.; Uwada, J.; Yazawa, T.; Kamiyama, K.; Nishimori, K. et al. (2020): AR420626, a selective agonist of GPR41/FFA3, suppresses growth of hepatocellular carcinoma cells by inducing apoptosis via HDAC inhibition. *Therapeutic advances in medical oncology* 12: 1758-1765. DOI: 10.1177/1758835920913432.
- Milligan, G.; Stoddart, L. A.; Smith, N. J. (2009): Agonism and allosterism: the pharmacology of the free fatty acid receptors FFA2 and FFA3. *British journal of pharmacology* 158: 146–153. DOI: 10.1111/j.1476-5381.2009.00421.x.
- Mills, C. (2012): M1 and M2 macrophages: Oracles of health and disease. *Critical reviews in immunology* 32: 463–488. DOI: 10.1615/critrevimmunol.v32.i6.10.
- Moore, S. F.; Mackenzie, A. B. (2008): Species and agonist dependent zinc modulation of endogenous and recombinant ATP-gated P2X7 receptors. *Biochemical pharmacology* 76: 1740–1747. DOI: 10.1016/j.bcp.2008.09.015.
- Mosallaei, M.; Ehtesham, N.; Rahimirad, S.; Saghi, M.; Vatandoost, N.; Khosravi, S. (2022): PBMCs: a new source of diagnostic and prognostic biomarkers. *Archives of physiology and biochemistry* 128: 1081–1087. DOI: 10.1080/13813455.2020.1752257.
- Moss, G. P.; Smith, P. A. S.; Tavernier, D. (1995): Glossary of class names of organic compounds and reactivity intermediates based on structure (IUPAC Recommendations 1995). *Pure and Applied Chemistry* 67: 1307–1375. DOI: 10.1351/pac199567081307.
- Mueller, N. T.; Zhang, M.; Juraschek, S. P.; Miller, E. R.; Appel, L. J. (2020): Effects of high-fiber diets enriched with carbohydrate, protein, or unsaturated fat on circulating short chain fatty acids: results from the Omni Heart randomized trial. *The American journal of clinical nutrition* 111: 545–554. DOI: 10.1093/ajcn/nqz322.
- Namour, F.; Galien, R.; van Kaem, T.; van der Aa, A.; Vanhoutte, F.; Beetens, J.; Van't Klooster, G. (2016): Safety, pharmacokinetics and pharmacodynamics of GLPG0974, a potent and selective FFA2 antagonist, in healthy male subjects. *British journal of clinical pharmacology* 82: 139–148. DOI: 10.1111/bcp.12900.
- Nelson, D. W.; Gregg, R. J.; Kort, M. E.; Perez-Medrano, A.; Voight, E. A.; Wang, Y. et al. (2006): Structure-activity relationship studies on a series of novel, substituted 1-benzyl-5-phenyltetrazole P2X7 antagonists. *Journal of medicinal chemistry* 49: 3659–3666. DOI: 10.1021/jm051202e.
- Neumann, S.; Razen, M.; Habermehl, P.; Meyer, C. U.; Zepp, F.; Kirkpatrick, C. J.; Wessler, I. (2007): The non-neuronal cholinergic system in peripheral blood cells: effects of nicotinic and muscarinic receptor antagonists on phagocytosis, respiratory burst and migration. *Life sciences* 80: 2361–2364. DOI: 10.1016/j.lfs.2007.01.010.
- Niedermann, R.; Buyle-Bodin, Y.; Lu, B.-Y.; Robinson, P.; Naleway, C. (1997): Short-chain carboxylic acid concentration in human gingival crevicular fluid. *Journal of Dental Research* 76: 575–579.

- Nielsen, M. C.; Andersen, M. N.; Møller, H. J. (2020): Monocyte isolation techniques significantly impact the phenotype of both isolated monocytes and derived macrophages in vitro. *Immunology* 159: 63–74. DOI: 10.1111/imm.13125.
- Nøhr, M. K.; Pedersen, M. H.; Gille, A.; Egerod, K. L.; Engelstoft, M. S.; Husted, A. S. et al. (2013): GPR41/FFAR3 and GPR43/FFAR2 as cosensors for short-chain fatty acids in enteroendocrine cells vs FFAR3 in enteric neurons and FFAR2 in enteric leukocytes. *Endocrinology* 154: 3552–3564. DOI: 10.1210/en.2013-1142.
- North, R. A. (2002): Molecular physiology of P2X receptors. *Physiological reviews* 82: 1013–1067. DOI: 10.1152/physrev.00015.2002.
- Olofsson, P. S.; Rosas-Ballina, M.; Levine, Y. A.; Tracey, K. J. (2012): Rethinking inflammation. Neural circuits in the regulation of immunity. *Immunological reviews* 248: 188–204. DOI: 10.1111/j.1600-065X.2012.01138.x.
- Oppenheim, J. J.; Kovacs, E. J.; Matsushima, K.; Durum, S. K. (1986): There is more than one interleukin 1. *Immunology today* 7: 45–56. DOI: 10.1016/0167-5699(86)90124-6.
- Ovchinnikov, D. A. (2008): Macrophages in the embryo and beyond: much more than just giant phagocytes. *Genesis* 46: 447–462. DOI: 10.1002/dvg.20417.
- Ozaki, E.; Campbell, M.; Doyle, S. L. (2015): Targeting the NLRP3 inflammasome in chronic inflammatory diseases: current perspectives. *Journal of inflammation research* 8: 15–27. DOI: 10.2147/JIR.S51250.
- Panda, S. K.; Ravindran, B. (2013): Isolation of human PBMCs. *Bio-protocol journal* 3: 323-326. DOI: 10.21769/BioProtoc.323.
- Pasare, C.; Medzhitov, R. (2004): Toll-like receptors and acquired immunity. *Seminars in immunology* 16: 23–26. DOI: 10.1016/j.smim.2003.10.006.
- Peng, L.; Li, Z.-R.; Green, R. S.; Holzman, I. R.; Lin, J. (2009): Butyrate enhances the intestinal barrier by facilitating tight junction assembly via activation of AMP-activated protein kinase in Caco-2 cell monolayers. *The Journal of nutrition* 139: 1619–1625. DOI: 10.3945/jn.109.104638.
- Perdiguer, E. G.; Geissmann, F. (2016): The development and maintenance of resident macrophages. *Nature immunology* 17: 2–8. DOI: 10.1038/ni.3341.
- Perregaux, D.; Gabel, C. A. (1994): Interleukin-1 beta maturation and release in response to ATP and nigericin. Evidence that potassium depletion mediated by these agents is a necessary and common feature of their activity. *Journal of Biological Chemistry* 269: 15195–15203. DOI: 10.1016/S0021-9258(17)36591-2.
- Peters, S. G.; Pomare, E. W.; Fisher, C. A. (1992): Portal and peripheral blood short chain fatty acid concentrations after caecal lactulose instillation at surgery. *Gut* 33: 1249–1252. DOI: 10.1136/gut.33.9.1249.
- Pétrilli, V.; Papin, S.; Dostert, C.; Mayor, A.; Martinon, F.; Tschopp, J. (2007): Activation of the NALP3 inflammasome is triggered by low intracellular potassium concentration. *Cell death and differentiation* 14: 1583–1589. DOI: 10.1038/sj.cdd.4402195.
- Pittet, M. J.; Nahrendorf, M.; Swirski, F. K. (2014): The journey from stem cell to macrophage. *Annals of the New York Academy of Sciences* 1319: 1–18. DOI: 10.1111/nyas.12393.
- Potula, R.; Gentile, T. A.; Meissler, J. J.; Shekarabi, A.; Wiah, S.; Farkas, D. J. et al. (2023): Purinergic P2X7 receptor antagonist inhibits methamphetamine-induced reward, hyperlocomotion, and cortical IL-7A levels in mice: A role for P2X7/IL-17A crosstalk in

- methamphetamine behaviors? *Brain, Behavior, and Immunity* 107: 47–52. DOI: 10.1016/j.bbi.2022.09.012.
- Prinyakupt, J.; Pluempitiwiriawej, C. (2015): Segmentation of white blood cells and comparison of cell morphology by linear and naïve Bayes classifiers. *Biomedical engineering online* 14: 63. DOI: 10.1186/s12938-015-0037-1.
- Qureshi, O. S.; Paramasivam, A.; Yu, Jowie C. H.; Murrell-Lagnado, R. D. (2007): Regulation of P2X4 receptors by lysosomal targeting, glycan protection and exocytosis. *Journal of cell science* 120: 3838–3849. DOI: 10.1242/jcs.010348.
- Ramírez, J.; Cañete, J. D. (2018): Anakinra for the treatment of rheumatoid arthritis: A safety evaluation. *Expert opinion on drug safety* 17: 727–732. DOI: 10.1080/14740338.2018.1486819.
- Ramos, M. G.; Rabelo, F. L. A.; Duarte, T.; Gazzinelli, R. T.; Alvarez-Leite, J. I. (2002): Butyrate induces apoptosis in murine macrophages via caspase-3, but independent of autocrine synthesis of tumor necrosis factor and nitric oxide. *Brazilian Journal of Medical and Biological Research* 32: 161–173. DOI: 10.1590/s0100-879x2002000200004.
- Ransohoff, R. M. (2016): A polarizing question: do M1 and M2 microglia exist? *Nature neuroscience* 19: 987–991. DOI: 10.1038/nn.4338.
- Rathinam, V. A. K.; Vanaja, S. K.; Fitzgerald, K. A. (2012): Regulation of inflammasome signaling. *Nature immunology* 13: 333–342. DOI: 10.1038/ni.2237.
- Ren, K.; Torres, R. (2009): Role of interleukin-1 $\beta$  during pain and inflammation. *Brain research reviews* 60: 57–64. DOI: 10.1016/j.brainresrev.2008.12.020.
- Repnik, U.; Knezevic, M.; Jeras, M. (2003): Simple and cost-effective isolation of monocytes from buffy coats. *Journal of immunological methods* 278: 283–292. DOI: 10.1016/s0022-1759(03)00231-x.
- Richter, K.; Asci, N.; Singh, V. K.; Yakoob, S. H.; Meixner, M.; Zakrzewicz, A. et al. (2023): Activation of endothelial NO synthase and P2X7 receptor modification mediates the cholinergic control of ATP-induced interleukin-1 $\beta$  release by mononuclear phagocytes. *Frontiers in immunology* 14: 1140–1157. DOI: 10.3389/fimmu.2023.1140592.
- Richter, K.; Mathes, V.; Fronius, M.; Althaus, M.; Hecker, A.; Krasteva-Christ, G. et al. (2016): Phosphocholine - an agonist of metabotropic but not of ionotropic functions of  $\alpha$ 9-containing nicotinic acetylcholine receptors. *Scientific reports* 6: 286. DOI: 10.1038/srep28660.
- Richter, K.; Sagawe, S.; Hecker, A.; Küllmar, M.; Askevold, I.; Damm, J. et al. (2018): C-reactive protein stimulates nicotinic acetylcholine receptors to control ATP-mediated monocytic inflammasome activation. *Frontiers in immunology* 9: 1604. DOI: 10.3389/fimmu.2018.01604.
- Rivero, V. J. P.; Bastien, D.; Yurcisin, G.; Pineau, I.; Dietrich, W. D.; Koninck, Y. de et al. (2012): P2X4 receptors influence inflammasome activation after spinal cord injury. *The Journal of Neuroscience* 32: 3058–3066. DOI: 10.1523/JNEUROSCI.4930-11.2012.
- Roberfroid, M. B. (2007): Inulin-type fructans: Functional food ingredients. *The Journal of nutrition* 137: 2493–2502. DOI: 10.1093/jn/137.11.2493S.
- Rokic, M.; Tvrdonova, V.; Vavra, V.; Jindrichova, M.; Obsil, T.; Stojilkovic, S. S.; Zemkova, H. (2010): Roles of conserved ectodomain cysteines of the rat P2X4 purinoreceptor in agonist binding and channel gating. *Physiological research* 59: 927–935. DOI: 10.33549/physiolres.931979.
- Romero, H. K.; Christensen, S. B.; Di Cesare Mannelli, L.; Gajewiak, J.; Ramachandra, R.; Elmslie, K. S. et al. (2017): Inhibition of  $\alpha$ 9 $\alpha$ 10 nicotinic acetylcholine receptors prevents

- chemotherapy-induced neuropathic pain. *Proceedings of the National Academy of Sciences of the United States of America* 114: 1825-1832. DOI: 10.1073/pnas.1621433114.
- Ross, G. D. (2000): Regulation of the adhesion versus cytotoxic functions of the Mac-1/CR3/alphaMbeta2-integrin glycoprotein. *Critical reviews in immunology* 20: 197–222.
- Rubartelli, A.; Cozzolino, F.; Talio, M.; Sitia, R. (1990): A novel secretory pathway for interleukin-1 beta, a protein lacking a signal sequence. *EMBO journal* 9: 1503–1510. DOI: 10.1002/j.1460-2075.1990.tb08268.x.
- Saeed, L.; Patnaik, M. M.; Begna, K. H.; Al-Kali, A.; Litzow, M. R.; Hanson, C. A. et al. (2017): Prognostic relevance of lymphocytopenia, monocytopenia and lymphocyte-to-monocyte ratio in primary myelodysplastic syndromes: a single center experience in 889 patients. *Blood cancer journal* 7: 550. DOI: 10.1038/bcj.2017.30.
- Sakaki, H.; Fujiwaki, T.; Tsukimoto, M.; Kawano, A.; Harada, H.; Kojima, S. (2013): P2X4 receptor regulates P2X7 receptor-dependent IL-1 $\beta$  and IL-18 release in mouse bone marrow-derived dendritic cells. *Biochemical and Biophysical Research Communications* 432: 406–411. DOI: 10.1016/j.bbrc.2013.01.135.
- Sameer, A. S.; Nissar, S. (2021): Toll-like receptors (TLRs): Structure, functions, signaling, and role of their polymorphisms in colorectal cancer susceptibility. *BioMed research international* 5: 1157–1163. DOI: 10.1155/2021/1157023.
- Savage, D. C. (1986): Gastrointestinal microflora in mammalian nutrition. *Annual Review of Nutrition* 6: 155–178. DOI: 10.1146/annurev.nu.06.070186.001103.
- Sawzdargo, M.; George, S. R.; Nguyen, T.; Xu, S.; Kolakowski Jr, L. F.; O’ Dowd, B. F. (1997): A cluster of four novel human G protein-coupled receptor genes occurring in close proximity to CD22 gene on chromosome 19q13.1. *Biochemical and biophysical research communications* 239: 542–547. DOI: 10.1006/bbrc.1997.7513.
- Sborgi, L.; Rühl, S.; Mulvihill, E.; Pipercevic, J.; Heilig, R.; Stahlberg, H. et al. (2016): GSDMD membrane pore formation constitutes the mechanism of pyroptotic cell death. *The EMBO journal* 35: 1766–1778. DOI: 10.15252/embj.201694696.
- Scheppach, W.; Weiler, F. (2004): The butyrate story: Old wine in new bottles? *Current Opinion in Clinical Nutrition and Metabolic Care* 7: 563–567. DOI: 10.1097/00075197-200409000-00009.
- Sealy, L. (1978): The effect of sodium butyrate on histone modification. *Cell* 14: 115–121. DOI: 10.1016/0092-8674(78)90306-9.
- Seman, M.; Adriouch, S.; Scheuplein, F.; Krebs, C.; Freese, D.; Glowacki, G. et al. (2003): NAD-induced T cell death: ADP-ribosylation of cell surface proteins by ART2 activates the cytosolic P2X7 purinoreceptor. *Immunity* 19: 0–582. DOI: 10.1016/s1074-7613(03)00266-8.
- Siebers, K.; Fink, B.; Zakrzewicz, A.; Agné, A.; Richter, K.; Konzok, S. et al. (2018): Alpha-1 antitrypsin inhibits ATP-mediated release of interleukin-1 $\beta$  via CD36 and nicotinic acetylcholine receptors. *Frontiers in immunology* 9: 877. DOI: 10.3389/fimmu.2018.00877.
- Singh, A. K.; Fechtner, S.; Chourasia, M.; Sicalo, J.; Ahmed, S. (2019): Critical role of IL-1 $\alpha$  in IL-1 $\beta$ -induced inflammatory responses: Cooperation with NF- $\kappa$ Bp65 in transcriptional regulation. *FASEB journal* 33: 2526–2536. DOI: 10.1096/fj.201801513R.
- Skinner, B. M.; Johnson, E. E. P. (2017): Nuclear morphologies: their diversity and functional relevance. *Chromosoma* 126: 195–212. DOI: 10.1007/s00412-016-0614-5.

- Sluyter, R.; Adriouch, S.; Fuller, S. J.; Nicke, A.; Sophocleous, R. A.; Watson, D. (2023): Animal models for the investigation of P2X7 receptors. *International journal of molecular sciences* 24: 265–270. DOI: 10.3390/ijms24098225.
- Srinivasula, S. M.; Poyet, J.-L.; Razmara, M.; Datta, P.; Zhang, Z.; Alnemri, E. S. (2002): The PYRIN-CARD protein ASC is an activating adaptor for caspase-1. *The Journal of biological chemistry* 277: 21119–21122. DOI: 10.1074/jbc.C200179200.
- Stoffels, M.; Zaal, R.; Kok, N.; van der Meer, J. W. M.; Dinarello, C. A.; Simon, A. (2015): ATP-induced IL-1 $\beta$  specific secretion: True under stringent conditions. *Frontiers in immunology* 6: 54. DOI: 10.3389/fimmu.2015.00054.
- Stokes, L.; Layhadi, J. A.; Bibic, L.; Dhuna, K.; Fountain, S. J. (2017): P2X4 receptor function in the nervous system and current breakthroughs in pharmacology. *Frontiers in pharmacology* 8: 291. DOI: 10.3389/fphar.2017.00291.
- Suurväli, J.; Boudinot, P.; Kanellopoulos, J.; Rüütel Boudinot, S. (2017): P2X4: A fast and sensitive purinergic receptor. *Biomedical journal* 40: 245–256. DOI: 10.1016/j.bj.2017.06.010.
- Takeda, K.; Akira, S. (2004): TLR signaling pathways. *Seminars in immunology* 16: 3–9. DOI: 10.1016/j.smim.2003.10.003.
- Tang, W. H. W.; Wang, Z.; Levison, B. S.; Koeth, R. A.; Britt, E. B.; Fu, X. et al. (2013): Intestinal microbial metabolism of phosphatidylcholine and cardiovascular risk. *The New England journal of medicine* 368: 1575–1584. DOI: 10.1056/NEJMoa1109400.
- Tansey, E. M. (2006): Henry Dale and the discovery of acetylcholine. *Comptes rendus biologies* 329: 419–425. DOI: 10.1016/j.crv.2006.03.012.
- Tedelind, S.; Westberg, F.; Kjerrulf, M.; Vidal, A. (2007): Anti-inflammatory properties of the short-chain fatty acids acetate and propionate: A study with relevance to inflammatory bowel disease. *World Journal of Gastroenterology* 13: 2826–2833. DOI: 10.3748/wjg.v13.i20.2826.
- Tolhurst, G.; Heffron, H.; Lam, Y. S.; Parker, H. E.; Habib, A. M.; Diakogiannaki, E. et al. (2012): Short-chain fatty acids stimulate glucagon-like peptide-1 secretion via the G-protein-coupled receptor FFAR2. *Diabetes* 61: 364–371. DOI: 10.2337/db11-1019.
- Topping, D. L.; Clifton, P. M. (2001): Short-chain fatty acids and human colonic function: Roles of resistant starch and nonstarch polysaccharides. *Physiological reviews* 81: 1031–1064. DOI: 10.1152/physrev.2001.81.3.1031.
- Toulmé, E.; Soto, F.; Garret, M.; Boué-Grabot, E. (2006): Functional properties of internalization-deficient P2X4 receptors reveal a novel mechanism of ligand-gated channel facilitation by ivermectin. *Molecular pharmacology* 69: 576–587. DOI: 10.1124/mol.105.018812.
- Trang, M.; Schmalzing, G.; Müller, C. E.; Markwardt, F. (2020): Dissection of P2X4 and P2X7 receptor current components in BV-2 microglia. *International journal of molecular sciences* 21: 47–55. DOI: 10.3390/ijms21228489.
- Trang, T.; Beggs, S.; Wan, X.; Salter, M. W. (2009): P2X4-receptor-mediated synthesis and release of brain-derived neurotrophic factor in microglia is dependent on calcium and p38-mitogen-activated protein kinase activation. *The Journal of Neuroscience* 29: 3518–3528. DOI: 10.1523/JNEUROSCI.5714-08.2009.
- Tripolt, N. J.; Leber, B.; Blattl, D.; Eder, M.; Wonisch, W.; Scharnagl, H. et al. (2013): Short communication: Effect of supplementation with Lactobacillus casei Shirota on insulin sensitivity,  $\beta$ -cell function, and markers of endothelial function and inflammation in subjects with metabolic syndrome--a pilot study. *Journal of dairy science* 96: 89–95. DOI: 10.3168/jds.2012-5863.

- Trouplin, V.; Boucherit, N.; Gorvel, L.; Conti, F.; Mottola, G.; Ghigo, E. (2013): Bone marrow-derived macrophage production. *Journal of visualized experiments* 81: 509-516. DOI: 10.3791/50966.
- Tsan, M.-F.; Gao, B. (2004): Endogenous ligands of Toll-like receptors. *Journal of leukocyte biology* 76: 514–519. DOI: 10.1189/jlb.0304127.
- Ulmann, L.; Hirbec, H.; Rassendren, F. (2010): P2X4 receptors mediate PGE2 release by tissue-resident macrophages and initiate inflammatory pain. *EMBO journal* 29: 2290–2300. DOI: 10.1038/emboj.2010.126.
- Ulven, T. (2012): Short-chain free fatty acid receptors FFA2/GPR43 and FFA3/GPR41 as new potential therapeutic targets. *Frontiers in endocrinology* 3: 111. DOI: 10.3389/fendo.2012.00111.
- Urbina-Treviño, L.; Mücke-Heim, I.-A. von; Deussing, J. M. (2022): P2X7 receptor-related genetic mouse models - Tools for translational research in psychiatry. *Frontiers in neural circuits* 16: 876–888. DOI: 10.3389/fncir.2022.876304.
- van Furth, R.; Cohn, Z. A. (1968): The origin and kinetics of mononuclear phagocytes. *The Journal of experimental medicine* 128: 415-135. DOI: 10.1084/jem.128.3.415.
- Vanaja, S. K.; Rathinam, V. A. K.; Fitzgerald, K. A. (2015): Mechanisms of inflammasome activation: Recent advances and novel insights. *Trends in cell biology* 25: 308–315. DOI: 10.1016/j.tcb.2014.12.009.
- Vaure, C.; Liu, Y. (2014): A comparative review of toll-like receptor 4 expression and functionality in different animal species. *Frontiers in immunology* 5: 316. DOI: 10.3389/fimmu.2014.00316.
- Venter, C. S.; Vorster, H. H.; Cummings, J. H. (1990): Effects of dietary propionate on carbohydrate and lipid metabolism in healthy volunteers. *The American journal of gastroenterology* 85: 549–553.
- Verbrugghe, A.; Hesta, M.; Daminet, S.; Polis, I.; Holst, J. J.; Buyse, J. et al. (2012): Propionate absorbed from the colon acts as gluconeogenic substrate in a strict carnivore, the domestic cat (*Felis catus*). *Journal of animal physiology and animal nutrition* 96: 1054–1064. DOI: 10.1111/j.1439-0396.2011.01220.x.
- Vince, A.; Killingley, M.; Wrong, O. M. (1978): Effect of lactulose on ammonia production in a fecal incubation system. *Gastroenterology* 74: 544–549.
- Vinolo, M. A. R.; Rodrigues, H. G.; Hatanaka, E.; Hebeda, C. B.; Farsky, S. H. P.; Curi, R. (2009): Short-chain fatty acids stimulate the migration of neutrophils to inflammatory sites. *Clinical science* 117: 331–338. DOI: 10.1042/CS20080642.
- Wawrocki, S.; Druszczynska, M.; Kowalewicz-Kulbat, M.; Rudnicka, W. (2016): Interleukin 18 (IL-18) as a target for immune intervention. *Acta biochimica Polonica* 63: 59–63. DOI: 10.18388/abp.2015\_1153.
- Weischenfeldt, J.; Porse, B. (2008): Bone marrow-derived macrophages (BMM): Isolation and applications. *CSH protocols* 1: 50-55. DOI: 10.1101/pdb.prot5080.
- Whiteaker, P.; Christensen, S.; Yoshikami, D.; Dowell, C.; Watkins, M.; Gulyas, J. et al. (2007): Discovery, synthesis, and structure activity of a highly selective alpha7 nicotinic acetylcholine receptor antagonist. *Biochemistry* 46: 6628–6638. DOI: 10.1021/bi7004202.
- Wiley, S. R.; Winkles, J. A. (2003): TWEAK, a member of the TNF superfamily, is a multifunctional cytokine that binds the TweakR/Fn14 receptor. *Cytokine & growth factor reviews* 14: 241–249. DOI: 10.1016/s1359-6101(03)00019-4.

Williams, N.; Coleman, P. S. (1982): Exploring the adenine nucleotide binding sites on mitochondrial F1-ATPase with a new photoaffinity probe, 3'-O-(4-benzoyl)benzoyl adenosine 5'-triphosphate. *Journal of Biological Chemistry* 257: 2834–2841. DOI: 10.1016/S0021-9258(19)81039-6.

Wong, J. M. W.; de Souza, R.; Kendall, C. W. C.; Emam, A.; Jenkins, D. J. A. (2006): Colonic health: Fermentation and short chain fatty acids. *Journal of Clinical Gastroenterology* 40: 235-243.

Young, M., T.; Pelegrin, P.; Surprenant, A. (2007): Amino acid residues in the P2X7 receptor that mediate differential sensitivity to ATP and BzATP. *Molecular pharmacology* 71: 92–100. DOI: 10.1124/mol.106.030163.

Zhang, C.; Franklin, C. L.; Ericsson, A. C. (2021): Consideration of gut microbiome in murine models of diseases. *Microorganisms* 9: 257–287. DOI: 10.3390/microorganisms9051062.

Zoli, M.; Pucci, S.; Vilella, A.; Gotti, C. (2018) Neuronal and extraneuronal nicotinic acetylcholine receptors. *Current Neuropharmacology* 16: 338-349. DOI: 10.2174/1570159X15666170912110450.

## Declaration

"I hereby declare that I have prepared the present work independently and without undue help or use of other than the specified aids. All textually or literally taken from published or unpublished texts, and all statements based on oral information, are identified as such. In the investigations I have conducted and mentioned in the dissertation, I have adhered to the principles of good scientific practice, as laid down in the "Statute of the Justus-Liebig-Universität Gießen for the safeguarding of good scientific practice", and adhered to ethical, data protection and animal welfare principles. I certify that third parties have not received from me, either directly or indirectly, benefits of any kind for work related to the content of the submitted dissertation or have specified them below. The work has not been submitted, either domestically or abroad, in the same or similar form to another examination authority for the purpose of a doctorate or other examination procedure. Any material taken from other sources and materials taken from others or used in the work has been identified as such. In particular, all persons were mentioned who were directly and indirectly involved in the creation of the present work. I agree with the review of my work by a plagiarism detection software or an internet-based software program."

---

Place, Date

---

Signature

## 11. Supplementary Material

**Table S1: Cell death in human peripheral blood mononuclear cells (hPBMCs) as estimated by the lactate dehydrogenase (LDH) activity in cell culture supernatants.**

Figure 6 A, B	Cells, treatment	Cell death [%]  median	n	Friedman test  P = 0.00
				Wilcoxon signed- rank test
	hPBMCs, LPS	2.0	16	
	hPBMCs, LPS, BzATP	5.5	16	*
	hPBMCs, LPS, BzATP, A438079 1 $\mu$ M	4.0	8	
	hPBMCs, LPS, BzATP, A438079 10 $\mu$ M	4.0	11	
	hPBMCs, LPS, BzATP, A438079 20 $\mu$ M	5.0	5	
	hPBMCs, LPS, BzATP, A438079 50 $\mu$ M	5.0	8	
	hPBMCs, LPS, BzATP, 5-BDBD 1 $\mu$ M	5.0	6	
	hPBMCs, LPS, BzATP, 5-BDBD 10 $\mu$ M	12.0	9	#
	hPBMCs, LPS, BzATP, 5-BDBD 20 $\mu$ M	16.5	6	#
	hPBMCs, LPS, BzATP, 5-BDBD 50 $\mu$ M	21.0	6	#
	hPBMCs, LPS, BzATP, 5-BDBD 100 $\mu$ M	10.0	3	
	hPBMCs, LPS, ATP	2.5	14	*
	hPBMCs, LPS, ATP, A438079 1 $\mu$ M	2.5	6	
	hPBMCs, LPS, ATP, A438079 10 $\mu$ M	2.0	9	
	hPBMCs, LPS, ATP, A438079 20 $\mu$ M	2.0	5	
	hPBMCs, LPS, ATP, A438079 50 $\mu$ M	3.0	6	
	hPBMCs, LPS, ATP, 5-BDBD 1 $\mu$ M	4.5	6	
	hPBMCs, LPS, ATP, 5-BDBD 10 $\mu$ M	6.0	9	§

	hPBMCs, LPS, ATP, 5-BDBD 20 $\mu$ M	15.5	4	
	hPBMCs, LPS, ATP, 5-BDBD 50 $\mu$ M	11.5	6	§
	hPBMCs, LPS, ATP, 5-BDBD 100 $\mu$ M	14.0	4	
	hPBMCs, LPS, A438079 10 $\mu$ M	2.0	5	
	hPBMCs, LPS, 5-BDBD 10 $\mu$ M	3.0	8	

Cell death was estimated via measurement of the release of lactate dehydrogenase (LDH) into the cell culture medium. The data depicted in this table corresponds to the experiments shown in the respective figures of the main part of this thesis. Human peripheral blood mononuclear cells (hPBMCs) were “pulsed” with lipopolysaccharide (LPS, 5 ng/ml, for 25 min). All cells were further stimulated with 3'-O-(4-benzoyl) benzoyl ATP (BzATP, 100 mM, 300 mM) or ATP (1 mM or 2 mM) and with further substances mentioned in the table above. \* $P \leq 0.05$  significantly different compared to data of cells treated with LPS; # $P \leq 0.05$  significantly different compared to data of cells treated with LPS + BzATP; § $P \leq 0.05$  significantly different compared to data of cells treated with LPS + ATP.

**Table S2: Cell death in human peripheral blood mononuclear cells (hPBMCs) as estimated by the lactate dehydrogenase (LDH) activity in cell culture supernatants.**

Figure 7	Cells, treatment	Cell death [%] median	n	Friedman test P = 0.00
	hPBMCs, LPS	4.5	6	
	hPBMCs, LPS, BzATP	1.9	6	
	hPBMCs, LPS, BzATP, 4-CMTB 0.5 $\mu$ M	2.1	4	
	hPBMCs, LPS, BzATP, 4-CMTB 1 $\mu$ M	2.3	6	
	hPBMCs, LPS, BzATP, 4-CMTB 10 $\mu$ M	3.6	6	#
	hPBMCs, LPS, BzATP, 4-CMTB 20 $\mu$ M	4.1	4	
	hPBMCs, LPS, BzATP, 4-CMTB 50 $\mu$ M	6.6	6	#
	hPBMCs, LPS, 4-CMTB 1 $\mu$ M	1.7	5	

Cell death was estimated via measurement of the release of lactate dehydrogenase (LDH) into the cell culture medium. The data depicted in this table corresponds to the experiments shown in the respective figures of the main part of this thesis. Human peripheral blood mononuclear cells (hPBMCs) were “pulsed” with lipopolysaccharide (LPS, 5 ng/ml, for 25 min). All cells were further stimulated with 3'-O-(4-benzoyl) benzoyl ATP (BzATP, 100 mM, 300 mM) or ATP (1 mM or 2 mM) and with further substances mentioned in the table above. #P ≤ 0.05 significantly different compared to data of cells treated with LPS + BzATP.

**Table S3: Cell death in human peripheral blood mononuclear cells (hPBMCs) as estimated by the lactate dehydrogenase (LDH) activity in cell culture supernatants.**

Figure 8	Cells, treatment	Cell death [%] median	n	Friedman test P = 0.17
				Wilcoxon signed-rank test
	hPBMCs, LPS	1.8	6	
	hPBMCs, LPS, BzATP	2.3	6	
	hPBMCs, LPS, BzATP, AR420626 1 μM	2.1	6	
	hPBMCs, LPS, BzATP, AR420626 10 μM	2.8	6	
	hPBMCs, LPS, BzATP, AR420626 50 μM	3.2	6	
	hPBMCs, LPS, AR420626 50 μM	1.9	6	

Cell death was estimated via measurement of the release of lactate dehydrogenase (LDH) into the cell culture medium. The data depicted in this table corresponds to the experiments shown in the respective figures of the main part of this thesis. Human peripheral blood mononuclear cells (hPBMCs) were “pulsed” with lipopolysaccharide (LPS, 5 ng/ml, for 25 min). All cells were further stimulated with 3'-O-(4-benzoyl) benzoyl ATP (BzATP, 100 mM, 300 mM) or ATP (1 mM or 2 mM) and with further substances mentioned in the table above. Since the Friedman test is above 0.05, the Wilcoxon test becomes redundant.

**Table S4: Cell death in human peripheral blood mononuclear cells (hPBMCs) as estimated by the lactate dehydrogenase (LDH) activity in cell culture supernatants.**

Figure 9	Cells, treatment	Cell death [%] median	n	Friedman test P = 0.00
				Wilcoxon signed-rank test
	hPBMCs, LPS	4.5	6	
	hPBMCs, LPS, BzATP	1.9	6	
	hPBMCs, LPS, BzATP, 4-CMTB 1 $\mu$ M	2.3	5	
	hPBMCs, LPS, BzATP, 4-CMTB 1 $\mu$ M, RgIA4 50 nM	2.9	5	
	hPBMCs, LPS, BzATP, 4-CMTB 1 $\mu$ M, ArIB [V11L, V16D] 500 nM	1.9	5	
	hPBMCs, LPS, BzATP, 4-CMTB 10 $\mu$ M	3.6	6	#
	hPBMCs, LPS, BzATP, 4-CMTB 10 $\mu$ M, RgIA4 50 nM	3.9	6	#
	hPBMCs, LPS, BzATP, 4-CMTB 10 $\mu$ M, ArIB [V11L, V16D] 500 nM	3.1	6	

Cell death was estimated via measurement of the release of lactate dehydrogenase (LDH) into the cell culture medium. The data depicted in this table corresponds to the experiments shown in the respective figures of the main part of this thesis. Human peripheral blood mononuclear cells (hPBMCs) were “pulsed” with lipopolysaccharide (LPS, 5 ng/ml, for 25 min). All cells were further stimulated with 3'-O-(4-benzoyl) benzoyl ATP (BzATP, 100 mM, 300 mM) or ATP (1 mM or 2 mM) and with further substances mentioned in the table above. #P  $\leq$  0.05 significantly different compared to data of cells treated with LPS + BzATP.

**Table S5: Cell death in human peripheral blood mononuclear cells (hPBMCs) as estimated by the lactate dehydrogenase (LDH) activity in cell culture supernatants.**

Figure 10	Cells, treatment	Cell death [%]	n	Friedman test
-----------	------------------	----------------	---	---------------

		<b>median</b>		<b>P = 0.002</b>
				<b>Wilcoxon signed-rank test</b>
	hPBMCs, LPS	1.2	5	
	hPBMCs, LPS, BzATP	1.1	5	
	hPBMCs, LPS, BzATP, AR420626 50 $\mu$ M	1.9	5	#
	hPBMCs, BzATP, AR420626 50 $\mu$ M, RgIA4 50 nM	2.0	5	#
	hPBMCs, BzATP, AR420626 50 $\mu$ M, Ar1B [V11L, V16D] 500 nM	1.8	5	#

Cell death was estimated via measurement of the release of lactate dehydrogenase (LDH) into the cell culture medium. The data depicted in this table corresponds to the experiments shown in the respective figures of the main part of this thesis. Human peripheral blood mononuclear cells (hPBMCs) were “pulsed” with lipopolysaccharide (LPS, 5 ng/ml, for 25 min). All cells were further stimulated with 3'-O-(4-benzoyl) benzoyl ATP (BzATP, 100 mM, 300 mM) or ATP (1 mM or 2 mM) and with further substances mentioned in the table above. # $P \leq 0.05$  significantly different compared to data of cells treated with LPS + BzATP.

**Table S6: Cell death in mouse peripheral blood mononuclear cells (mPBMCs) as estimated by the lactate dehydrogenase (LDH) activity in cell culture supernatants.**

<b>Figure 12</b>	<b>Cells, treatment</b>	<b>Cell death [%]</b>	<b>n</b>	<b>Friedman test</b>
		<b>median</b>		<b>P = 0.08</b>
				<b>Wilcoxon signed-rank test</b>
	mPBMCs, LPS	2.0	9	
	mPBMCs, LPS, BzATP	9.0	5	
	mPBMCs, LPS, ATP	3.0	9	
	mPBMCs, LPS, ATP, PC (200 $\mu$ M)	5.0	5	

mPBMCs, LPS, ATP, Acetate (20 mM)	2.0	7	
mPBMCs, LPS, ATP, Butyrate (20 mM)	10.0	7	
mPBMCs, LPS, ATP, Propionate (20 mM)	3.0	7	
mPBMCs, LPS, Acetate (20 mM)	2.0	6	
mPBMCs, LPS, Butyrate (20 mM)	2.5	6	
mPBMCs, LPS, Propionate (20 mM)	1.0	5	

Cell death was estimated via measurement of the release of lactate dehydrogenase (LDH) into the cell culture medium. The data depicted in this table corresponds to the experiments shown in the respective figures of the main part of this thesis. Mouse peripheral blood mononuclear cells (mPBMCs) were “pulsed” with lipopolysaccharide (LPS, 5 ng/ml, for 25 min). All cells were further stimulated with 3'-O-(4-benzoyl) benzoyl ATP (BzATP, 100 mM) or ATP (1 mM) and with further substances mentioned in the table above. Since the Friedman test is above 0.05, the Wilcoxon test becomes redundant.

**Table S7: Cell death in mouse peripheral blood mononuclear cells (mPBMCs) as estimated by the lactate dehydrogenase (LDH) activity in cell culture supernatants.**

Figure 13	Cells, treatment	Cell death [%] median	n	Friedman test P = 0.02
				Wilcoxon signed-rank test
	wild-type mPBMCs, LPS	0.5	6	
	wild-type mPBMCs, LPS, ATP	0.5	6	
	wild-type mPBMCs, LPS, ATP, PC (200 μM)	8.5	6	#
	wild-type mPBMCs, LPS, ATP, Acetate (20 mM)	0.5	6	

wild-type mPBMCs, LPS, ATP, Propionate (20 mM)	6.0	6	
wild-type mPBMCs, LPS, ATP, Butyrate (20 mM)	2.5	6	
wild-type mPBMCs, LPS, Acetate (20 mM)	3.3	6	
wild-type mPBMCs, LPS, Propionate (20 mM)	3.5	6	
wild-type mPBMCs, LPS, Butyrate (20 mM)	2.5	6	
			<b>Friedman test</b> <b>P = 0.19</b>
			<b>Wilcoxon signed-rank test</b>
gene-deficient mPBMCs, LPS	2.0	5	
gene-deficient mPBMCs, LPS, ATP	0.0	5	
gene-deficient mPBMCs, LPS, ATP, PC (200 $\mu$ M)	2.5	5	
gene-deficient mPBMCs, LPS, ATP, Acetate (20 mM)	9.0	5	
gene-deficient mPBMCs, LPS, ATP, Propionate (20 mM)	1.0	5	
gene-deficient mPBMCs, LPS, ATP, Butyrate (20 mM)	0.0	5	
gene-deficient mPBMCs, LPS, Acetate (20 mM)	3.2	4	
gene-deficient mPBMCs, LPS, Propionate (20 mM)	1.5	3	
gene-deficient mPBMCs, LPS, Butyrate (20 mM)	3.0	3	

Cell death was estimated via measurement of the release of lactate dehydrogenase (LDH) into the cell culture medium. The data depicted in this table corresponds to the experiments shown in the respective figures of the main part of this thesis. Mouse peripheral blood mononuclear cells (mPBMCs) were “pulsed” with lipopolysaccharide (LPS, 5 ng/ml, for 25 min). All cells were further stimulated with ATP (1 mM) and with further substances mentioned in the table above. The wild-type and the gene-deficient data were statistically analyzed separately. In the wild-type group, # $p \leq 0.05$  significantly different compared to data of cells treated with LPS + ATP. Since the Friedman test in the gene-deficient group is above 0.05, the Wilcoxon test becomes redundant.

**Table S8: Cell death in mouse peripheral blood mononuclear cells (mPBMCs) as estimated by the lactate dehydrogenase (LDH) activity in cell culture supernatants.**

Figure 14	Cells, treatment	Cell death [%] median	n	Friedman test P = 0.12
				Wilcoxon signed- rank test
	mPBMCs, LPS	0.5	6	
	mPBMCs, LPS, ATP	3.5	6	
	mPBMCs, LPS, ATP, 4-CMTB (10 $\mu$ M)	18.0	5	
	mPBMCs, LPS, ATP, AR420626 (20 $\mu$ M)	22.0	5	
	mPBMCs, LPS, 4-CMTB (10 $\mu$ M)	1.5	2	
	mPBMCs, LPS, AR420626 (20 $\mu$ M)	0.0	2	

Cell death was estimated via measurement of the release of lactate dehydrogenase (LDH) into the cell culture medium. The data depicted in this table corresponds to the experiments shown in the respective figures of the main part of this thesis. Mouse peripheral blood mononuclear cells (mPBMCs) were “pulsed” with lipopolysaccharide (LPS, 5 ng/ml, for 25 min). All cells were further stimulated with ATP (1 mM) and with further substances mentioned in the table above. Since the Friedman test is above 0.05, the Wilcoxon test becomes redundant.

**Table S9: Cell death in mouse peripheral blood mononuclear cells (mPBMCs) as estimated by the lactate dehydrogenase (LDH) activity in cell culture supernatants.**

Figure 15	Cells, treatment	Cell death [%] median	n	Friedman test P = 0.06
	wild-type mPBMCs, LPS	0.5	6	
	wild-type mPBMCs, LPS, ATP, DMSO	0.5	6	
	wild-type mPBMCs, LPS, ATP, 4-CMTB (20 $\mu$ M)	1.0	6	
	wild-type mPBMCs, LPS, ATP, AR420626 (20 $\mu$ M)	4.5	6	
				Friedman test P = 0.19
				Wilcoxon signed- rank test
	gene-deficient mPBMCs, LPS	2.0	5	
	gene-deficient mPBMCs, LPS, ATP, DMSO	8.0	5	
	gene-deficient mPBMCs, LPS, ATP, 4- CMTB (20 $\mu$ M)	0.0	5	
	gene-deficient mPBMCs, LPS, ATP, AR420626 (20 $\mu$ M)	10.0	5	
	gene-deficient mPBMCs, LPS, 4-CMTB (20 $\mu$ M)	2.0	5	

Cell death was estimated via measurement of the release of lactate dehydrogenase (LDH) into the cell culture medium. The data depicted in this table corresponds to the experiments shown in the respective figures of the main part of this thesis. Mouse

peripheral blood mononuclear cells (mPBMCs) were “pulsed” with lipopolysaccharide (LPS, 5 ng/ml, for 25 min). All cells were further stimulated with ATP (1 mM) and with further substances mentioned in the table above. The wild-type and the gene-deficient data were statistically analyzed separately. In the wild-type group and gene-deficient group the Friedman test is above 0.05, the Wilcoxon test becomes redundant.

**Table S10: Cell death in mouse bone marrow-derived macrophages (BMDMs) as estimated by the lactate dehydrogenase (LDH) activity in cell culture supernatants.**

Figure 19	Cells, treatment	Cell death [%] median	n	Friedman test P = 0.03
	Mouse BMDMs	0.0	15	
	Mouse BMDMs, ATP	0.0	7	
	Mouse BMDMs, LPS	1.0	13	
	Mouse BMDMs, LPS, BzATP (100 µM)	1.0	5	
	Mouse BMDMs, LPS, BzATP (300 µM)	0.0	5	
	Mouse BMDMs, ATP, LPS	4.0	15	
	Mouse BMDMs, ATP, LPS, A438079 (10 µM)	57.0	7	#
	Mouse BMDMs, LPS, A438079 (10 µM)	15.0	4	

Cell death was estimated via measurement of the release of lactate dehydrogenase (LDH) into the cell culture medium. The data depicted in this table corresponds to the experiments shown in the respective figures of the main part of this thesis. Bone marrow-derived macrophages (BMDMs) were primed with lipopolysaccharide (LPS, 1 µg/ml, for 5 h). All cells were further stimulated with 3'-O-(4-benzoyl) benzoyl ATP (BzATP, 100 mM, 300 mM) or ATP (1 mM) and with further substances mentioned in the table above. #P ≤ 0.05 significantly different compared to data of cells treated with LPS + ATP.

**Table S11: Cell death in mouse bone marrow-derived macrophages (BMDMs) as estimated by the lactate dehydrogenase (LDH) activity in cell culture supernatants.**

Figure 20	Cells, treatment	Cell death [%] median	n	Friedman test P = 0.001
				Wilcoxon signed-rank test
	Mouse BMDMs	17.0	12	
	Mouse BMDMs, LPS	15.8	12	
	Mouse BMDMs, LPS, ATP	17.8	12	
	Mouse BMDMs, LPS, ATP, 5-BDBD (1 $\mu$ M)	32.5	8	#
	Mouse BMDMs, LPS, ATP, 5-BDBD (10 $\mu$ M)	31.5	12	#
	Mouse BMDMs, LPS, ATP, 5-BDBD (50 $\mu$ M)	49.5	4	
	Mouse BMDMs, LPS, ATP, 5-BDBD (100 $\mu$ M)	35.5	6	#
	Mouse BMDMs, LPS, ATP, A438079 (0.5 $\mu$ M)	33.0	4	
	Mouse BMDMs, LPS, ATP, A438079 (1 $\mu$ M)	17.5	8	
	Mouse BMDMs, LPS, ATP, A438079 (5 $\mu$ M)	20.0	4	
	Mouse BMDMs, LPS, ATP, A438079 (10 $\mu$ M)	16.0	8	#
	Mouse BMDMs, LPS, ATP, A438079 (100 $\mu$ M)	17.0	6	
	Mouse BMDMs, LPS, 5-BDBD (10 $\mu$ M)	23.0	8	
	Mouse BMDMs, LPS, A438079 (10 $\mu$ M)	29.0	6	

Cell death was estimated via measurement of the release of lactate dehydrogenase (LDH) into the cell culture medium. The data depicted in this table corresponds to the experiments shown in the respective figures of the main part of this thesis. Bone marrow-derived macrophages (BMDMs) were primed with lipopolysaccharide (LPS, 1 µg/ml, for 5 h). All cells were further stimulated with ATP (2 mM) and with further substances mentioned in the table above. #P ≤ 0.05 significantly different compared to data of cells treated with LPS + ATP.

**Table S12: Cell death in mouse bone marrow-derived macrophages (BMDMs) as estimated by the lactate dehydrogenase (LDH) activity in cell culture supernatants.**

Figure 21	Cells, treatment	Cell death [%] median	n	Friedman test P = 0.01
				Wilcoxon signed- rank test
	Mouse BMDMs	0.0	8	
	Mouse BMDMs, ATP	0.0	6	
	Mouse BMDMs, LPS	1.0	8	
	Mouse BMDMs, LPS, ATP	2.0	8	
	Mouse BMDMs, LPS, ATP, ACh (10 µM)	0.0	7	
	Mouse BMDMs, LPS, ATP, Butyrate (20 mM)	17.0	7	#
	Mouse BMDMs, LPS, ATP, 4-CMTB (10 µM)	5.8	8	#
	Mouse BMDMs, LPS, ATP, AR420626 (20 µM)	24.9	7	#

Cell death was estimated via measurement of the release of lactate dehydrogenase (LDH) into the cell culture medium. The data depicted in this table corresponds to the experiments shown in the respective figures of the main part of this thesis. Bone marrow-derived macrophages (BMDMs) were primed with lipopolysaccharide (LPS, 1 µg/ml, for 5 h). All cells were further stimulated with ATP (2 mM) and with further substances mentioned in the table above. #P ≤ 0.05 significantly different compared to data of cells treated with LPS + ATP.

**Table S13: Cell death in mouse bone marrow-derived macrophages (BMDMs) as estimated by the lactate dehydrogenase (LDH) activity in cell culture supernatants.**

Figure 22 A, B	Cells, treatment	Cell death [%] median	n	Friedman test P = 0.00
	Mouse BMDMs	11.0	5	
	Mouse BMDMs, LPS	14.0	5	*
	Mouse BMDMs, LPS, ATP	21.0	5	#
	Mouse BMDMs, LPS, ATP, 4-CMTB (20 µM)	18.0	5	
	Mouse BMDMs, LPS, 4-CMTB (20 µM), RgIA4 50 nM	17.0	5	
	Mouse BMDMs, LPS, 4-CMTB (20 µM), ArIB [V11L, V16D] 500 nM	18.0	5	
	Mouse BMDMs, LPS, ATP, AR420626 (50 µM)	17.0	5	
	Mouse BMDMs, LPS, AR420626 (50 µM), RgIA4 50 nM	18.0	5	
	Mouse BMDMs, LPS, AR420626 (50 µM), ArIB [V11L, V16D] 500 nM	19.0	5	§
	Mouse BMDMs, LPS, RgIA4 50 nM	20.0	5	
	Mouse BMDMs, LPS, ArIB [V11L, V16D] 500 nM	24.0	5	
				Friedman test P = 0.00

			<b>Wilcoxon signed- rank test</b>
Mouse BMDMs	11.0	5	
Mouse BMDMs, LPS	13.0	5	*
Mouse BMDMs, LPS, ATP	23.0	5	#
Mouse BMDMs, LPS, ATP, 4-CMTB (20 $\mu$ M)	18.0	5	
Mouse BMDMs, LPS, 4-CMTB (20 $\mu$ M), RgIA4 50 nM	17.0	5	
Mouse BMDMs, LPS, 4-CMTB (20 $\mu$ M), ArIB [V11L, V16D] 500 nM	18.0	5	
Mouse BMDMs, LPS, ATP, AR420626 (50 $\mu$ M)	17.0	5	
Mouse BMDMs, LPS, AR420626 (50 $\mu$ M), RgIA4 50 nM	18.0	5	
Mouse BMDMs, LPS, AR420626 (50 $\mu$ M), ArIB [V11L, V16D] 500 nM	19.0	5	§
Mouse BMDMs, LPS, ArIB [V11L, V16D] 500 nM	24.0	5	

Cell death was estimated via measurement of the release of lactate dehydrogenase (LDH) into the cell culture medium. The data depicted in this table corresponds to the experiments shown in the respective figures of the main part of this thesis. Bone marrow-derived macrophages (BMDMs) were primed with lipopolysaccharide (LPS, 1  $\mu$ g/ml, for 5 h). All cells were further stimulated with ATP (2 mM) and with further substances mentioned in the table above. Part A and B were statistically analyzed separately. \* $P \leq 0.05$  significantly different compared to data of untreated cells; # $P \leq 0.05$  significantly different compared to data of cells treated with LPS; § $P \leq 0.05$  significantly different compared to data of cells treated with LPS + ATP.

## 12. Note of thanks

*I praise you, for I am fearfully and wonderfully made.*

*Wonderful are your works;*

*my soul knows it very well. Psalm 139;14*

I would like to express my deepest appreciation to everyone who helped me in every step of performing the experiments and writing this thesis.

Moreover, I would like to extend my deepest gratitude to Prof. Dr. Veronika Grau for permitting me to conduct this work under her direction as well as accompanying and helping me in every stage needed.

Without Dr. Katrin Richter I would not have been able to complete this project. Katrin played a decisive role, assisting me from the first day, answering all my questions and emotionally uplifting me with guiding words.

Thanks to the Institute of Anatomy in Giessen and also thanks to Prof. Dr. Offermann from the Max-Planck Institute in Bad Nauheim for providing the wild-type and gene-deficient mice.

Furthermore, I would like to give a special thanks to my dear husband and mother for providing me with encouragement and patience throughout the duration of this project.

I would like to acknowledge the assistance and help of the whole lab team, including Gabi Fuchs-Moll, Sabine Stumpf, Katrin Petri and Sigrid Wilker. It was also a great pleasure working with Philipp, Alisa and Leon. Thank you for the good time we had together.